GEMS & GEMOLOGY

VOLUME XXXIII

FALL 1997

GEMS & GEMOLOGY

FALL 1997   VOLUME 33 NO. 3

TABLE OF CONTENTS

pg. 185

pg. 189

pg. 205

pg. 214

ABOUT THE COVER: Commercial quantities of gem-quality benitoite are found at only one location in the world, the Benitoite Gem mine, in San Benito County, California. This historic locality continues to produce fine-quality gemstones and mineral specimens, and an extension of the deposit was found in the spring of 1997. The feature article in this issue looks at the history of the Benitoite Gem mine, the geology of the New Idria district and current mining there, and the gemological properties of this distinctive material. The benitoite and diamond necklace illustrated here is shown with the largest faceted benitoite to date, a 15.42 carat stone from the Benitoite Gem mine. An artistic rendering, by GIA designer Lainie Mann, features this stone mounted in a pendant. Jewelry and gemstone from the collection of Michael M. Scott.

Photo © Harold & Erica Van Pelt—Photographers, Los Angeles, California.

Color separations for Gems & Gemology *are by Pacific Color, Carlsbad, CA. Printing is by Cadmus Journal Services, Richmond, VA.*

S Y M P O S I U M 1999

Meeting the Millennium

*I*n June 1991, GIA celebrated its 60th Anniversary with the Second International Gemological Symposium in Los Angeles, California. Many of you came to that event and have since told us that these were the most exciting and memorable four days of your career. Having successfully completed the building of our new world headquarters and campus in Carlsbad, California, we are now turning our attention to hosting the Third International Gemological Symposium, June 21–24, 1999, in beautiful San Diego, California.

For GIA, this event will mark a seminal moment in the future of the gem and jewelry industry. Focusing on the theme Meeting the Millennium, the Third International Symposium will feature more than 100 speakers and panelists, a "poster session" of reports on cutting-edge research, world-renowned opening and closing keynote speakers, and a special day designed to stimulate the members of our industry to move beyond traditional boundaries to meet the challenges of the new century. We anticipate more than 2,000 participants in this unique event—a mixture of academic enrichment, gemological insight, cultural experience, and networking opportunities that will be unlike any seen before in our industry. For those who have not yet had an opportunity to visit our new world headquarters in Carlsbad, a full day of tours and other activities is being planned immediately following the Symposium.

Although the event is still many months away, I suggest that you mark your calendars now. Reserve your place for the experience of a lifetime. Come celebrate with us and *meet the millennium* at the Third International Gemological Symposium, June 21–24, 1999.

William E. Boyajian
President, Gemological Institute of America

BENITOITE FROM THE NEW IDRIA DISTRICT, SAN BENITO COUNTY, CALIFORNIA

By Brendan M. Laurs, William R. Rohtert, and Michael Gray

Commercial quantities of gem-quality beni-toite are known from a single location in the world, the Benitoite Gem mine in the New Idria district of San Benito County, California. A barium titanium silicate, benitoite is typically colorless to blue, and is noteworthy for its high refractive indices, moderate bire-fringence, and strong dispersion. Benitoite occurs in altered blueschist within serpenti-nite. The gem crystals formed within frac-tures as a result of the alteration of blueschist by hydrothermal fluids derived from the regional metamorphism of the serpentinite. An extension of the historic deposit at the Benitoite Gem mine was discovered in the spring of 1997, which should contribute to continued stability in price and supply. The gemological properties of benitoite readily identify it from similar-appearing gems.

ABOUT THE AUTHORS

Mr. Laurs is senior editor of Gems & Gemology, *Gemological Institute of America, Carlsbad, California (blaurs@gia.edu). Mr. Rohtert is Manager of Gemstones, Kennecott Exploration Company, Reno, Nevada (wrohtert@sierra.net). Mr. Gray is owner of Graystone Enterprises, and a partner in Coast to Coast Rare Stones; he lives in Missoula, Montana (west@rarestone.com).*

Please see acknowledgments at end of article.

*G*em-quality benitoite has been mined intermittent-ly from only one region in the world, the New Idria district of San Benito County, California. Benitoite was first discovered there in 1907; it was named after the county, as well as the San Benito River, which runs through the property, and the nearby San Benito Mountain (Louderback, 1909). Stones are strongly dichroic, typically violetish blue and colorless. Exceptionally rare gemstones are colorless and pink. A few orange benitoites have been produced by heat treatment of colorless material. Benitoite has high refractive indices, moderate birefringence, and strong dispersion (exceeding that of diamond in some direc-tions), which render the faceted gems comparable in appear-ance and price to fine sapphire and tanzanite (figure 1). Although production has been sporadic throughout the life of the deposit, hundreds of carats of faceted material are cur-rently available, in sizes up to 2–3 ct.

Benitoite is a barium titanium silicate ($BaTiSi_3O_9$) that forms under unusual conditions. At the New Idria district, benitoite is found exclusively in bodies of blueschist within serpentinite. During 1995, the senior author conducted a detailed study of blueschist bodies throughout the New Idria district on behalf of the Kennecott Exploration Company. The main occurrence, the Benitoite Gem mine, was mapped in detail, and other known benitoite occur-rences at the Mina Numero Uno and Victor prospects were examined. Microscopic benitoite crystals were detected for the first time in a blueschist body on Santa Rita Peak. After nearly a decade of inactivity, a small prospect containing minute amounts of gem-quality benitoite was rediscovered along a tributary of Clear Creek; this locality is now known as the Junnila claim. More recently, an extension of the Benitoite Gem mine deposit was found in spring 1997, dur-ing exploration down slope of the historic pit.

The Benitoite Gem mine was referred to as the "Dallas mine" until the mid-1960s, but it has been variously called the "Benitoite mine," "Dallas Benitoite mine," and "Dallas

Figure 1. Because of its beauty, rarity, and singularity of occurrence, benitoite was declared the official California State Gemstone in 1985. This assortment of stones from the Benitoite Gem mine (1.10–4.77 ct) shows the range of colors that are typically encountered in benitoite. All stones were faceted by Elvis (Buzz) and Michael Gray. From the collection of Michael M. Scott; photo © Harold & Erica Van Pelt.

Gem mine" (Wise and Gill, 1977). Today the locality is designated as the Benitoite Gem mine by the mine owners, after the notation on topographic maps of the U.S. Geological Survey which identify the site simply as the "Gem mine."

HISTORY

Although there is general agreement in the literature that benitoite was discovered in early 1907, there is considerable controversy about who actually discovered it. Louderback (1907) originally attributed the discovery to L. B. Hawkins and T. E. Sanders. However, two years later, he identified J. M. Couch (figure 2), a prospector who was grubstaked by R. W. Dallas, as having first found a number of mineral deposits that merited further investigation (Louderback, 1909). Dallas "induced" Hawkins to accompany Couch back into the mountains. According to Louderback (1909, p. 333), "While out to examine some copper deposits they happened upon the benitoite deposit and each claims to be responsible for the discovery." In 1961, Couch's eldest son, Oscar, published *The Benitoite Story*, in which he outlined the reasons why his father should be given sole credit finding the deposit. Austin (1988) provides further evidence for Couch being the sole discoverer of what, at the time, he thought was a sapphire deposit. Frazier and

Frazier (1990a) reviewed the controversial history surrounding the discovery and development of the mine without making any judgment, and provided a comprehensive bibliography (1990b).

The first documented piece of benitoite to be faceted was brought to a lapidary in the San Francisco Bay area by Sanders' brother. While an expert from the Los Angeles area proclaimed the new material "volcanic glass," this lapidary called the stone spinel: "It was too soft for a sapphire, so I decided it must be a spinel; [since] that's the only other stone there is of that color" (Marcher, 1939). The lapidary showed some of the stones to George Eacret, the manager of Shreve & Co., one of the largest jewelry stores in San Francisco at that time. According to Marcher (1939), Eacret checked the stone with a dichroscope and found that it was doubly refractive, so he delivered a sample to Dr. George Louderback, a mineralogist at the University of California (Berkeley) who determined that it was a new, undescribed mineral.

In the company of Mr. Eacret, Dr. Louderback made his first visit to the mine on July 19, 1907, and confirmed the discovery. He revisited the deposit on October 11 of that year to study the geology. When Louderback returned to the mine with Eacret on August 12, 1908, he took the first photographs of benitoite for use in his 1909 full-length

Figure 2. Although there has been considerable controversy surrounding who actually discovered benitoite, much of the evidence supports the claim of J. M. Couch, shown here at a campsite near the Benitoite Gem mine. Photo from the Dallas Mining Company archives.

article describing the mineral. Louderback's documentation of the ditrigonal-dipyramidal crystal habit finally proved the natural existence of this crystal form, which had been predicted mathematically 77 years earlier (Hessel, 1830).

Soon after the discovery, the Dallas Mining Company was formed to finance the development of the deposit, which was then called the "Dallas mine." Cabins and corrals were built nearby, and mining equipment was hauled in by horse and wagon over tortuous roads from Coalinga, the nearest town. According to a diary of the Dallas Mining Company, active mining began in July 1907. An open cut and a series of underground workings were developed during the first few years of mining (figure 3), and numerous plates of gem-bearing rock were recovered.

Most of the benitoite crystals were covered with natrolite, which could have been dissolved in acid without harming the benitoite crystals. However, it was decided that this process was too time-consuming, so the "knobs" formed by benitoite crystals lying underneath the natrolite were initially broken off the rock matrix by use of hammer and chisel or a punch press. As a result, few well-crystallized mineral specimens were recovered during the early period of mining, as the main focus was on the production of gem rough. The Dallas Mining Company diary records quantities of rough measured in "quart jars" and "cigar boxes" that were sent to Dallas's offices in Coalinga.

The Dallas Mining Company continued opera-

tions until 1912, when it ceased being economical (Bradley et al., 1917). In October 1913, the mining equipment was auctioned off and the property was vacated. The mine was issued mineral patent papers in 1917, five years after active mining ceased. The ownership of the mine remained in the Dallas family until 1987.

Between 1920 and 1940, little activity took place at the locality, except for occasional unauthorized mining by various parties, including enterprising teenagers Edward Swoboda and Peter Bancroft (Bancroft, 1984). Miller Hotchkiss, from the nearby San Joaquin Valley town of Firebaugh, leased the mine in the 1940s. Hotchkiss was the first to take a bulldozer to the mine, which he used to rework the mine tailings. From 1952 to 1967, a lease was held by Clarence Cole, a mineral dealer from Oakland, California. Cole used a bulldozer and dynamite to enlarge the historic pit. In 1966, Cole granted a sublease to Gerold Bosley, of San Diego, California (Sinkankas, 1976). Backed by noted mineral collector Josephine Scripps, Bosley used a bulldozer to expose more of the open pit near the entrance of the original tunnels. Bosley ultimately found very little gem rough, but he did recover some notable mineral specimens.

Cole died in 1967, and the lease subsequently was transferred to William "Bill" Forrest, of Fresno, California, and Elvis "Buzz" Gray, currently of Missoula, Montana. They purchased the mine from the Dallas family in 1987, and they remain the sole owners today.

LOCATION AND ACCESS

The Benitoite Gem mine is located 32 km (20 miles) northwest of the town of Coalinga, California, at approximately 1,380 m (4,520 feet) above sea level. Paved county roads provide access to the New Idria district from the southwest via Coalinga, or from the northeast via Panoche Road along Interstate 5 in the San Joaquin Valley (figure 4). These roads lead 63 km (39 miles) and 85 km (53 miles), respectively, to a network of four-wheel-drive trails that are infrequently maintained by the U.S. Bureau of Land Management. Both routes require an additional 30 to 40 km of travel over rough dirt roads to reach the mine.

The Benitoite Gem mine is located on 16.2 hectares (40 acres) of private patented mining property, which is secured by a locked gate. The site is patrolled regularly by law enforcement officers, and visitors must obtain written permission from the owners to enter the mine area. Four other benitoite prospects in the district are claimed as follows: (1) The Junnila claim, owned by Leza Junnila of Fresno, California; (2) The Mina Numero Uno claim, owned by Sharon and Eugene Cisneros of San Jose, California; (3) The Victor claim, owned by Craig Stolberg of San Jose, California; and (4) The Santa Rita Peak property, controlled by Kennecott Exploration Company. All of these mineral prospects are closed to the public.

WORLDWIDE OCCURRENCE
OF BENITOITE

Benitoite has been confirmed from nine locations around the world, but only the historic Benitoite Gem mine and the Junnila claim have produced gem-quality material. All of the commercial gem production has come from the Benitoite Gem mine. At the three other deposits in the New Idria district, benitoite has been found only as small, platy (non-gem quality) crystals, up to a few millimeters in diameter (see descriptions of the Mina Numero Uno claim, Victor claim, and Santa Rita Peak property in the Geology section, below).

Outside the New Idria district, benitoite has been found *in situ* at four areas. At Big Creek–Rush Creek—in the Sierra Nevada foothills of eastern Fresno County, California—small grains of benitoite are found in gneissic metamorphic rocks near a type of igneous rock known as granodiorite (Alfors et al., 1965; Hinthorne, 1974). This occurrence is located nearly 160 km (100 miles) northeast of the

Figure 3. This photo, taken around 1910, shows benitoite miners and an adit at the Benitoite Gem mine. Photo from the Dallas Mining Company archives.

Benitoite Gem mine, and is not geologically related to the New Idria district. In Japan, benitoite was noted from albite-amphibole rock in a serpentinite body, along the Kinzan-dani River, at Ohmi in the Niigata Prefecture (Komatsu et al., 1973; Chihara et al., 1974; Sakai and Akai, 1994). At Broken Hill, New South Wales, Australia, Dr. Ian R. Plimer reported benitoite as a rare mineral in high-grade granite gneiss (Worner and Mitchell, 1982). Most recently, crystals of colorless, blue, and pink benitoite averaging 1–2 mm in diameter were detected in gas cavities in syenite at the Diamond Jo quarry in Hot Springs County, Arkansas (Barwood, 1995; H. Barwood, pers. comm., 1997).

Detrital grains of benitoite (not *in situ*) were recovered from Pleistocene lake sediments at the Lazzard estate, a few kilometers west of Lost Hills, in the San Joaquin Valley, Kern County, California (Reed and Bailey, 1927). On the basis of geologic considerations, sediments from this location could not have been derived from the New Idria district or from the Big Creek–Rush Creek area.

Two previously reported benitoite locations should be discredited. Anten (1928) probably

misidentified benitoite in a thin section from Owithe Valley, Belgium (Petrov, 1995). Lonsdale et al. (1931) tentatively identified benitoite in sediments from the Eocene Cook Mountain formation of southwest Texas; Smith (1995) suggested that the locality should be discredited because the authors confused the spelling of bentonite (a clay mineral) with benitoite, but we recommend discreditation because the available data provided by Lonsdale et al. suggest that they misidentified grains that were actually sapphirine. Rumors of benitoite from Korea have not been confirmed.

GEOLOGY

Geologic Setting. The New Idria district is located in the southern Diablo Range of the California Coast Range geologic province. Since 1853, the district has been mined and prospected for numerous mineral resources, including mercury, chromium, gold, asbestos, gems, and mineral specimens. The district encompasses a serpentinite body that was tectonically emplaced into surrounding sedimentary and metamorphic rocks. During the late Jurassic, when two of the earth's plates collided (see, for example, Hopson et al., 1981), the relatively low-density serpentinite rose through the overlying layers of rock, which included the Franciscan Formation. Slices of the Franciscan Formation were incorporated into the highly sheared serpentinite body during its emplacement; these are called tectonic inclusions (see Coleman, 1957). The serpentinite breached the paleo-surface in the mid- to late-Miocene (Coleman,
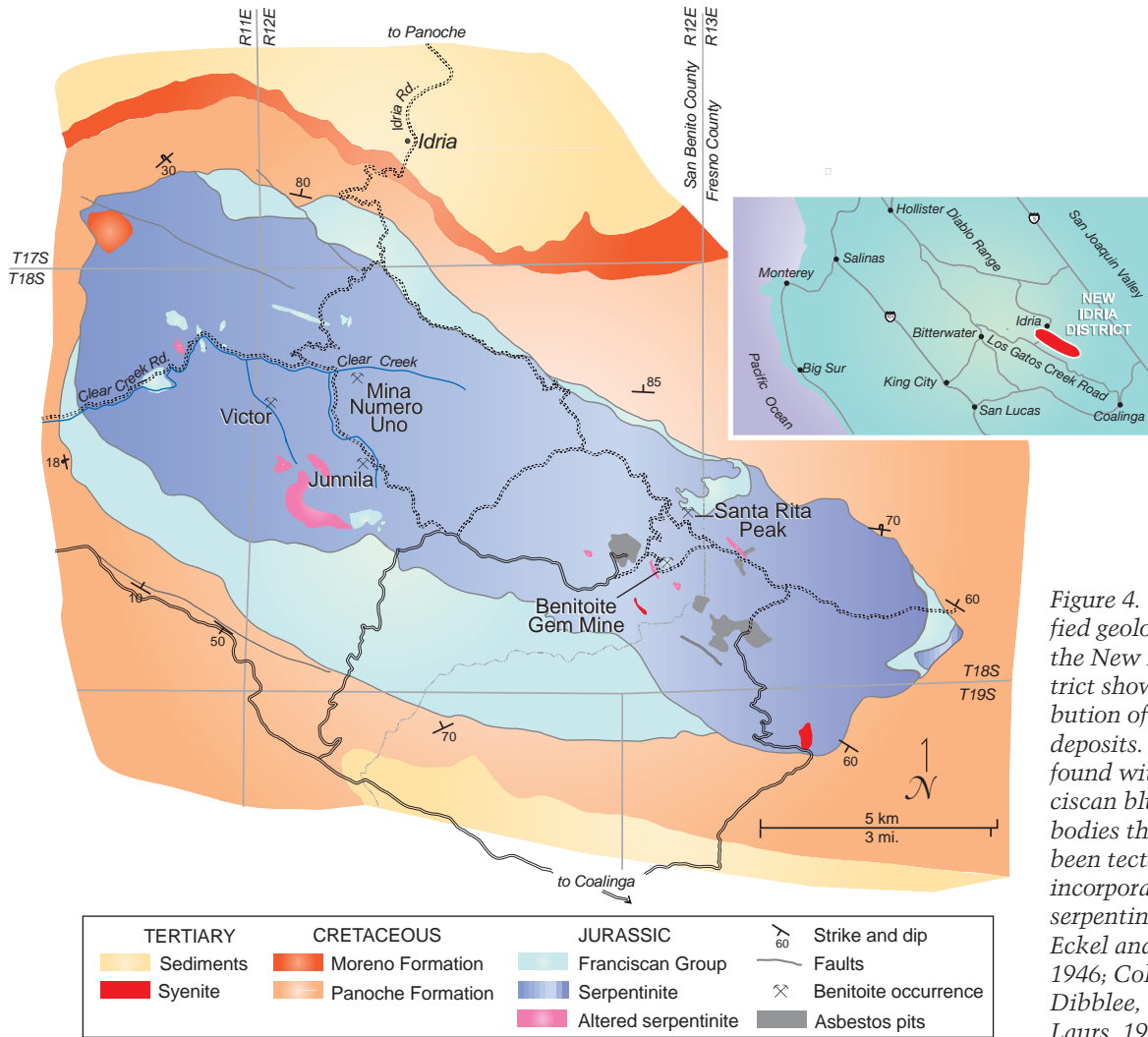

Figure 4. This simplified geologic map of the New Idria district shows the distribution of benitoite deposits. Benitoite is found within Franciscan blueschist bodies that have been tectonically incorporated into the serpentinite (after Eckel and Myers, 1946; Coleman, 1957; Dibblee, 1979; and Laurs, 1995).

1961). It is now exposed along the crest of the Diablo Range (figure 5) over an area 23 km by 8 km, elongate to the northwest.

Tectonic inclusions of Franciscan rocks within the serpentinite consist dominantly of blueschist and graywacke, with lesser mica schist, greenstone, and amphibolite schist (Coleman, 1957; Laurs, 1995). All of these rocks are derived from oceanic crust and overlying sediments that were accreted onto the continental margin during the Jurassic period. Two blueschist protoliths (parent rocks) may be differentiated on the basis of texture and composition: (1) metavolcanic, which are largely basaltic lavas and volcaniclastics; and (2) metasedimentary, which are largely marine sediments. Depending on the composition of the protolith, the blueschist contains variable amounts of very fine-grained albite, glaucophane-crossite, actinolite-tremolite, aegerine-augite, and titanite, with or without stilpnomelane, quartz, K-feldspar, epidote, and apatite. Benitoite is found in blueschist derived from both protoliths (Laurs, 1995).

Prior to breaching the surface, the New Idria serpentinite was intruded by small bodies of igneous rocks, predominantly syenite (Coleman, 1957; again, see figure 4). The mid-Miocene age of the syenite correlates well with Neogene magmatism in the California Coast Range, which is associated with the plate tectonic reconfiguration of western California (Van Baalen, 1995). Metamorphism associated with this reconfiguration is probably responsible for forming calc-silicate vein assemblages that are scattered through the serpentinite, as well as benitoite-bearing veins in the blueschist bodies (Van Baalen, 1995). Tentative age data suggests that the benitoite crystallized about 12 million years ago (M. Lanphere, pers. comm., in Van Baalen, 1995), so it is much younger than the enclosing blueschist, which formed about 100 to 160 million years ago (see, for example, Lee et al., 1964).

Benitoite Gem Mine. *Previous Work.* Arnold (1908) and Sterrett (1908, 1911) summarized the early mining activity. Coleman (1957), Van Baalen (1995), and Wise and Moller (1995) wrote district-wide geological reports, which include discussions of the Benitoite Gem mine. Geologic maps of the mine were prepared first by Coleman (1957), and later by Rohtert (1994) and Laurs (1995). Laird and Albee (1972) made physical, chemical, and crystallographic measurements on benitoite and associated minerals from the district, and Wise and Gill (1977) provided

a detailed description of the complicated mineralogy.

Geology. The mine is situated on a low hill (figure 6), which is underlain by Franciscan rocks emplaced into serpentinite (Coleman, 1957; Wise and Gill, 1977). These rocks consist of blueschist and greenstone, which are locally sheared (figure 7). The blueschist is dark bluish gray where unaltered, and lighter blue-green within the mineralized zone. This zone is at least 60 m long, strikes N60°W, dips moderately northeast, and is about 3 m thick. Recent field observations by the authors suggest that the deposit is offset along two north- to northwest-trending faults (again, see figure 7). All of the historic lode production was obtained from the central section of the deposit. However, in the spring of 1997 an extension of the mineralized zone was discovered in the western offset portion. The faulting apparently down-dropped a portion of the mineralized blueschist, which lay buried beneath up to 10 m of unconsolidated eluvium and dump material.

Mineralization. Benitoite mineralization is confined entirely to the blueschist, in a hydrothermally

Figure 5. This low-altitude oblique aerial photograph, looking northeast, shows the Benitoite Gem mine workings (small brown cut). The large open pit on the left is an active asbestos mine being worked by the King City Asbestos Corp. Santa Rita Peak, where benitoite has also been found, is visible above the Benitoite Gem mine and forms the highest point on the skyline. Photo courtesy of Kennecott Exploration Company.
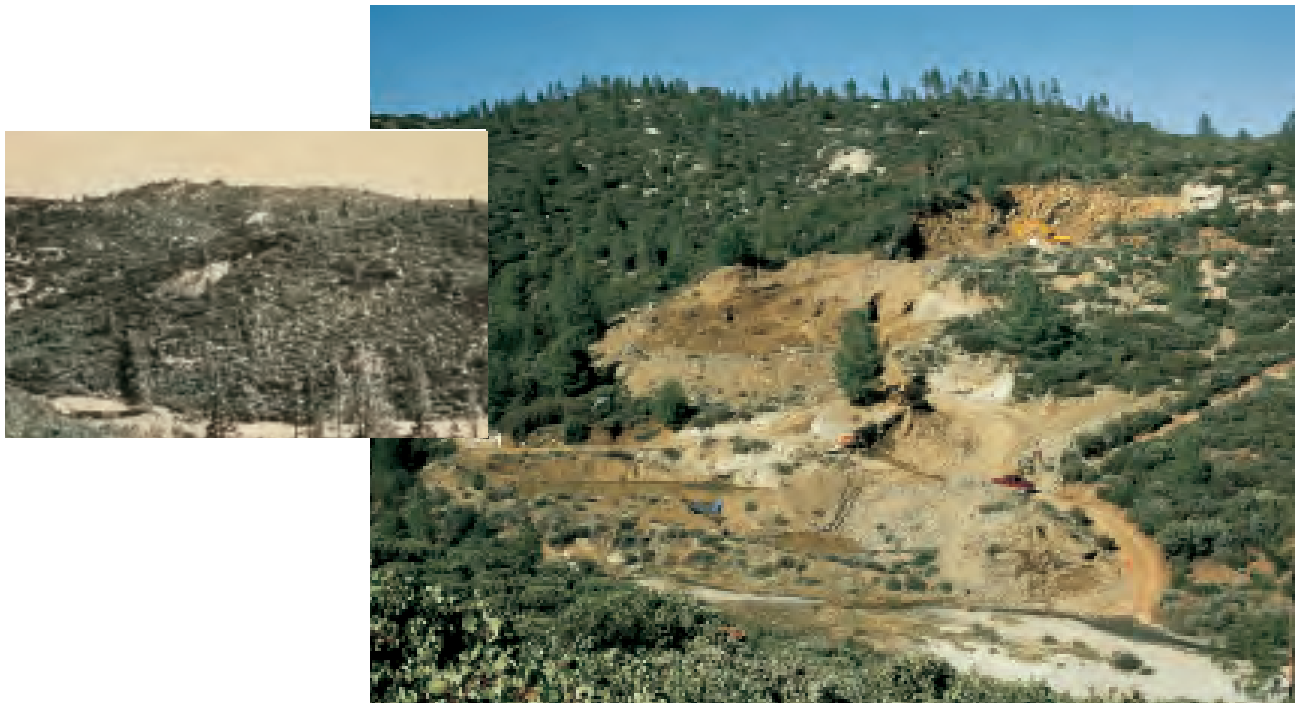
Figure 6. In this 1997 photo (by Michael Gray) of the Benitoite Gem mine, a backhoe sits in the main open cut, and the equipment processing colluvial material can be seen in the center, just below the single pine tree. Two settling ponds are visible below this equipment. Water is pumped from the San Benito River at the base of the workings into the ponds, from where it is recirculated through the processing equipment. The inset (after Louderback, 1909) shows a view of this same area in 1907, shortly after the discovery of the deposit.

Figure 7. This simplified geologic map (top) and cross-section (bottom) of the Benitoite Gem mine show the altered blueschist where benitoite is found, in lenses that are tectonically incorporated into the sheared greenstone. After Coleman (1957), Rohtert (1994), and Laurs (1995).
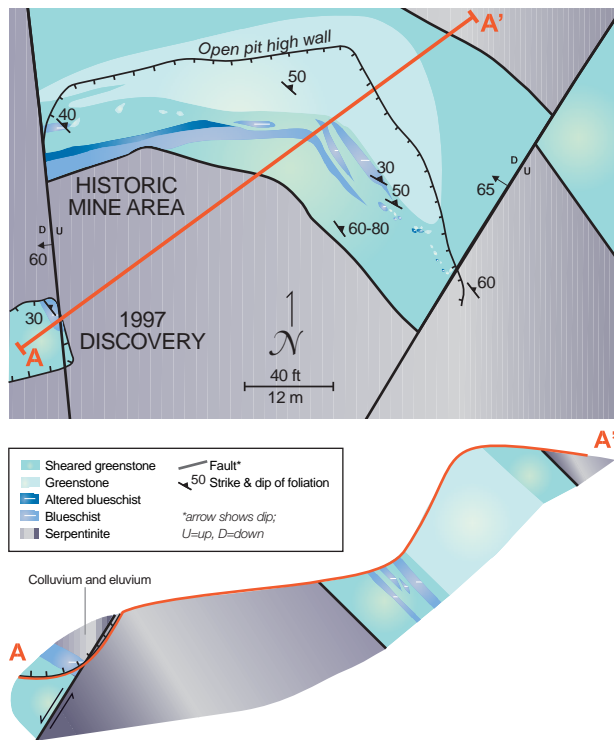
altered zone, which is characterized by: (1) recrystallization of fibrous amphibole and pyroxene, (2) local albite dissolution, and (3) veining and pervasive infiltration by natrolite. Benitoite formed during the first two stages of the alteration (inasmuch as many crystals contain amphibole and pyroxene inclusions), but prior to the formation of natrolite—which coats benitoite in the veins (figure 8). The natrolite veins average less than 1 cm wide, and contain benitoite only locally, commonly where the veins narrow or terminate.

The benitoite forms as euhedral crystals (figure 9) up to 5.6 cm in diameter, 1–1.5 cm on average, that are attached to the vein walls. Other minerals on the blueschist vein walls include neptunite, silica pseudomorphs after serandite, joaquinite group minerals, apatite, albite, jonesite, and the copper sulfides djurleite, digenite, and covellite (Wise and Gill, 1977), as well as traces of other minerals described by Van Baalen (1995) and Wise (1982). Natrolite coats all of the vein minerals and, in most cases, completely fills in and closes the veins. Natrolite also has infiltrated the altered blueschist adjacent to the veins, filling interstitial space that was previously occupied by albite.

Two types of benitoite were noted by Wise and Gill (1977): (1) gem-quality crystals attached to the walls of cross-cutting veins; and (2) disseminated, euhedral, non-gem benitoite with abundant amphi-

bole and pyroxene inclusions that formed within the altered blueschist. Some crystals show both characteristics, since they apparently grew into both the vein and the adjacent host-rock substrate. Benitoite in the veins commonly forms simple triangular crystals with dominant π $\{01\bar{1}1\}$ faces (Wise and Gill, 1977; figure 10). The crystals typically show a frosty appearance on the π faces due to natural etching, whereas the μ faces are mirror smooth. Color zoning is common, with a milky white or colorless core grading outward into transparent blue corners. However, gem-quality blue crystals recently discovered in the western offset portion of the deposit typically lack color zoning and show only π faces (A in figure 10). In general, the relatively small size of faceted material is due to the abundant cloudy areas and the flattened morphology of the crystals.

The disseminated non-gem benitoites closely resemble the host rock in color, because of the abundant fibrous inclusions from the altered blueschist. As described by Wise and Gill (1977), such crystals commonly show dominant c faces, as well as variably developed pyramid (π and p) and prism (μ and m) faces, resulting in tabular crystals with triangular to hexagonal outlines (D and E in figure 10). Rarely, the non-gem crystals form star-shaped twins caused by penetration twinning due to a Dauphiné-type 180° rotation about the c-axis (W. S. Wise, pers. comm., 1997; figure 11). The mine owners know of
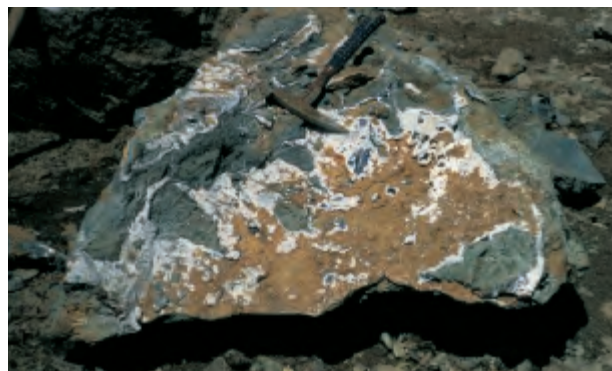

Figure 9. This specimen, which was mined during the late 1980s, shows an unusually transparent benitoite crystal on a matrix of white natrolite and light green altered blueschist. The natrolite originally covered the benitoite crystals as well, but it was removed with dilute hydrochloric acid. Photo © Harold & Erica Van Pelt.

only nine twinned crystals recovered thus far (E. Gray, pers. comm., 1997).

Junnila Claim. The Junnila claim is located 7 km northwest of the Benitoite Gem mine, on a low hill overlooking a tributary of Clear Creek (again, see

Figure 8. On May 1, 1997, this remarkable boulder of benitoite-bearing blueschist was excavated from the newly discovered extension of the Benitoite Gem mine. Knobs on the surface of the natrolite (which covers 40 cm × 70 cm of the boulder) indicate the presence of benitoite and neptunite crystals, which are attached to the vein wall and overgrown by natrolite. Several gem-quality pieces were removed from the outside edge of the vein. Photo by Michael Gray.

Figure 10. The common crystal habits of benitoite are redrawn from Louderback (1909) and Wise and Gill (1977). The π face decreases in importance in the sequence from (A) to (E). The morphology of the gem-quality crystals generally resembles (C), except for crystals from the recently discovered western extension of the deposit, which resemble (A). Non-gem crystals typically resemble (D).
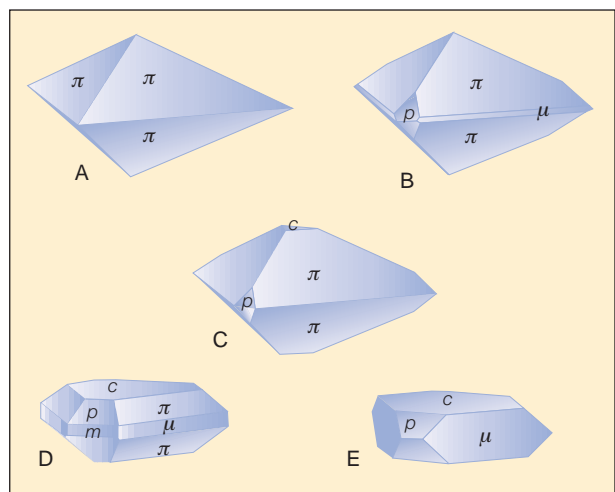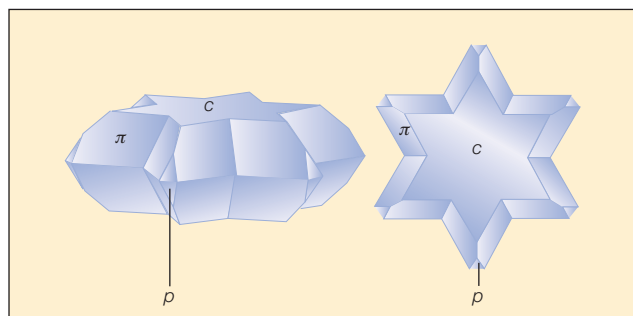
Figure 11. Twinned benitoite crystals show a 180° rotation about the c-axis. In this drawing (courtesy of William S. Wise), the c faces of the two crystals are merged and indistinguishable from one another, resulting in flat, star-shaped faces. The photo shows some of the twinned benitoite crystals (2–3 cm wide) recovered from the Benitoite Gem mine. Note the characteristic opaque appearance, resulting from abundant inclusions of fibrous amphibole and pyroxene. Photo © Harold & Erica Van Pelt.

figure 4). The claim was worked intermittently by A. L. McGuinness and Charles Trantham from 1982 to 1986. The deposit lay forgotten after the death of Mr. McGuinness in the late 1980s, but was rediscovered in 1995 by the Kennecott Exploration Company and almost simultaneously by L. Junnila of Fresno, California. At the time of rediscovery, thick brush covered the area and only a small benitoite-containing prospect pit was found (Laurs, 1995). In fall 1995, the property was excavated using a D-8 tractor (figure 12) in a cooperative effort by Junnila and several mineral dealers (Moller, 1996; Ream, 1996). Although only small amounts of benitoite were found, a few crystals (figure 13), up to 2.6 cm in diameter (Ream, 1996), reportedly contained material suitable for faceting; it is from this material that the two stones (0.42 ct and 0.21 ct) shown in figure 14 were cut.

As at the Benitoite Gem mine, benitoite at the Junilla claim is found in a body of blueschist within the serpentinite. The blueschist crops out over an area approximately 50 m by 20 m; it is brownish gray and weathered into platy fragments (Laurs, 1995). Near the center of the body is a zone of altered blueschist that contains benitoite. This vertical zone is resistant to weathering, massive in texture, and has a distinctive light grayish blue color; it strikes northeast and ranges from 1 to 2 m thick over a length of 6 m. Sparse amounts of benitoite form along vertical tension gashes (commonly less than 1 cm wide), and also along foliation and cross-fractures. In contrast to the natrolite gangue present at the Benitoite Gem mine, the benitoite-bearing veins at the Junnila claim are filled with a calcium-rich mineral assemblage consisting mostly of thomsonite, pectolite, calcite, and stevensite; neptunite and joaquinite-group minerals are present locally (Laurs, 1995).

The benitoite crystals are translucent (rarely transparent), tabular (see, e.g., figure 10D), and average 1 cm in their longest dimension. The crystals are intergrown with other vein minerals, and therefore they rarely show more than two or three faces. Blue, colorless, or color-zoned crystals (typically with colorless cores and blue rims, as at the Benitoite Gem mine) have been found.

Mina Numero Uno Claim. Located along upper Clear Creek, 7.8 km northwest of the Benitoite Gem mine, the Mina Numero Uno claim consists of boulders and rare outcrops of blueschist scattered through dense brush over an area approximately 20 m by 100 m, elongate to the east-northeast. Benitoite mineralization was noted in boulders at opposite ends of the deposit (Laurs 1995). The boulders at the eastern end contain rare vugs, up to 6 cm long and 3 cm wide, that are elongated parallel to foliation. The vugs are commonly lined with albite and silvery gray fibrous amphibole; in places, they contain benitoite, neptunite, or joaquinite-group minerals (Wise, 1982; Laurs, 1995). Benitoite forms pale blue, platy, euhedral crystals that are up to 5 mm in diameter. Less common are tan grains, previously reported as "pink" by Chromy (1969).

In the boulders at the western end, benitoite and neptunite form along narrow, randomly oriented fractures less than 1 mm wide (Laurs, 1995). These fractures typically contain no gangue minerals except for minor amounts of quartz locally (there is no albite). Benitoite forms pale blue or colorless, tabular, pseudo-hexagonal plates and rosettes up to 10 mm in diameter, with most crystals averaging 2 mm in diameter. The crystals occur with neptunite and lay flat against the fracture walls.

Figure 12. The Junnila claim was excavated with heavy equipment in 1995. Benitoite was recovered from the narrow, vertical zone of resistant blueschist that is visible here beneath the slender pine tree. Photo by William Larson.

Figure 13. This is one of the largest benitoite crystals (2.2 cm wide) recovered from the Junnila claim during the 1995 excavation. The benitoite is intergrown with thomsonite and actinolite. The irregular surface texture is due to intergrowth with calcite, which was removed from the specimen by acid dissolution. Specimen courtesy of William Larson; photo © Jeffrey Scovil.

Victor Claim. The Victor claim is located along a tributary 1 km south of Clear Creek, and 9.2 km northwest of the Benitoite Gem mine. According to documentation at an old claim marker on the property, the Victor claim was first staked in 1974 as the Franciscan mine by Steven M. Dwyer of Palm Desert, California. During the early 1980s, the claim was owned by Ed Oyler of the San Francisco Bay area; in 1991, the deposit was acquired by Craig Stolberg of San Jose, California. Outcrops of blueschist up to 3 m in diameter are surrounded by a sheared tremolite-chlorite zone within the serpentinite (Laurs, 1995). Millage (1981) inferred that the blueschist body measures 150 m × 100 m. The central blueschist outcrops contain small (up to 5 mm in diameter) colorless benitoite platelets and rosettes, in thin veinlets along the foliation.

Santa Rita Peak Property. This occurrence is located 1.2 km north-northeast of the Benitoite Gem mine, on the southeast flank of Santa Rita Peak (elevation 5,165 feet, 1,574 m). The blueschist is exposed as a field of boulders, at least 30 m wide, that is surrounded by a sheared tremolite-chlorite-jadeite zone within the serpentinite (Laurs, 1995). Some of the boulders are hydrothermally altered and cut by natrolite veins up to 2 cm thick. In places, the altered blueschist shows a nodular texture similar

Figure 14. These two benitoites (0.42 and 0.21 ct) were reportedly faceted from material found at the Junnila claim. Stones courtesty of William Larson; photo © GIA and Tino Hammid.

Figure 15. With 52 faceted benitoites weighing a total of about 33 ct (the largest stone is 2.84 ct), this benitoite and diamond necklace is unique in the world. All of the benitoites were cut and matched by E. (Buzz) Gray, and the necklace was designed by William McDonald of McDonald's Jewelry, Fresno, California. Necklace courtesy of Michael M. Scott; photo © Harold & Erica Van Pelt.

to that observed at the Benitoite Gem mine; electron microprobe analysis revealed microscopic crystals of benitoite in this altered blueschist (R. L. Barnett, pers. comm., in Laurs, 1995).

ORIGIN OF BENITOITE

Ever since benitoite's discovery, its origin has been a persistent enigma. The formation of benitoite at the New Idria district has been generally ascribed to hydrothermal processes that caused the unusual combination of barium (Ba) and titanium (Ti). Coleman (1957) suggested that Ti was derived from fluids associated with the crystallization of small syenite intrusions in the district; Ba was liberated from the alteration of blueschist. However, Ti is relatively immobile in hydrothermal fluids (Van Baalen, 1993), and the closest syenite to any of the

benitoite deposits in the district is 1 km. Wise and Gill (1977) proposed that fluids derived Ti, Fe, and rare-earth elements from the serpentine, and Ba from the blueschist, to form benitoite and the associated vein minerals. Most recently, Van Baalen (1995) proposed that benitoite formed as a result of metamorphism localized along the contact between blueschist and greenstone, in the presence of sodium-rich, low-silica metamorphic fluids. He suggested that more than enough Ba and Ti were present in the blueschist and greenstone to produce the inferred amount of benitoite and neptunite.

We generally concur with Van Baalen's (1995) model, subject to some modification. Van Baalen (1995) stated that benitoite formed along the contact between blueschist and greenstone at the Benitoite Gem mine; it is actually contained entirely within the blueschist, regardless of proximity to the greenstone. Greenstone is not required for benitoite formation, as indicated by its absence at the Junnila and Mina Numero Uno claims, although it is possible that it contributed to Benitoite formation at the Benitoite Gem mine. Throughout the New Idria district, there is also a strong correlation between the amounts of blueschist alteration and benitoite mineralization. We suggest that benitoite formed at the Benitoite Gem mine when Ba and Ti were released by the alteration of blueschist, and possibly greenstone, in the presence of magnesium- and calcium-rich fluids generated during the regional metamorphism of serpentinite (rather than in the presence of sodium-rich fluids, as postulated by Van Baalen [1995]). This model is based on detailed geologic mapping and the collection of chemical data on blueschist minerals and whole-rock samples at all the known benitoite occurrences in the district (Laurs, 1995).

MODERN MINING

The present owners of the Benitoite Gem mine, Forrest and Gray, initially worked the open pit for mineral specimens, including neptunite and jonesite. One boulder produced a small quantity of pink benitoite, which yielded gems of one-quarter carat to just over one carat, but overall the amount of gem material recovered from the lode was not substantial. In 1970, Forrest and Gray began washing the mine-dump material by pumping water uphill through a fire hose. Then (as now) they worked only during the spring months, to take advantage of the favorable weather as well as the water available from the headwaters of the San Benito River, which

runs through the property. After washing the dump materials, they picked out mineralized blueschist and loose pieces of benitoite by hand (Gray, 1986). Using this very simple method during the early 1970s, they recovered significant quantities of faceting rough that produced some fine stones. Among these was the flawless 6.53 ct pear-shaped brilliant that was the center stone of the pendant to the famous benitoite and diamond necklace that was stolen in Europe in 1974. The necklace (figure 15) was recovered in 1975, but the pendant was never found.

After working through most of the mine dump, the two owners processed the underlying colluvium and eluvium using the same mining methods. The natrolite coating protected many of the benitoite and neptunite crystals during weathering and transport, so many fine mineral specimens were recovered. The gem rough recovered during this mining operation was generally of high quality, since the crystals that weathered out of the veins had typically broken along existing fractures to isolate the gemmy tips and nodules.

Since 1982, the owners have used a more systematic and mechanized recovery method (Gray, 1992). A front-end loader feeds dirt and rock through a grizzly, to separate out boulders, into a hopper (figure 16), where water is used to wash the material down a chute to a layered screening apparatus fitted with high-pressure water jets (figure 17). Material larger than 25 mm (1 inch) moves over the top screen, where it is again cleaned by water jets and checked for specimen potential. Material smaller than 25 mm falls onto a lower screen with a 3

Figure 16. The mine owners at the Benitoite Gem mine process colluvial and alluvial material using mechanized equipment. Here a loader dumps material through a grizzly and into a hopper. Rocks larger than 15 cm roll off the grizzly and are examined individually; stones smaller than 15 cm are washed down a chute to the apparatus pictured in figure 17. Photo by Brendan M. Laurs.

mm (1/8 inch) mesh. Pieces smaller than 3 mm are discharged into settling ponds, and material between 3 and 25 mm is washed into a gravitational separation jig, where the heavier benitoite is trapped in several parallel trays. Rough gem benitoite (figure 18) is removed from the trays by hand at the end of each work day. In the late 1980s, Forrest and Gray recovered a piece of rough from which the 10.47 ct gem pictured in figure 19 was cut. The largest,

Figure 17. At the Benitoite Gem mine, material is fed first into a layered screening apparatus fitted with high-pressure water jets, and then into a gravitational separation jig. Pieces over 25 mm are separated by the screening apparatus and checked for specimen potential, while material between 3 and 25 mm is washed into the jig where the heavier benitoite is trapped in several parallel trays. Photo by Brendan M. Laurs.
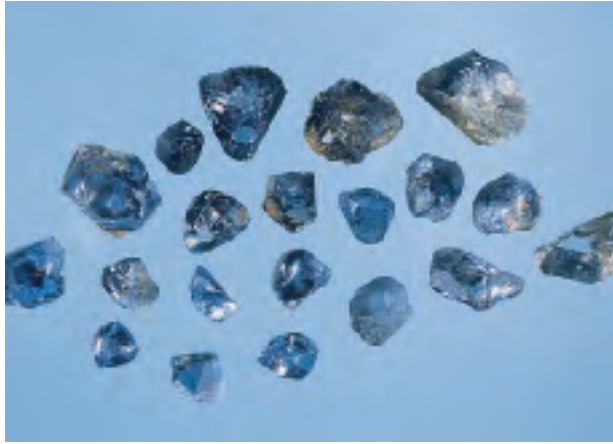
Figure 18. Rough benitoite gem nodules and crystal fragments, such as these, are removed from the gravitational separation jig by hand. The largest stone on the upper right is 1.0 cm wide. Photo by Maha DeMaggio.

finest rough found to date was recovered in the early 1990s; it was cut into a 15.42 ct gem (see cover of this issue).

By the end of the 1996 mining season, the colluvium and eluvium were largely exhausted. Using larger machinery, mine owners Forrest and Gray found a new productive area down slope of the open pit during spring 1997 (figure 20). Excavation during the 1997 season (March through May) revealed mineralized lode material that contained fine mineral specimens, as well as colluvium and eluvium with abundant gem rough. Mining of this new area will continue in 1998.

PRODUCTION

The Benitoite Gem mine is the only commercial source of gem-quality benitoite in the world. From the time of its discovery in 1907 until 1967, when Forrest and Gray began working the mine, it is estimated that about 2,500 carats of faceted benitoite were produced (E. Gray, pers. comm., 1997). Of that amount, nearly 1,000 carats were produced during the period of active mining between 1907 and 1911, based on the amount of rough reported in the Dallas Mining Company's account books. It was during that time that the gem rough that produced the 7.6 ct gem pictured in Louderback's 1909 report was recovered; this was subsequently recut to the 7.53 ct stone that is now in the Smithsonian Institution. Few other stones exceeded 3 ct, however, and most of the gems weighed less than 1 ct.

The balance of 1,500 carats believed to have been recovered between 1911 and 1967 was estimated from verbal information provided by previous miners (E. Gray, pers. comm., 1997). Most of these stones were faceted by cutters in the United States, and weights of up to 5 ct were obtained. Clarence Cole retrieved most of the rough during the interval from 1952 to 1962.

Since 1967, Forrest and Gray have produced approximately 2,000 carats of faceted benitoite. According to E. Gray (pers. comm., 1997), this inventory can be divided into six weight classes: (1) About 2,000 pieces were cut in commerical factories, and generally finished to less than 0.25 ct each; (2) another 1,500 pieces ranged between 0.25 and 1 ct; (3) some 500 stones weighed between 1 and 2 ct; (4) a total of 50 stones ranged between 2 and 3 ct; (5) only 25 stones weighed between 3 and 4 ct; and (6) the 15 largest stones exceeded 4 ct. Thus, 89% of the stones were under 1 ct; 9% were between 1 and 2 ct; and 2% were over 2 ct. All but the commercially cut stones were faceted by the families of the current owners or in their own facilities. Forrest and Gray have not marketed cuttable rough except, in a few cases, as mineral specimens.

Forrest and Gray also estimate that about 500 carats of finished goods have entered the market through informal channels and other sources, such as the cutting of older rough and the faceting of mineral specimens. Thus, a total of about 5,000 carats of faceted benitoites have been produced over the life of the mine. Because of this small produc-

Figure 19. This exceptional faceted benitoite weighs 10.47 ct. From the collection of Michael M. Scott; photo © Harold & Erica Van Pelt.

tion, benitoite is a collector's gem, one of the rarest in the world.

PHYSICAL AND CHEMICAL PROPERTIES

Materials and Methods. We examined a total of 139 benitoite samples, of which 83 were faceted stones and four were cabochons. With the exception of two faceted stones reportedly from the Junnila claim, all of the benitoites examined were from the Benitoite Gem mine. The rough stones (52) were all of gem quality, and were provided by Forrest and Gray from their gravity-separation apparatus. The fashioned samples were selected for their various internal features; consequently, they were not as clean as benitoites typically seen in the marketplace.

The faceted stones in our study ranged from 0.10 to 1.46 ct (see, e.g., figure 21), and the cabochons ranged from 1.06 to 5.31 ct. All of the sam-

Figure 21. These faceted benitoites from the Benitoite Gem mine, which show a range of tone and saturation, were among the samples studied for this investigation. Clockwise from the top, the stones weigh 0.95 ct, 0.87 ct, 0.49 ct, and 0.54 ct. Photo by Maha DeMaggio.

Figure 20. The backhoe is excavating the newly discovered western extension of the deposit at the Benitoite Gem mine. Boulders of altered blueschist, some bearing benitoite, are piled near the left rim of the pit. The high wall of the main pit can be seen on the skyline. Photo by Brendan M. Laurs.

ples—both rough and fashioned—were examined with magnification to locate and describe inclusions and color zoning. Refractive index measurements were made on the 21 faceted stones that were larger than 0.20 ct. Specific gravity, fluorescence, and visible absorption spectra were also determined for these faceted stones, as well as for the four cabochons.

Refractive indices and birefringence were measured on a GIA GEM Instruments Duplex II refractometer, using a 1.815 contact liquid and a monochromatic sodium-equivalent light source. Because the upper R.I. of benitoite (1.804) is close to the upper limit of the Duplex II (1.810), we also measured the four benitoites pictured in figure 21 with a specially designed refractometer fitted with a cubic zirconia hemicylinder. Specific gravity was measured by the hydrostatic method (three measurements per sample) with a Mettler CM1200 digital balance. All of the samples were examined with a standard gemological microscope, a Leica Stereozoom with 10× to 60× magnification; the rough specimens were immersed in methylene iodide. Absorption spectra were observed with a Beck spectroscope on a GIA GEM Instruments base.
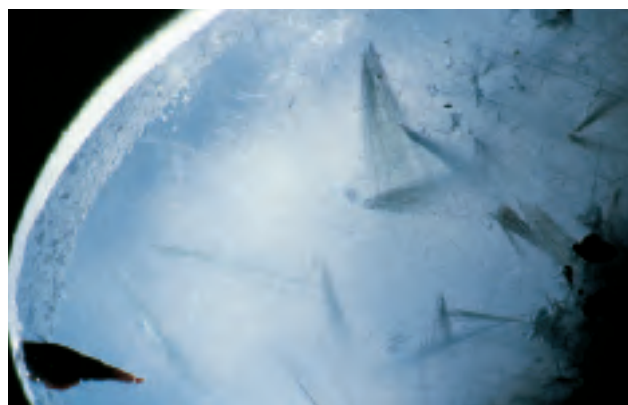
Electron microprobe analyses of some of the mineral inclusions in benitoite were performed at the University of Manitoba in Winnipeg, Canada, on two gem-quality pieces of rough that contained inclusions visible with 10× magnification.

Figure 22. Weighing from 0.30 to 1.70 ct, these benitoites show a range in size, color, and faceting style that is representative of commercially available benitoite. Courtesy of Edward Swoboda; photo © Harold & Erica Van Pelt.

Dark colors were seen in melee (less than 0.20 ct), as well as in larger stones. Most of the gems were medium to medium-dark in tone, with strong saturation, a color range sometimes referred to as "cornflower" blue. A green tinge was evident in some of the paler cabochons due to inclusions of fibrous green amphibole or pyroxene (discussed below). Strong dichroism (figure 23), from colorless to blue or violetish blue, was evident when the stones were viewed through a dichroscope in any direction. To the unaided eye, pleochroism was visible as light and dark tones that mingled with the brilliance and dispersion. The dispersion is masked somewhat by the blue body color. Color zoning was common.

As described previously, colorless and pink faceted stones are extremely rare; consequently, they were not included in this portion of the study. Heat treatment of lighter colored material may result in an orange hue similar to that associated with Imperial topaz (see, e.g., figure 24); the dichroic colors of this material are pink and orange. The orange color has not been observed in untreated benitoite. Heat treatment has been successful for only a small portion of the material treated, and some of the crystals have exploded in the furnace because of differential expansion of inclusions. The heat-treatment procedure is proprietary, and experiments were not performed as part of this study.

Physical Properties. The standard gemological properties of benitoite are shown in table 1 and discussed below.

Refractive Indices. Most of the stones showed $n_\omega =$ 1.757 to 1.759, and $n_\varepsilon =$ 1.802 to 1.804. The accura-

Visual Appearance. The samples ranged from blue to violetish blue in color, and from very light to medium dark in tone. This color range is representative of the stones commonly marketed (figure 22).

Figure 23. This benitoite cabochon (5.31 ct) displays strong dichroism and contains fibrous inclusions of amphibole and/or pyroxene. The dark reddish brown inclusion on the lower left is neptunite. Darkfield illumination; photomicrograph by John I. Koivula.

Figure 24. Shown here, clockwise from the top left, are some of the more unusual benitoites that have been found at the Benitoite Gem mine: a 0.79 ct light blue round brilliant, with unusually large two-phase inclusions; a 1.29 ct pinkish blue round brilliant; a 1.07 ct nearly colorless lozenge-shaped mixed cut, with a slight blue tint; a 0.34 ct dark purplish pink round brilliant; a 0.53 ct heat-treated pinkish orange oval mixed cut; a 0.61 ct heat-treated particolored (pinkish orange and blue) rectangular modified emerald cut; and a 0.91 ct heat-treated particolored shield shape mixed cut. The particolored stones resulted from heat treatment of material that was originally colorless and blue. All stones were faceted by Elvis (Buzz) and Michael Gray. From the collection of Michael M. Scott; photo © Harold & Erica Van Pelt.

cy of the upper measurements was compromised by their proximity to the upper limit of the refractometer. Nevertheless, these measurements compare favorably to the published values of n_ω = 1.757 and n_ε = 1.804 (Webster, 1994). In addition, the four stones tested with the cubic zirconia refractometer showed n_ε = 1.804 to 1.805. The measured birefringence ranged from 0.043 to 0.047, which compares favorably to the published value of 0.047 (Webster, 1994). Because of the high birefringence, doubling of pavilion facet junctions is easily seen through the table with 10× magnification.

Specific Gravity. The measured values for the faceted stones ranged from 3.65 to 3.80. In most of the stones larger than 0.40 ct, the S.G. values were near 3.70. This differs somewhat from the published *measured* value of 3.65, but it is close to the published *calculated* value of 3.68 (Anthony et al., 1995). The largest scatter in measured values was noted for the smaller stones, which is due to measurement error. The S.G. of the cabochons ranged from 3.31 to 3.69; the lighter measurements were obtained for stones containing abundant fibrous inclusions (described below).

Ultraviolet Fluorescence. Similar to the descriptions by Wise and Gill (1977) and Mitchell (1980), the sample blue benitoites fluoresced strong blue to short-wave UV radiation, and appeared inert to long-wave UV; the colorless benitoite fluoresced slightly stronger blue to short-wave, and showed dull red fluorescence to long-wave. Some light-colored samples examined in this study also fluoresced dull red to long-wave UV. Moderate chalkiness is characteristic of the fluorescence to both short- and long-wave UV. Because of benitoite's conspicuous fluorescence, miners have recovered some crystals by scanning the ground surface at night with a portable UV lamp.

Internal Features. *Inclusions.* Microcrystals, "fingerprints," and fractures are commonly seen in benitoite. Many of the 83 faceted stones examined for this study contained white needles as disseminations and intergrown clusters (figure 25). We did not note any preferred orientation of the needles. The needles are probably actinolite-tremolite, as suggested by petrography and by electron microprobe analyses of similar crystals in the host rock (Laurs, 1995). Because the needles are so small (typically less than 0.5 mm long), they are rarely visible with the unaided eye unless they are abundant. With 10× magnification, they resemble lint particles in appearance and texture. Also present in heavily included samples were dark blue and green needles that formed elongate tufts on the order of several millimeters long (again, see figure 23). Electron microprobe analyses of benitoite inclusions showed the presence of aegerine-augite and diopside, which

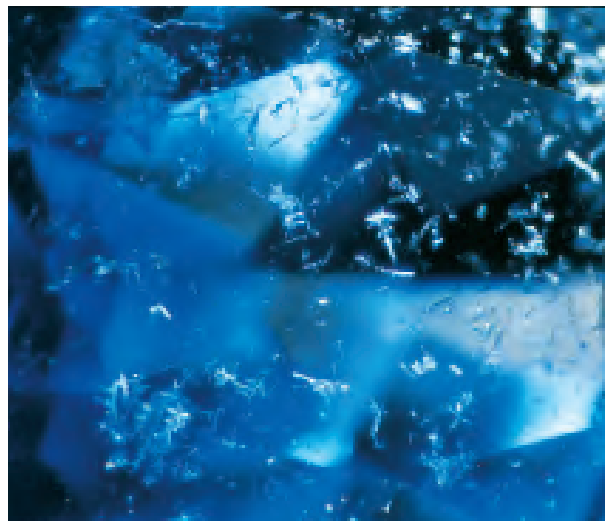|	
Composition	$BaTiSi_3O_9$
Color	Colorless, and blue to violetish blue (commonly zoned); rarely pink. Heat treatment may (rarely) cause colorless → orange hue. Light to medium dark in tone, typically strong in saturation.
Pleochroism	Strongly dichroic; colorless (ω) and blue to violetish blue (ε)
Clarity	Translucent to transparent
Refractive indices	$n_\omega = 1.757$, $n_\varepsilon = 1.804$[b] $n_\omega = 1.757–1.759$*, $n_\varepsilon = 1.802–1.805$*
Birefringence	0.047[b]; 0.043–0.047*
Optic character	Uniaxial positive
Specific gravity	3.65 (measured); 3.68 (calculated)[c] 3.65–3.80 (measured, this study)
Dispersion	$\varepsilon = 0.039$, $\omega = 0.046$[d] (diamond is 0.044)
Hardness	6–6.5[c]
Polish luster	Vitreous to sub-adamantine[e]
Fracture luster	Vitreous on conchoidal to uneven surfaces[e]
Cleavage	None
Toughness	Fair; brittle
UV Fluorescence	
Short-wave (254 nm)	All stones—moderately chalky, strong blue
Long-wave (365 nm)	Blue stones—inert Pale blue to colorless stones— moderately chalky, dull red
Cathodo- luminescence	Intense blue[f]
Morphology	Hexagonal system; crystals are tri- angular, flattened on the c-axis, and pyramidal or tabular
Inclusions	Minerals (actinolite-tremolite, aegirine-augite, diopside, serandite pseudomorphs[g], neptunite[g], joaquinite[g], albite[g], apatite[g], djurleite[g]), "fingerprints,"[h] fractures, two-phase[h]
Typical size range	Cut stones, 10 points to 1 ct; rough crystals, 1 cm in diameter
Largest cut stone	15.42 ct
Stability[e]	Sensitive to rapid temperature changes and ultrasonic vibration. Insoluble in hydrochloric and sulfuric acids. Easily attacked by hydrofluoric acid.
May be confused with	Sapphire, tanzanite (depending on orientation), blue diamond, iolite, blue tourmaline, blue spinel, sap- phirine, blue zircon

Figure 25. Lint-like needles of amphibole (probably actinolite-tremolite) are the most frequently encountered mineral inclusions in benitoite. Dark-field illumination, magnified 20×; photomicrograph by John I. Koivula.

are seldom seen in faceted stones (see the center right photomicrograph in Gübelin and Koivula, 1986, p. 416; these crystals were apparently mis-identified as neptunite). Other inclusions seen only rarely were anhedral to euhedral dark reddish brown neptunite and euhedral honey-colored joaquinite-group minerals (specific species not determined). Albite, apatite, and metallic greenish gray djurleite crystals have been reported as inclusions in benitoite (Wise and Gill, 1977), but they were not observed in this study. Two-phase (liquid and gas) inclusions (figure 26) were noted in only two sam-ples, along healed fractures. The "fingerprints" are commonly planar, but they appeared curved in sev-eral stones. Unhealed fractures typically showed step-like conchoidal break patterns.

Color and Growth Zoning. Color zoning was most apparent in emerald-cut stones, which commonly displayed a gradation from blue to colorless when viewed face-up with the unaided eye. When the stones were viewed from different angles at 10× magnification, sharp planar boundaries between the blue and colorless areas were eye-visible in one or more directions. These boundaries are situated near the core of the rough crystals.

Growth zoning was seen at 10× magnification in some stones as multiple bands that showed vari-able tones and spacing (figure 27). Such growth zon-

are both pyroxenes (F. Hawthorne, pers. comm., 1997).

Silica pseudomorphs after serandite form pris-matic euhedral inclusions in benitoite, but these

Figure 26. Two-phase inclusions are not commonly seen in benitoite. The larger inclusions in the healed fracture of this 0.95 ct stone contain vapor bubbles of variable shape and size. Darkfield illumination, magnified 25×; photomicrograph by John I. Koivula.
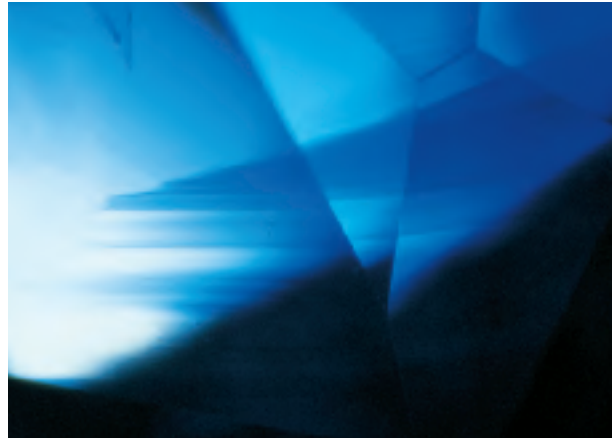

Figure 27. Planar color zoning is commonly visible at some angles within benitoite. The color zones appear curved in this 0.81 ct stone, because of refraction through adjacent facets. Shadow-like internal graining bounds and truncates the color zones, and is visible as the stone is tilted from side to side. Darkfield illumination, magnified 15×; photomicrograph by John I. Koivula.

ing is much less regular or apparent than that typically seen in corundum. Less commonly than planar growth zoning, our samples showed irregular, patchy, diffuse areas of color.

A distinctive characteristic of benitoite, noted in more than half the samples examined for this study, were sharp planar features that closely resemble the internal graining seen in some diamonds. This "graining" appeared as shadow-like planes that, at 10× magnification, were commonly seen along the boundaries of color zones. It also truncated color zones at oblique angles (again, see figure 27). The graining was almost always uniform and straight, but in some stones it was step-like or jagged. No surface graining or other polishing irregularities were noted where the internal graining reached the surface of the stone.

Chemistry and Spectroscopy. A tabulation of previous data and recently acquired compositions of benitoite is shown in table 2. No new analyses were obtained for this study, because routine electron microprobe analyses have shown a constant composition, and the data reported by Laird and Albee (1972) are considered very reliable (G. Rossman, pers. comm., 1997). The measured amounts of Ba, Ti, and Si are remarkably constant, regardless of color or locality, and fall near the ideal values that are calculated from the chemical formula. The greatest chemical variation in benitoite was reported by Gross et al. (1965) for samples from the Big Creek–Rush Creek area in Fresno County, California, which contained up to 4.1% tin oxide. A zirconium-bearing blue benitoite from Japan was found to contain 1.77 wt.% ZrO_2; and up to 1.51 wt.% ZrO_2 was measured in a colorless benitoite from Arkansas (H. Barwood, pers. comm., 1997). It is not surprising that Sn and Zr show the greatest variations, since these elements form barium silicate minerals analogous to benitoite that are called pabstite and bazirite, respectively (Hawthorne, 1987). Other elements show minor variations, most notably Nb, Na, Ca, K, and Fe.

Numerous investigators have attempted to link the chemical composition of benitoite to its coloration. Louderback (1907) initially attributed the blue color to traces of reduced Ti, but in 1909 he reported that no reduced Ti could be measured. Coleman (1957) suggested that trace impurities of V, Nb, and Cu might cause the blue coloration. Laird and Albee (1972) noted slightly higher concentrations of Fe in blue than in colorless benitoite. Burns et al. (1967) suggested that the coloration is caused by crystal defects due to an oxygen deficiency. Burns (1970) suggested that the pleochroism of benitoite and other minerals might be caused by $Fe^{2+} \rightarrow Fe^{3+}$ charge transfer. Millage (1981) also proposed metal-metal charge transfer, such as

TABLE 2. Chemical compositions of benitoite from California, Arkansas, and Japan.[a]

Oxide (wt.%)	Benitoite Gem mine[b] California Colorless (6)	Benitoite Gem mine[b] California Blue (6)	Victor[c] California Colorless (1)	Diamond Jo[d] Arkansas Colorless (3)	Diamond Jo[d] Arkansas Blue (6)	Diamond Jo[d] Arkansas Pink (3)	Ohmi[e] Japan Colorless (1)	Ohmi[e] Japan Blue (1)	Ohmi[e] Japan Blue (1)
SiO_2	42.62	43.10	43.66	43.52	43.55	43.49	43.55	43.16	41.05
TiO_2	19.44	19.51	19.29	17.90	18.47	18.99	19.30	19.11	19.82
ZrO_2	0.108*	0.016*	nd	1.16	0.33	0.08	nd	nd	1.77
Al_2O_3	0.04*	0.20*	0.30	0.29	0.22	0.21	0.18	0.10	nd
FeO	0.01*	0.05*	0.01	0.15	0.04	0.01	0.081†	0.033†	nd
MnO	nd	nd	0.03	0.03	0.04	0.03	0.05	0.11	nd
MgO	trace*	trace*	nd	nd	nd	nd	0.12	0.14	0.16
CaO	0.006*	0.10*	0.11	nd	nd	nd	0.28	0.24	0.12
BaO	37.27	37.23	36.48	36.70	36.21	36.36	34.82	36.04	36.78
SrO	0.003*	0.004*	nd	nd	nd	nd	nd	nd	nd
Na_2O	0.14	0.13	0.20	0.23	0.22	0.18	0.84	0.75	0.27
K_2O	nd	nd	nd	0.01	0.20	0.13	0.44	0.21	nd
Nb_2O_5	0.20*	<0.10*	nd	bdl	0.74	0.34	nd	nd	nd
V_2O_5	0.002*	0.003*	nd	nd	nd	nd	nd	nd	nd
S	nd	nd	nd	nd	nd	nd	0.06	0.02	—
Cl	nd	nd	nd	nd	nd	nd	0.28	0.10	—
Total	99.84	100.34	100.08	99.99	100.02	99.82	100.00	100.01	99.97

[a]*Comments: Ideal formula concentrations (wt.%): SiO_2 43.59, TiO_2 19.32, BaO 37.09 (Laird and Albee, 1972). Values determined by electron micro-probe, except: * – emission spectroscopy, and † – atomic absorption. Total iron is reported as FeO. Number of samples in parentheses. Looked for by Laird and Albee (1972), but not detected: Ag, As, Au, B, Be, Bi, Cd, Co, Cr, Cu, Ga, La, Mo, Mn, Nd, Ni, Pb, Pt, Sb, Sc, Sn, Ta, Th, Tl, W, Y, Yb, and Zn. The abbreviation "nd" = not determined; "bdl" = below detection limit.*
[b]*Laird and Albee (1972).*   [c]*Millage (1981).*   [d]*H. Barwood, pers. comm. (1997).*
[e]*Sakai and Akai (1994).*

$Fe^{2+} \rightarrow Ti^{4+}$ or $Fe^{2+} \rightarrow Fe^{3+}$, as a coloring agent, but then negated this possibility because these atoms are separated too far from one another in the benitoite lattice. Instead, Millage attributed the blue coloration to traces of Zr in the Ti site. The compositions of colorless and blue benitoite from Arkansas and the Benitoite Gem mine contradict this, however, since more Zr is present in the colorless samples than in the blue material (again, see table 2).

In this study, no spectral characteristics could be resolved in any of the samples tested, regardless of color, with a desk-model type of spectroscope. Spectral data have been collected by means of a spectrophotometer for blue, pink, and heat-treated orange benitoite (Burns et al., 1967; Rossman, 1997). Blue benitoite shows a broad peak at about 700 nm (figure 28), most of which appears in the near-infrared region. Infrared spectra have also been collected, but the data in this region are inconsistent and of little use (G. Rossman, pers. comm., 1997). In spite of much effort to interpret the spectral data, the cause of color in benitoite remains elusive.

Synthesis and Scientific Use. Synthetic benitoite has been successfully grown in the laboratory (Rase

and Roy, 1955a and b; Hinthorne, 1974; Christophe et al., 1980), but only in minute crystals that are colorless and too small to facet. Natural benitoite has an important industrial application in electron

Figure 28. The absorption spectra for blue benitoite from the Benitoite Gem mine, shown here in the range from UV to near-infrared at orientations parallel (red line) and perpendicular (blue line) to the c-axis, do not provide any clues to the cause of color in this material. Courtesy of George R. Rossman.
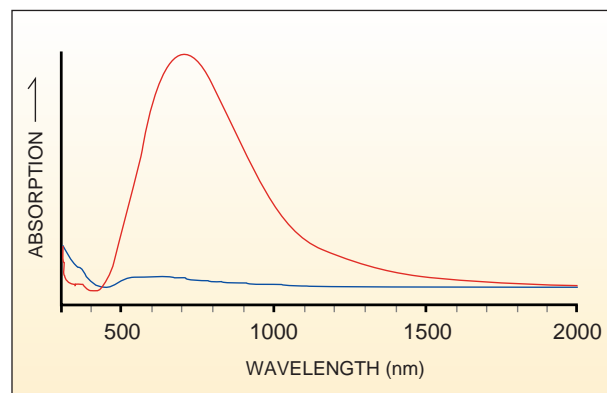
Figure 29. This 1.16 ct modified pear shape benitoite mimics the shape of the perfect 1-cm-wide rough crystal; both are from the Benitoite Gem mine. The specimen was recovered from the upper portion of the main pit by the present owners. It is one of only three found in which the benitoite apparently crystallized contemporaneously with albite crystals. From the collection of Michael M. Scott; photo © Harold & Erica Van Pelt.

microprobes: Because it fluoresces strongly to an electron beam, benitoite is used to align and adjust the beam size. Benitoite is also employed as an analytical standard for Ba and Ti, because of the constancy of its chemical composition. Webster (1994) suggested that benitoite could be used as a known standard for measuring dispersion in gemstones.

Identification. Benitoite may be distinguished from sapphire by its greater birefringence, strong dispersion, and its strong blue-and-colorless pleochroism. When set in a piece of jewelry, benitoite also will abrade more easily than sapphire. Natural and irradiated blue diamonds can also give the appearance of the lighter shades of benitoite because of similarities in color and dispersion, but the separation is easily made because diamond is singly refractive and has a much higher R.I. Benitoite can be distinguished from tanzanite on the basis of pleochroism, since benitoite lacks the purple trichroic component that is almost always apparent at some angle within tanzanite. In addition to the differences in gemological properties, sapphirine is too dark to be confused with benitoite, and zircon does not occur in the same hue. Iolite and blue tourmaline have much lower dispersion, refractive indices, and birefringence than benitoite. As described previously, benitoite also commonly has distinctive growth-zoning patterns and lint-like mineral inclusions.

CUTTING

Benitoite is one of the easiest gemstones to facet. There are no directional weaknesses (e.g., cleavage). At 6.0–6.5 on the Mohs scale, benitoite is about as hard as tanzanite and peridot, harder than sunstone and other feldspars, and softer than quartz and tourmaline. Benitoite can be oriented so that color zoning is rarely evident in the face-up direction (figure 29). Since the dichroic colors of blue benitoite are blue and colorless, there are no ancillary hues to mix through optical orientation. As a result, the alignment of the rough crystal for faceting requires only the placement of the desired color within the culet of the finished stone. In most cases, however, this is not important, since blue coloration is evident regardless of the direction in which the stone is oriented.

One of the authors (MG) has cut thousands of benitoites. Because of the typically small finished sizes, faceting can generally be accomplished using a single lap—in most cases, 1200 grit. Polishing is so rapid that the lapidary has to be careful not to enlarge a facet by overpolishing. The best grit is 0.04 micron aluminum oxide, generally known as Linde B, which is a hundred times finer than the more common Linde A. It works very well on a tin or tin/lead polishing lap. The fineness of the powder helps eliminate the polishing lines that are typically imparted to softer gemstones.

The critical angle of benitoite is 34.7°. Successful makes have crown angles that range from 30° to 40°, with optimum results obtained at 38°. The pavilion angle range is narrower, from 40° to 42° with the optimum at 41°. Benitoite is amenable to all styles and makes (see again, figure 22), but it tends to show maximum dispersion when finished as a round brilliant or a trilliant.

CONCLUSION

It is likely that future production of faceting-quality benitoite will come solely from the Benitoite Gem mine. The recent discovery of additional mineralized material down slope from the historic open pit is highly encouraging for the stability of price and future supply. Although rare, faceted stones and mineral specimens of benitoite are commercially available, and mining is ongoing. The formation of relatively large, locally abundant, gem-quality crystals at the Benitoite Gem mine resulted from a combination of unusual geologic processes. The distinctive gemological properties of benitoite make it readily identifiable from other gem materials.

REFERENCES

Alfors J.T., Stinson M.C., Mathews R.A., Pabst A. (1965) Seven new barium minerals from eastern Fresno County, California. *American Mineralogist*, Vol. 50, pp. 314–340.
Anten J. (1928) Sur la composition lithologiques des psammites du Condroz. *Société Géologique de Belgique, Annales*, Vol. 51, pp. B330–331.
Anthony J.W., Bideaux R.A., Bladh K.W., Nichols M.C. (1995) *Handbook of Mineralogy*, Vol. 2: Silica, Silicates; Part 1. Mineral Data Publishing, Tucson, AZ.
Arnold R. (1908) Notes on the occurrence of the recently described gem mineral, benitoite. *Science*, Vol. 27, No. 686, pp. 312–314.
Austin D.H. (1988) *The Benitoite Story*. Independently published, 80 pp.
Bancroft P. (1984) *Gem and Crystal Treasures*. Western Enterprises, Fallbrook, CA, pp. 94–95.
Barwood H. (1995) Benitoite and joaquinite in Arkansas. *Mineral News*, Vol. 11, No. 5, pp. 2, 5.
Bradley W.W., Huguenin E., Logan C.A., Waring C.A. (1917) Gems. *Mines and Mineral Resources of the Counties of Monterey, San Benito, San Luis Obispo, Santa Barbara, Ventura*. California State Mining Bureau, San Francisco, CA, pp. 42–43.
Burns R.G. (1970) *Mineralogical Applications of Crystal Field Theory*. Cambridge University Press, Cambridge, England.
Burns R.G., Clark R.H., Fyfe W.S. (1967) Crystal field theory and some geochemical applications. In A.P. Vinogradov, Ed., *Chemistry of the Earth's Crust*, Vol. 2, Israel Program for Scientific Translations, Jerusalem, pp. 93–112.
Chihara K., Komatsu M., Mizota T. (1974) A joaquinite-like mineral from Ohmi, Niigata Prefecture, central Japan. *Mineralogical Journal*, Vol. 7, No. 4, pp. 395–399.
Christophe M., Gouet G., Wyart J. (1980) Synthèse hydrothermale de la bénitoite. *Bulletin de Minéralogie*, Vol. 103, pp. 118–119.
Chromy B. (1969) Pink benitoite. *Gems and Minerals*, No. 279, p. 32.
Coleman R.G. (1957) Mineralogy and petrology of the New Idria district, California. Ph.D. dissertation, Stanford University, Stanford, CA.
Coleman R.G. (1961) Jadeite deposits of the Clear Creek area, New Idria district, San Benito County, California. *Journal of Petrology*, Vol. 2, pp. 209–247.
Couch O. (1961) *The Benitoite Story*. Independently published, 10 pp.
Dibblee T.W. Jr. (1979) Geologic map of the central Diablo Range between Hollister and New Idria, San Benito, Merced and Fresno Counties, California. *U.S. Geological Survey Open File Map 79–358*, scale 1:125,000.
Eckel E.B., Myers W.B. (1946) Quicksilver deposits of the New Idria district, San Benito and Fresno counties, California. *California Journal of Mines and Geology*, Vol. 42, pp. 81–124.
Frazier S., Frazier A. (1990a) A rare bit of history. *Lapidary Journal*, Vol. 44, No. 8, pp. 46–58.
Frazier S., Frazier A. (1990b) A benitoite bibliography. *Lapidary Journal*, Vol. 44, No. 8, pp. 61–68.
Gemological Institute of America (1993) *Gem Reference Guide*. Gemological Institute of America, Santa Monica, California.
Gray M. (1986) Benitoite mining today. *Canadian Gemmologist*, Vol. 7, No. 3, pp. 82–83.
Gray M. (1992) Recent developments at the Benitoite mine. *Canadian Gemmologist*, Vol. 13, No. 4, pp. 118–119.
Gross E.B., Wainwright J.E.N., Evans B.E. (1965) Pabstite, the tin analogue of benitoite. *American Mineralogist*, Vol. 50, pp. 1164–1169.
Gübelin E.J., Koivula J.I. (1986) *Photoatlas of Inclusions in Gemstones*, ABC Edition, Zurich, Switzerland.
Hawthorne F.C. (1987) The crystal chemistry of the benitoite group minerals and structural relations in (Si_3O_9) ring structures. *Neues Jahrbuch für Mineralogie, Monatshefte*, Vol. 1, pp. 16–30.
Hessel J.F.C. (1830) Krystallometrie. Reprinted as: *Nr. 88. Ostwald's Klassiker der exakten Wissenschaften* (1897),

Wilhelm Engelmann, Leipzig.

Hinthorne J.R. (1974) The origin of sanbornite and related minerals. Ph.D. dissertation, University of California at Santa Barbara.

Hopson C.A., Mattinson J.M., Pessagno E.A. (1981) Coast Range ophiolite, western California. In W.G. Ernst., Ed., *The Geotectonic Development of California*, Prentice Hall, Englewood Cliffs, NJ, pp. 418–510.

Komatsu M., Chiara K., Mizota T. (1973) A new strontium-titanium hydrous silicate mineral from Ohmi, Niigata Prefecture, central Japan. *Mineralogical Journal*, Vol. 7, No. 3, pp. 298–301.

Laird J., Albee L. (1972) Chemical composition and physical, optical, and structural properties of benitoite, neptunite, and joaquinite. *American Mineralogist*, Vol. 57, pp. 85–102.

Laurs B.M. (1995) Progress report: Benitoite exploration in the New Idria mining district, San Benito County, California. Report submitted to the Kennecott Exploration Company, Reno, NV.

Lee D.E., Thomas H.H., Marvin R.F., Coleman R.G. (1964) Isotopic ages of glaucophane schists from the area of Cazadero, California. *U.S. Geological Survey Professional Paper* 475, pp. D105–D107.

Lonsdale J.T., Metz M.S., Halbouty M.T. (1931) The petrographic characters of some Eocene sands from southwest Texas. *Journal of Sedimentary Petrology*, Vol. 1, pp. 73–81.

Louderback G.D. (1907) Benitoite, a new California gem mineral. *University of California, Department of Geological Sciences Bulletin*, Vol. 5, pp. 149–153.

Louderback G.D. (1909) Benitoite, its paragenesis and mode of occurrence. *University of California, Department of Geological Sciences Bulletin*, Vol. 5, pp. 331–380.

Marcher G.H. (1939) Story of a gemstone christening. *The Mineralogist*, pp. 200, 217–219.

Millage A.H. (1981) Mineralogy of the Victor claim, New Idria district, San Benito County, California. M.S. thesis, Stanford University, Stanford, CA.

Mitchell R.K. (1980) The fluorescence of benitoite. *Journal of Gemmology*, Vol. 17, No. 3, p. 149.

Moller W.P. (1996) A new discovery of benitoite. *Mineralogical Society of Southern California Bulletin*, September, pp. 3–4.

Payne C.J. (1939) Dispersions of some rarer gemstones. *Gemmologist*, Vol. 9, pp. 33–35.

Petrov A. (1995) More benitoite locality information, another new one and another discredited. *Mineral News*, Vol. 11, No. 8, p. 9.

Rase D.E., Roy R. (1955a) Phase equilibria in the system BaTiO$_3$-SiO$_2$. *Journal of the American Ceramic Society*, Vol. 38, pp. 389–395.

Rase D.E., Roy R. (1955b) On the stability and hydrothermal synthesis of benitoite. *American Mineralogist*, Vol. 40, pp. 542–544.

Ream L.R. (1996) Benitoite from the Junnila mine. *Mineral News*, Vol. 12, No. 3, p. 3.

Reed R.D., Bailey J.P. (1927) Subsurface correlation by means of heavy minerals. *Bulletin of the American Association of Petroleum Geologists*, Vol. 11, pp. 359–368.

Rohtert W.R. (1994) Preliminary geologic map of the Benitoite Gem mine. Report submitted to the Kennecott Exploration Company, Reno, NV.

Rossman G.R. (1997) Benitoite visible spectra (350–1100 nm). Web page, *http://minerals.gps.caltech.edu/files/benitoit/*.

Sakai M., Akai J. (1994) Strontium, barium and titanium-bearing minerals and their host rocks from Ohmi, Japan. *Scientific Reports of the Niigata University, Series E: Geology and Mineralogy*, Vol. 9, pp. 97–118.

Sinkankas J. (1976) *Gemstones of North America*, Volume II. Van Nostrand, Princeton, NJ, pp. 280–288.

Smith A.E. (1995) The reported benitoite occurrence in Texas—doubtful? *Mineral News*, Vol. 11, No. 5, p. 5.

Sterrett D.B. (1908) Benitoite. *U.S. Bureau of Mines Minerals 1907 Yearbook, Part 2: Non-metallic Products*. Washington, DC, pp. 798–799.

Sterrett D.B. (1911) Benitoite. *U.S. Bureau of Mines Minerals 1909 Yearbook, Part 2: Non-metals*. Washington, DC, pp. 742–748.

Van Baalen M.R. (1993) Titanium mobility in metamorphic systems: A review. *Chemical Geology*, Vol. 110, pp. 233–249.

Van Baalen M.R. (1995) The New Idria serpentinite. Ph.D. dissertation, Harvard University, Cambridge, MA.

Webster R. (1994) *Gems: Their Sources, Descriptions, and Identification*, 5th ed. Rev. by P.G. Read., Butterworth Heinemann, London.

Wise W.S. (1982) Strontiojoaquinite and bario-orthojoaquinite: Two new members of the joaquinite group. *American Mineralogist*, Vol. 67, pp. 809–816.

Wise W.S., Gill R.H. (1977) Minerals of the Benitoite Gem mine. *Mineralogical Record*, Vol. 8, pp. 7–16.

Wise W.S., Moller W.P. (1995) Geology and mineralogy of the New Idria district, San Benito and Fresno Counties, California. *Rocks and Minerals*, Vol. 70, No. 1, pp. 27–35.

Worner H.K., Mitchell R.W., Eds. (1982) *Minerals of Broken Hill*. Australian Mining & Smelting Ltd., Melbourne, pp. 54, 87, and 202.

TAIRUS HYDROTHERMAL SYNTHETIC SAPPHIRES DOPED WITH NICKEL AND CHROMIUM

By Victor G. Thomas, Rudolf I. Mashkovtsev, Sergey Z. Smirnov, and Vadim S. Maltsev

Researchers of the Tairus joint venture have developed the technology for the hydrothermal growth of gem-quality crystals of synthetic sapphire. They have achieved a broad spectrum of attractive colors by varying the concentrations of Ni^{2+}, Ni^{3+}, and Cr^{3+}. Comprehensive testing of 18 faceted synthetic sapphires and 10 synthetic crystals, representing the range of colors, revealed a typical set of internal features that are specific to hydrothermally grown crystals (microscopy), as well as the presence of OH^- and various carbon-oxygen groups in the sapphire structure (infrared spectroscopy). The reactions of the test samples to ultraviolet radiation and visible light were also found to be useful in distinguishing the Tairus synthetic sapphires from their natural counterparts and other synthetics.

ABOUT THE AUTHORS

Dr. Thomas is a senior researcher, and Mr. Maltsev is a technological researcher, at Tairus (a joint venture between the Siberian Branch of the Russian Academy of Sciences and Pinky Trading Co. Ltd. of Bangkok, Thailand). Dr. Mashkovtsev is a senior researcher, and Dr. Smirnov is a research scientist, at the Siberian Gemological Center, Novosibirsk

*T*he history of hydrothermally grown synthetic corundum began nearly 40 years ago, when Laudise and Ballman (1958) produced the first colorless synthetic sapphire. Their technique, when modified, also can be used to grow rubies (Kuznetsov and Shternberg, 1967). Until recently, however, attempts to grow blue sapphire by the hydrothermal method had failed. This problem is significant because flux-grown and flame-fusion synthetic sapphire crystals typically have uneven color distribution. In blue flame-fusion material, an intense blue hue is usually concentrated in thin outer zones of boules, while most of the bodycolor is much lighter. In blue flux-grown synthetic sapphires, color inhomogeneity is apparent as a sequence of blue and colorless angular growth zones that conform to the crystal shape. Such color inhomogeneity makes cutting difficult and greatly decreases the yield of faceted material.

To address this market gap, the authors investigated the use of hydrothermal growth techniques to produce blue crystals that would be free from the defects of synthetic sapphire grown by other methods. This problem was approached in two ways: (1) by doping hydrothermal synthetic sapphire with iron (Fe^{2+}) and titanium (Ti^{4+}) ions (as proposed by, for example, Burns, 1981); and (2) by using other doping impurities that could reproduce the blue color of sapphire. Research into the development of a commercial technique by the first approach is still ongoing. However, the second approach has led to success: The use of nickel (Ni^{2+}) as a dopant has resulted in crystals of "sky" blue synthetic sapphire, from which thousands of faceted stones as large as 4 ct have been produced by the Tairus joint venture and marketed internationally since 1995.

The next step in the development of this technique was to produce sapphires of different colors by varying the concentrations of Ni^{2+}, Ni^{3+}, and chromium (Cr^{3+}). At this time, the Tairus research group has created the technology

Figure 1. Tairus experts have produced hydrothermal synthetic sapphires in a broad range of colors, as illustrated here. These Tairus synthetic sapphires range from 1.00 to 4.74 ct. Photo © GIA and Tino Hammid.
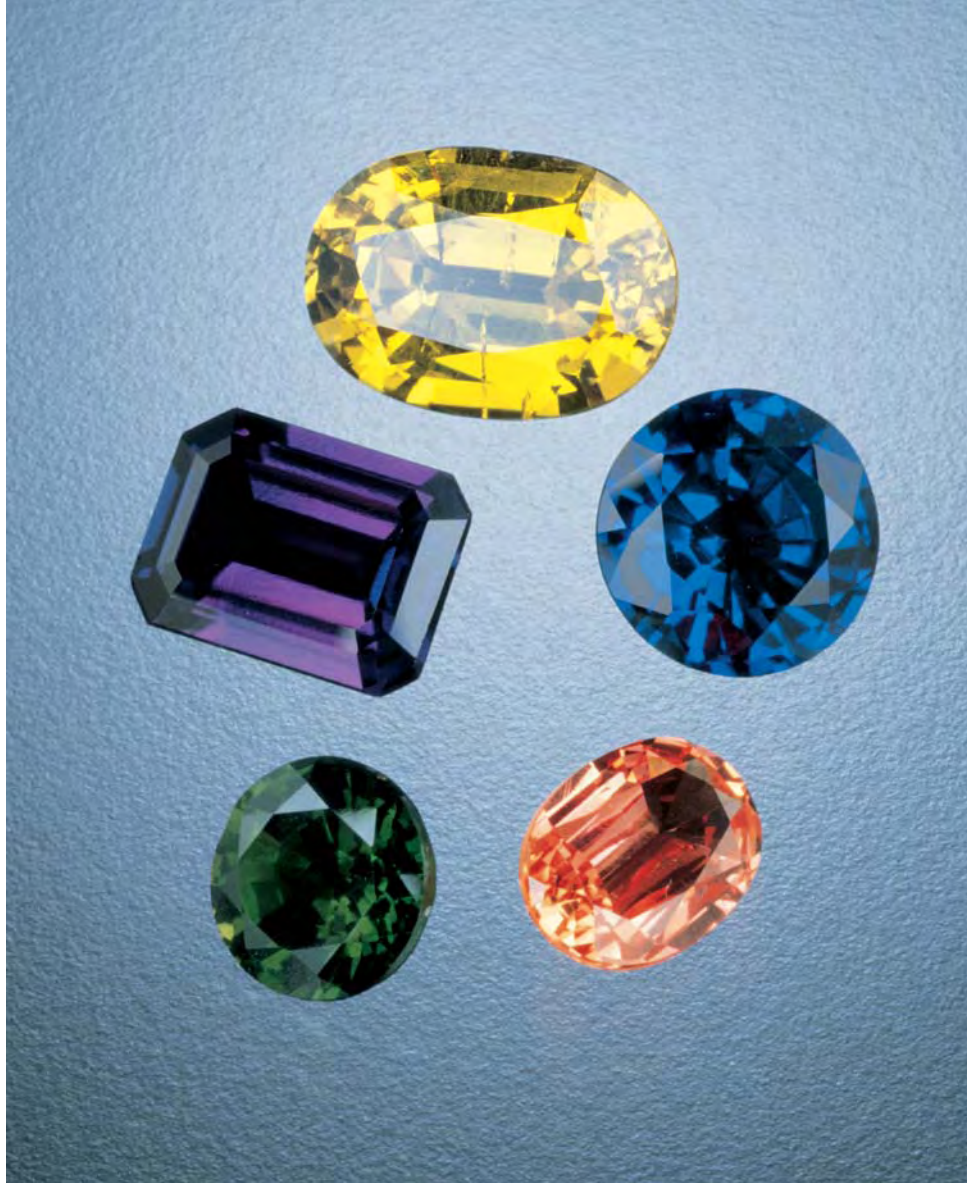
to grow commercial quantities of sapphires in blue and a wide range of other colors (see, e.g., figure 1). This article presents the results of our research into the growth of hydrothermal synthetic sapphires and their characterization, including the chemistry, gemological properties, and distinctive internal features of these new synthetics.

GROWTH TECHNIQUES

The autoclave arrangement used to grow Tairus hydrothermal synthetic sapphire is illustrated in figure 2. The growth process is carried out in a hermetically sealed "floating" gold ampoule with a volume of almost 175 ml inside the autoclave, a temperature of 600°C, and a pressure of about 2000 bar. Growth takes place when the initial synthetic colorless sapphire feed is transferred and crystallized onto seeds, via a vertical temperature gradient of 60° to 70°C, through a carbonate solution with a complex composition (the details of which are pro-

prietary). Seed plates oriented parallel to the hexagonal prism {10$\overline{1}$0} are used to grow cuttable crystals. For research purposes, we also grew two crystals on a spherical seed to investigate the ideal arrangement of the crystal faces. All of the seeds in the samples used for this study were cut from Czochralski-grown colorless synthetic sapphire. The dopant (NiO and, for certain colors, Cr_2O_3) is introduced via unsealed capsules placed at the bottom of the ampoule. The concentrations of Ni and Cr in the growing crystal are controlled by the diameter of the opening in these capsules.

An oxygen-containing buffer plays a significant role in the sapphire growth process. It is a powdered reagent that is placed at the bottom of each ampoule. This substance governs the valence state of Ni in the solution, so that sapphires with different $Ni^{2+}:Ni^{3+}$ ratios can be grown. Various metals and their oxides (none of which produces any color in the synthetic sapphire) have been used for this
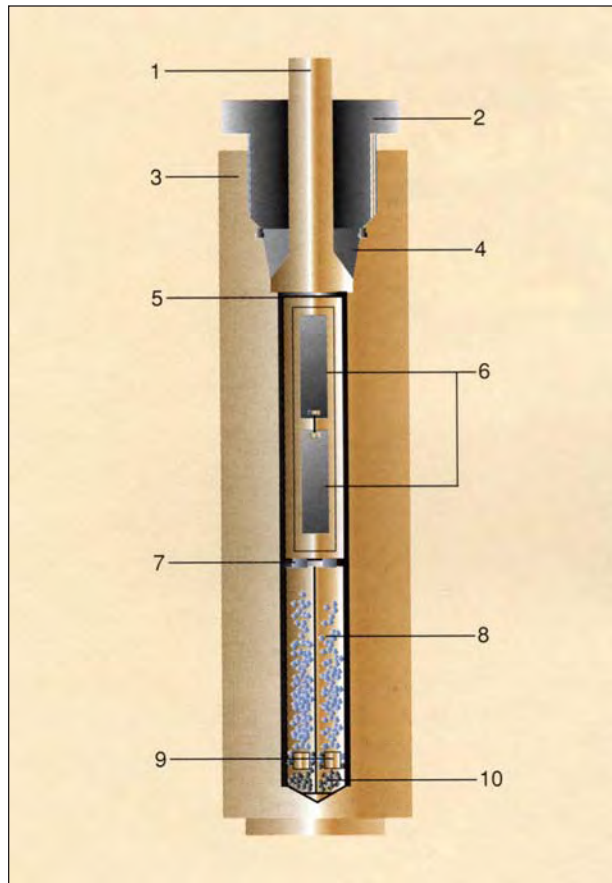
Figure 2. Hydrothermal synthetic sapphires are grown by Tairus scientists in an autoclave that measures 60 cm high and 8 cm in diameter. The components are as follows: (1) lid; (2) push nut; (3) autoclave body; (4) seal ring; (5) gold ampoule; (6) synthetic sapphire seeds; (7) diaphragm; (8) crushed synthetic colorless corundum charge; (9) capsules with Ni/Cr oxides; (10) powdered oxygen-containing buffer. Crystal growth proceeds via dissolution of the corundum charge (8) in a hydrothermal solution in the lower (i.e., hotter) part of the autoclave, followed by convective transfer of the saturated solution to the upper (i.e., cooler) part of the autoclave, where the synthetic sapphire crystallizes on the seeds (6). The autoclave is heated from the bottom and the side in a special furnace.

buffer (e.g., coupled Cu-Cu_2O, Cu_2O-CuO, etc. [see table 1]). Synthetic sapphire crystals as large as 7 × 2.5 × 2 cm have been grown in a month, with a growth rate of almost 0.15 mm per day.

MATERIALS AND METHODS

Two crystals of each color (10 pairs total) were grown under uniform conditions as described above. One crystal in each pair was used to produce faceted gems (from one to five faceted stones, each weighing approximately 1 ct). The other was cut into plates or used whole for crystallographic measurements. Detailed crystallographic measurements were also made on the two greenish blue crystals (each about 0.8 cm across) that were grown on spherical seeds. (These latter crystals were grown both to illustrate the ideal arrangement of crystal faces for corundum produced under the experimental conditions described above, and because it was easier to obtain accurate goniometric measurements on them.). We selected 18 faceted samples (round and oval mixed cuts, weighing about 1 ct each) that ranged from very light pink through orange, yellow, and green to blue (see, e.g., figure 3) for gemological testing. More than 20 polished (on

both sides) plates were used for spectroscopy, inclusion study, and microprobe analysis.

Standard gemological testing was carried out at the Siberian Gemological Center, Novosibirsk. The face-up colors of the 18 faceted synthetic sapphires were determined with a standard daylight-equivalent light source (the fluorescent lamp of a GIA GEM Instruments Gemolite microscope) and an ordinary incandescent lamp. For each faceted sample, the color was compared to standards from the GIA GemSet and described in terms of hue, tone, and saturation. Specific gravity was determined hydrostatically. Refractive indices were measured with a GIA GEM Duplex II refractometer and a filtered, near-monochromatic, sodium-equivalent light source. To examine internal features and polarization behavior, we used a GIA GEM Illuminator polariscope and gemological microscope with various types of illumination.

Detailed observations of inclusions, color zoning, and growth sectors were made on crystal plates of all 10 color varieties with a Zeiss Axiolab polarizing microscope. Some samples were also immersed in methylene iodide for microscopic examination. Appearance in visible light was observed with the incandescent illumination provided by a GIA GEM Instruments spectroscope base, and UV luminescence was observed with the aid of a GIA GEM Instruments ultraviolet cabinet. Samples with weak luminescence were examined in a completely darkened room. Dichroism was determined with a calcite dichroscope and a GIA GEM Instruments FiberLite 150 fiber-optic illuminator.

The arrangement of crystal faces was studied by means of a Zeiss ZRG-3 two-circle goniometer. The

TABLE 1. Colors and partial chemistry of the Tairus synthetic sapphires.[a]

Sample	Color	Concentration (wt.%)					Oxygen buffer
		Cr_2O_3	NiO[b]	FeO	MnO	TiO_2	
1	Greenish blue	bdl[c]	0.23	tr	tr	tr	Cu-Cu$_2$O
2	Greenish blue	0.15	0.24	tr	tr	tr	Cu-Cu$_2$O
3	Greenish blue	0.26	0.34	tr	tr	tr	Cu-Cu$_2$O
4	Light reddish purple	0.07	0.04	tr	tr	tr	Cu-Cu$_2$O
5	Pink	0.07	bdl	tr	tr	tr	Cu-Cu$_2$O
6	"Padparadscha"	0.08	bdl	tr	tr	tr	PbO-Pb$_3$O$_4$
7	Yellow	tr[d]	tr	tr	tr	tr	PbO-Pb$_3$O$_4$
8	Light greenish yellow[e]	bdl	tr	tr	tr	tr	Cu-Cu$_2$O
9	Green	bdl	0.35	tr	tr	tr	Cu$_2$O-CuO
10	Blue-green	bdl	0.23	tr	tr	tr	not controlled
11	Colorless	bdl	bdl	tr	tr	tr	not controlled

[a] Analyses by electron microprobe.
[b] Total $NiO+Ni_2O_3$.
[c] bdl — below the detection limit = <0.01 wt.%.
[d] tr — trace = about 0.02 wt.% for each element.
[e] This sample was gamma-irradiated to produce the yellow color (details in Materials and Methods section of text).

compositions (including major and trace elements) of 11 samples representative of the different colors were determined with a Camebax-Micro electron microprobe. We observed visible-range spectra of the 18 faceted stones using a GIA GEM Instruments Prism 1000 spectroscope. In addition, UV-visible spectra were obtained with a Zeiss Specord M40 spectrophotometer, and infrared spectra were measured with Zeiss Specord M80 and SF-20 spectrophotometers, on 1-mm-thick plates. A processor built into the M40 locates the position of absorption band peaks. Color coordinates calculated from the unpolarized absorption spectra were plotted on a CIE chromaticity diagram, to compare color ranges of synthetic sapphires doped with Ni^{2+}, Ni^{3+}, Cr^{3+}, Ni^{2+}-Cr^{3+}, and Ni^{3+}-Cr^{3+}. The accuracy of these calculations was checked by a catalogue of colored glass (Catalogue . . ., 1967). One hydrothermal synthetic ruby (donated by Alexander Dokukin) and one flame-fusion synthetic ruby were used for comparison in the CIE diagram as examples of corundum doped with Cr^{3+} only.

Some of the very light greenish blue sapphires doped with Ni^{2+} were gamma irradiated (^{60}Co source, dose 0.1–1 Mrad) to convert part of the Ni^{2+} to Ni^{3+}, which changed the color to yellow. We investigated the ultraviolet and visible spectra on these treated samples.

RESULTS AND DISCUSSION

Crystal Morphology. Crystals grown on flat and spherical seeds are shown in figure 4. These crystals have several sets of major flat faces (i.e., forms) consisting of the hexagonal prism a {11$\bar{2}$0}, dipyramid n {22$\bar{4}$3}, and rhombohedron r {10$\bar{1}$1}. These forms are common on natural corundum crystals (Goldschmidt, 1916; Yakubova, 1965). In addition, we observed minor faces of the following forms: rhombohedra ϕ {10$\bar{1}$4} and d {10$\bar{1}$2}, as well as rough flat surfaces θ {0.1.$\bar{1}$.11} and c {0001} (again, see figure 4).

Figure 3. Although this photo shows the full color range (including colorless and red) of the hydrothermal synthetic corundum produced by Tairus researchers to date (here, 1.11–4.74 ct), the present study focused on those pink, yellow, and green-to-blue synthetic sapphires produced by doping with Ni^{2+}, Ni^{3+}, and/or Cr^{3+}. Photo by Evgeny Krayushin.
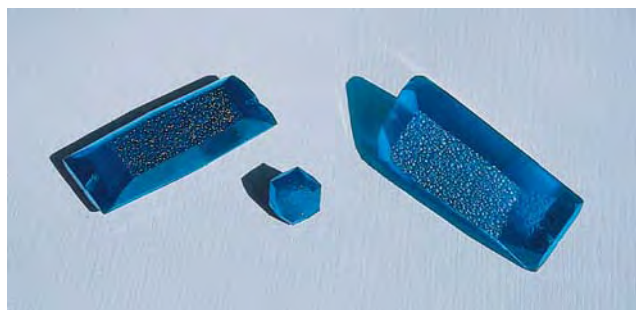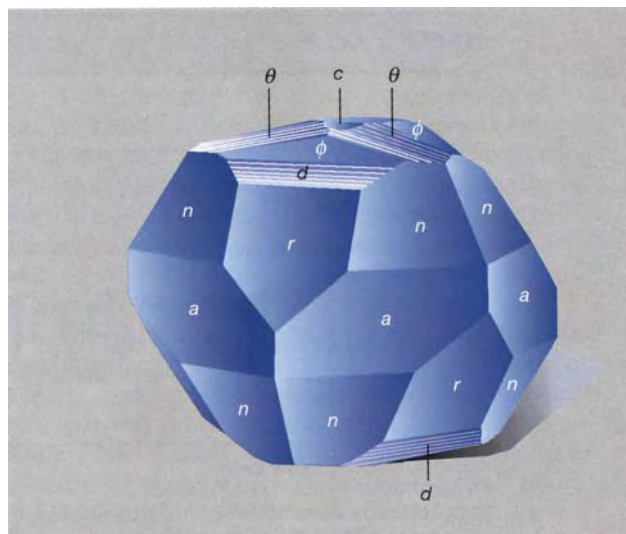
Figure 4. The photo on the left shows two large (5←2 cm) crystals of greenish blue synthetic sapphire that were grown on seed plates, and a small (about 0.8 cm) crystal grown on a spherical seed. (Photo by Evgeny Krayushin.) The line illustration on the right shows the actual crystal faces obtained on a crystal grown on a spherical seed.

With the exception of *c*, these forms are not typical of natural corundum crystals. The Miller indices of the ϕ and θ faces were calculated from goniometric measurements, but we could not find a reference to either face in the available literature on corundum crystal morphology.

The habit of the samples grown on spherical seeds is transitional between some natural and some flux-grown—e.g., Knischka (Gübelin, 1982)—crystals. By comparison, the habit of crystals grown on flat seeds is similar to that seen on spherical seeds, but the overall shape of the crystals (e.g., the relative sizes of the different faces) is distorted, because of the different crystallographic orientation and size of the seed plate. Crystals grown on seed plates showed *r*, *n*, and θ as major faces, with a smoother surface than their equivalents on crystals with a spherical seed. Minor faces include the hexagonal prism *a* and scalenohedral faces for which indices have not yet been determined.

Chemistry. The electron microprobe analyses (table 1) indicate that the chemical composition of the nickel- and chromium-doped hydrothermal synthetic sapphires was about 99.4–99.9 wt.% Al_2O_3. Special attention was paid to measuring the possible chromophores Cr, Ni, Ti, manganese (Mn), and Fe. (Ti, Mn, and Fe are the components of autoclave steel, so they could have entered the growing sapphire through the possible unsealing of the ampoule during the run.) All of the samples including the colorless synthetic sapphire (sample 11; table 1), contain traces of Ti, Mn, and Fe. Since these elements were present in the colorless sample, they apparently do not affect the color at the concentrations present in the Tairus synthetic sapphires.

Optical Absorption Spectra and Color. *Optical Absorption Spectra.* Ni-doped sapphire crystals grown by the Verneuil method are known to contain trivalent nickel (Ni^{3+}). To convert the Ni to a divalent state (Ni^{2+}), synthetic sapphire has been annealed in a reducing (hydrogen) atmosphere (Muller and Gunthard, 1966). Minomura and Drickamer (1961) produced Ni^{2+}- and Ni^{3+}-doped sapphire by annealing pure Al_2O_3 crystals in NiO powder. For the samples in our study, however, the Ni^{2+}:Ni^{3+} ratio was set *in situ* during the growth process by controlling the oxidation-reduction potential (see Growth Techniques section), and it varied widely.

The absorption spectrum (in unpolarized light) of Ni^{2+}-doped greenish blue Tairus synthetic sapphire (sample 1, table 1) includes three intense bands—at 377, 599, and 970 nm—and two weak bands, at 435 and 556 nm. In polarized light (figure 5A), each intense band is resolved into two bands—that is, 370 and 385 nm, 598 and 613 nm, and 950 and 990 nm (The last two bands are not shown in figure 5A but were detected with the SF-20 spectrophotometer.) These results differ somewhat from the positions reported earlier for Ni^{2+} absorption bands in synthetic sapphires grown by other methods (Minomura and Drickamer, 1961; Muller and Gunthard, 1966), which in turn differ noticeably from one another. In particular, lines at 995 and 1020 nm were observed by Minomura and Drickamer, but not by Muller and Gunthard. These differences are understandable given the radically different methods of sapphire growth.

Green synthetic sapphire (sample 9, table 1) grows under relatively high oxidizing conditions, so a greater ratio of Ni^{3+} to Ni^{2+} is to be expected in a

green crystal. The absorption spectrum of this sapphire (figure 5B) is similar to a Ni^{2+} absorption spectrum, but with intense absorption between 380 and 420 nm, rapidly increasing toward the ultraviolet.

The spectra in figure 5C were derived by subtracting the spectra in figure 5A from those in figure 5B: They correlate well with the reported Ni^{3+} ion absorption spectrum (Muller and Gunthard, 1966; Boksha et al., 1970). Thus, we believe that the green color of the hydrothermal synthetic sapphires is caused by the simultaneous absorption of Ni^{2+} and Ni^{3+} ions. As will be shown below, the absorption characterized by the spectrum in figure 5C will produce a yellow color in sapphire. In practice, we have found that by increasing the oxidation potential from a Cu_2O-CuO to a PbO-Pb_3O_4 buffer, we can grow yellow sapphire (sample 7, table1) with a spectrum similar to those in figure 5C.

Another way to produce yellow sapphire doped with Ni^{3+} is by gamma irradiation of Ni^{2+}-doped pale greenish blue sapphire. The absorption spectra of one of the samples that was gamma-irradiated with 0.5 Mrad (sample 8 in table1) also resemble those in figure 5C. Moreover, following irradiation, only a weak decrease in Ni^{2+} absorption is observed, whereas Ni^{3+} absorption increases to become comparable to Ni^{2+} absorption.
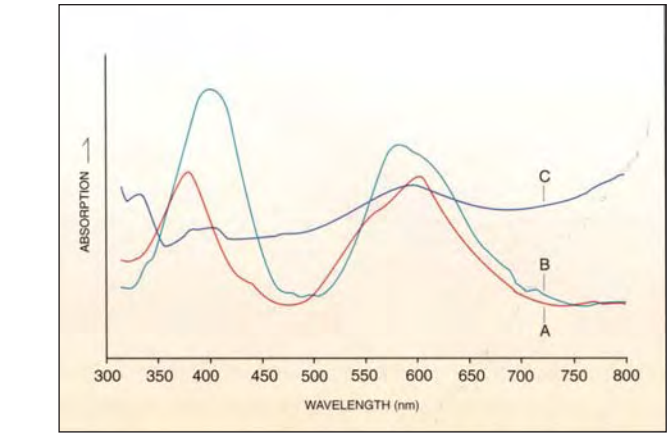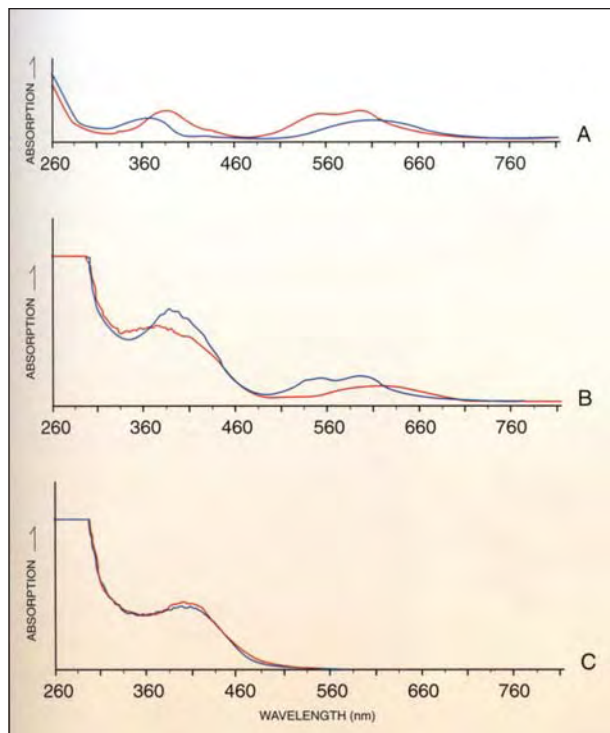

Figure 6. The unpolarized absorption spectra of (A) Ni^{2+}-doped and (B) Ni^{2+}-Cr^{3+}–doped Tairus greenish blue synthetic sapphires are quite different from the absorption spectrum of ordinary blue Verneuil-grown Fe^{2+} + Ti^{4+} synthetic sapphire (C). Spectrum C is similar to that of natural Fe^{2+} + Ti^{4+} sapphires.

The addition of small amounts of Cr (up to 0.3 wt.% Cr_2O_3) to Ni-containing sapphires (NiO>0.2 wt.%) results in a greenish blue color, and the simple superposition of Ni and Cr spectra (figure 6). The spectrum of a greenish blue Ni^{2+}-Cr^{3+}-doped sapphire is similar to that of ruby, with characteristic Cr lines at 469, 475 nm, and 690 nm. The band at 510 to 620 nm is a result of the superposition of Ni (580–620 nm) and Cr (510–620 nm) bands. Since this feature is clearly seen in a gemological spectroscope, it can be regarded as a good identifying feature of Tairus greenish blue Cr-containing sapphires.

Color Varieties. There are two ways to study and describe color. The first is the "comparison" method, whereby the color of the sample is simply compared to a standard with known color. This method is used in most gemological investigations and for gemological testing. The second way is to calculate color characteristics from the absorption spectra of the gemstones. This method allows us not only to describe the color of these synthetic sap-

Figure 5. These optical absorption spectra are of (A) greenish blue (sample 1, table 1) and (B) green (sample 9, table 1) Tairus synthetic sapphires doped with Ni^{2+} and Ni^{2+}-Ni^{3+}, respectively. Spectrum C was produced by subtracting spectrum A from spectrum B and represents a hypothetical yellow synthetic sapphire doped only with Ni^{3+}. Blue = parallel to the c-axis; red = perpendicular to the c-axis.

phires, but also to compare them quantitatively to natural sapphires and other synthetics. To quantify the different colors of Tairus hydrothermal synthetic sapphires, we converted their absorption spectra to color coordinates in the CIE color system. The CIE system is fully described elsewhere (Wright, 1964), but a brief explanation of the chromaticity diagram, which is integral to this system, will be made here.

A set of coordinates was developed to express the relationship among all colors in the spectrum on the basis of a "standard observer" response (the average of observations by a large number of people) to different color stimuli. The chromatic portions of these measurements were plotted on an x-y coordinate graph to produce the chromaticity diagram (figure 7). The skewed parabolic curve on this diagram is the location of saturated hue coordinates. The points representing saturated blue and violet colors are located in the left corner of the region, while points of saturated red and orange are on the right. The curved top corresponds to green and yellow saturated colors. The area along the straight line between the violet and red corners is the location of nonspectral purple colors. The point for white color is located in the approximate center of the region; point C marks the white daylight source.

Thus, any hue and saturation can be represented by a set of x-y coordinates and plotted along or within the chromaticity curve. The points shown on the curve are the dominant wavelengths (in nanometers) of each saturated color. Along any radial line drawn between white color and a saturated hue lie colors with decreasing saturation as one approaches the white color point.

The synthetic sapphires doped with Ni^{2+} (point 1 in figure 7) have a greenish blue hue. The synthetic sapphires grown under oxidizing conditions and colored predominantly by Ni^{3+} (point 7) are yellow. The position of this point is close to hypothetical Ni^{3+} sapphire (point 12), which is calculated from the spectra in figure 5C, as well as greenish yellow sapphire (point 8) produced by gamma irradiation. Variations in the ratio of Ni^{2+} to Ni^{3+} can produce all of the colors in the region bounded by points 1, 8, 9, and 10.

When significant concentrations of Ni^{2+} (more than 0.2 wt.% oxide) are present, Cr content has very little impact on the hue of the greenish blue synthetic sapphires. The saturation is slightly lowered (points 2 and 3) and the tone is darkened in the relatively Cr rich samples. When both NiO and Cr_2O_3 are present at concentrations below 0.1 wt.% each, a light reddish purple (e.g., points 4 and 5) is

Figure 7. On this CIE chromaticity diagram, points are plotted for the Tairus synthetic sapphires (diamond shapes) and for natural and other synthetic sapphires (circles). Points 1 through 10 correspond to the Tairus sample numbers from table 1. Sample 11 is a hydrothermally grown ruby; sample 12 (pure Ni^{3+}) was calculated from the spectrum for hypothetical yellow sapphire in figure 5C; and sample 13 is a flame-fusion synthetic ruby. Points 14 through 18 were calculated from representative spectra of natural sapphires by Platonov et al. (1984): 14 is a yellow sapphire from the Ural Mountains, Russia; 15 is a greenish blue sapphire from Australia; 16 is a pale greenish blue sapphire from the Ural Mountains; 17 is a deep blue sapphire that is also from the Urals; and 18 is a deep blue sapphire from Burma. Point "C" represents a standard daylight source. The triangular region defined by the dotted lines illustrates the approximate range of colors produced in Tairus synthetic sapphires by various amounts of Ni^{2+}, Ni^{3+}, and Cr. Note the overlap in color between the Tairus synthetic sapphires and the natural and other synthetic samples.
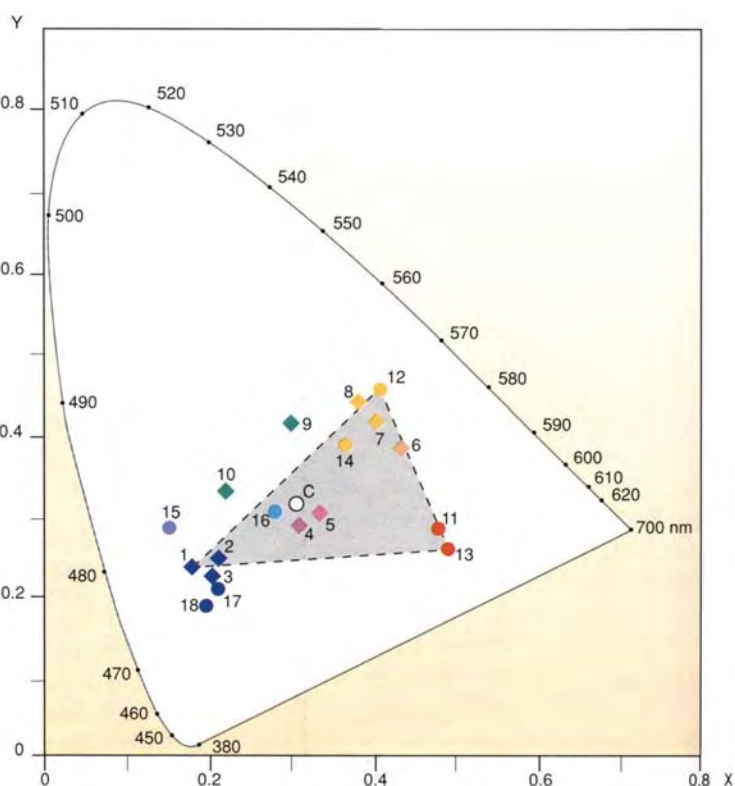
TABLE 2. Properties of Tairus greenish blue (Ni^{2+} and Ni^{2+}-Cr^{3+}) synthetic sapphires and some of their natural and other synthetic counterparts.

Property	Tairus hydrothermal synthetic	Chatham Flux-grown synthetic	Flame-fusion synthetic	Natural, from Vietnam	Natural, from Australia	Natural, from China	Natural, from Sri Lanka
Color	Moderately strong, medium to dark greenish blue	Blue	Medium-dark violetish blue (diffusion treated)	Predominantly blue to greenish blue to bluish green, medium-light to very dark	Very slightly greenish blue to greenish blue, and near-colorless to extremely dark "royal" blue	Dark blue with areas bluish green	"Fine" blue of blue and
Color distribution (eye-visible)	Even	Uneven; strong color zoning	Uneven; tiny curved color banding	Uneven; distinct color banding (colorless/blue)	Uneven; color banding (colorless or pale yellow/blue)	Uneven; very strong color zoning	Uneven; very strong color zoning
Pleochroism	Weak (Ni^{2+}-Cr^{3+}) to strong green blue to blue (Ni^{2+}); in some cases (Ni^{2+}-Cr^{3+}), none	Strong; violetish blue to greenish blue	Strong; violetish blue to grayish blue	Distinct to strong; blue or violetish blue to blue-green or yellow-green	Not reported	Strong	Moderate greenish blue to inky blue
R.I. (n_ω)	1.768–1.769	1.770	1.768	1.769–1.772	1.769–1.772	1.769–1.771	1.768
R.I. (n_ε)	1.759–1.761	1.762	1.759	1.760–1.764	1.761–1.763	1.761–1.762	1.760
Birefringence	0.007–0.010	0.008	0.009	0.008–0.009	0.008–0.009	0.008–0.009	0.008
S.G.	3.98–4.03	3.974–4.035	Not determined	3.99–4.02	3.99–4.02	3.99–4.02	4.00
Fluorescence to LWUV	Typically inert, but in some cases (with high Cr) purplish red	Variable, inert to strong in yellow to orange	Inert	Inert	Inert	Inert	Inert
Fluorescence to SWUV	Typically inert, but in some cases (with high Cr) very weak purplish red	Variable, inert to strong in green, yellow to orange colors	Chalky light blue	Inert	Inert	Inert	Light blue
Reference	Present study	Kane (1982)	SGC Databank[a]	Smith et al. (1995)	Coldham (1985)	Furui (1988)	Gunawardene and Rupasinghe (1986)

[a]Stones tested in the Siberian Gemological Center (SGC).

produced. The addition of small amounts of Cr^{3+} to Ni^{3+}-doped synthetic sapphire shifts the hue from yellow (such as for point 7) to the orange part of the spectrum, producing a "padparadscha" type pinkish orange color (point 6). Thus, addition of Cr to either Ni^{2+} or Ni^{3+} shifts the color coordinates toward purple, near the lines connecting point 13 with points 1 and 12.

The combination of different amounts of Cr^{3+}, Ni^{2+}, and Ni^{3+} permits the production of synthetic sapphires in virtually any color in the vicinity of triangle 1-12-13 (shaded triangle on figure 7). The hue and saturation are strongly dependent on the concentrations of these elements. Thus, although the triangle 1-12-13 does not represent absolute boundaries (e.g., points 3, 9, and 10 do lie away from the triangle), it helps to illustrate the range of colors represented by the samples grown in our experiments and discussed in this article. In addition, figure 7 shows that the colors of some Tairus synthetic sapphires overlap the colors of their natural counterparts, as well as the colors of synthetic sapphires grown by other methods.

Gemological Characteristics. The properties for greenish blue, pinkish orange (padparadscha), and yellow Tairus hydrothermal synthetic sapphires are reported in tables 2, 3, and 4, respectively. Sample stones are illustrated in figures 8, 9, and 10, respectively. The blue and pinkish orange samples are compared to Chatham flux-grown synthetic sapphires and flame-fusion samples from an unknown

TABLE 3. Properties of Tairus pinkish orange "padparadscha" (Ni^{3+}-Cr^{3+}) synthetic sapphires and some of their natural and other synthetic counterparts.

Property	Tairus hydrothermal synthetic	Chatham Flux-grown synthetic	Flame-fusion synthetic	Natural, from Sri Lanka
Color	Medium-light moderate pinkish orange	Orange to reddish orange, in moderate to vivid saturation	Orange to yellowish orange, in medium-light to medium-dark tones, moderate to strong saturation	Pinkish orange[a]
Color distribution (eye-visible)	Even	Color zoned	Even	Not reported
Pleochroism	Weak reddish orange and light reddish orange	Strong pink and orange to brownish yellow	Weak to moderate orangy yellow and yellowish-orange	Orange-yellow and yellowish orange
R.I. (n_ω)	1.765	1.770	1.768	1.768
R.I. (n_ε)	1.757	1.762	1.759	1.760
Birefringence	0.008	0.008	0.009	0.008
S.G.	4.00	4.00 ± 0.003	3.97	4.00
Fluorescence to LWUV	Moderate orange	Strong to very strong orange-red to yellowish orange	Weak orange-red	Strong "apricot"[b]
Fluorescence to SWUV	Weak orange	Very weak to weak in same colors as LW	Inert	Strong "apricot"[b]
Reference	Present study	Kane (1982)	SGC Databank[c]	Gunawardene and Rupasinghe (1986)

[a]Crowningshield (1983).
[b]Type of UV radiation was not specified.
[c]Stones tested in the Siberian Gemological Center (SGC).

manufacturer; all three hue types are compared to natural sapphires from various sources worldwide.

The refractive indices of the Tairus synthetic greenish blue samples were found to be near the lower limits of corundum (see, e.g., Feklichev, 1989). As shown in table 2, they overlap the R.I. values reported for Sri Lankan sapphires and flame-fusion synthetic sapphires, and they are slightly below the values reported for the flux-grown synthetic sapphires and natural sapphires from the other sources. The values obtained for the yellow and pinkish orange Tairus synthetic sapphires were somewhat lower still. Some of the pinkish orange Tairus samples had values below the known range for corundum (see, e.g., Feklichev, 1989). The pink (n_ω=1.765, n_ε=1.758) and dark green (n_ω=1.768, n_ε=1.760) samples—not reported in the tables—showed values that were between those of the yellow-to-orange (including padparadscha) and greenish blue samples. The refractive indices of the pink samples were close to those reported for Chatham flux-grown synthetic pink sapphires (n_ω=1.768, n_ε=1.759; Kammerling et al., 1994), and they fell within the ranges reported for

other hydrothermal lab-grown sapphires. As indicated in tables 2–4, the values for birefringence and specific gravity of the Tairus hydrothermal synthetic sapphires overlap those for these natural and other synthetic sapphires.

Dichroism. Ni^{2+}-doped synthetic sapphires (e.g., sample 1 in table 1) showed a strong green-blue to blue dichroism. In the blue-green Ni^{2+}-Ni^{3+}–doped samples (e.g., sample 10), dichroism was strong violetish blue to blue-green; in the green (e.g., sample 9) Ni^{2+}-Ni^{3+}–doped samples, the colors were somewhat weaker brownish green and green. Increasing Cr content in the greenish blue Ni^{2+}-Cr^{3+}–doped synthetic sapphires weakens their dichroism. In greenish blue Cr-rich sapphires (e.g., sample 3), dichroism was clearly visible only with a bright incandescent light source: A light purple tint was seen in one direction. This purple tint is due to chromium's characteristic red luminescence to incandescent light. Even with an ordinary incandescent lamp, purple flashes can be seen in faceted samples viewed face-up. These features of greenish blue Cr-rich Tairus synthetic sap-

Figure 8. Tairus researchers produced these greenish blue hydrothermal synthetic sapphires by doping them with Ni^{2+} and Ni^{3+} and, in some cases, Cr^{3+}. Photo © GIA and Tino Hammid.

Figure 9. The colors of these pinkish orange "padparadscha" (Ni^{3+}-Cr^{3+}) Tairus hydrothermal synthetic sapphires are similar to those seen in nature or in other synthetic sapphires. Photo © GIA and Tino Hammid.

Figure 10. Yellow Tairus hydrothermal synthetic sapphires are colored predominantly by Ni^{3+}. Photo © GIA and Tino Hammid.

phires can help to distinguish them from their natural and other synthetic counterparts. The yellow sapphires colored predominantly by Ni^{3+} showed no dichroism, whereas the addition of Cr to Ni^{3+} resulted in weak dichroism in the pinkish orange (padparadscha) sapphires.

Reaction to Ultraviolet Radiation. Sapphire's luminescence to UV radiation strongly depends on Cr content. The greenish blue Cr-rich synthetic sapphires in this study fluoresced red to both short-wave (SW) and long-wave (LW) ultraviolet, whereas the greenish blue Ni-rich samples were inert to both. The fluorescence of the greenish blue Cr-rich samples was much weaker to SWUV than to LWUV. Red fluorescence has not been observed in most natural (except some light blue Sri Lankan and some rare dark blue stones [*Gem Reference Guide*, 1995]) or other synthetic blue sapphires, so it can be used as a diagnostic feature for greenish blue Cr-rich Tairus synthetic sapphires.

"Padparadscha"-colored samples fluoresced moderate orange to LWUV and weak orange to SWUV—reactions different from those of the natural and other synthetic sapphires of similar color reported in table 3. However, the reaction of natural yellow sapphires to UV radiation varies considerably, so this feature cannot serve to separate Tairus synthetic sapphires from natural stones of this color.

Inclusions and Other Internal Features. Some of the samples studied were internally flawless; others contained various amounts of inclusions. These internal features consisted of fluid inclusions, crystalline inclusions, and optical inhomogeneities.

TABLE 4. Properties of Tairus yellow (Ni^{3+}-Ni^{2+}) synthetic sapphires and some of their natural and other synthetic counterparts.

Property	Tairus hydrothermal synthetic	Natural, from Australia	Natural, from Sri Lanka
Color	Yellow to greenish yellow, light tones, strong saturation	Light yellow to strong "golden" yellow	Intense "golden" yellow to light or pale yellow
Color distribution (eye-visible)	Even	Occasionally color zoned	Not reported
Pleochroism	None	Not reported	Orangy yellow to grayish yellow
R.I. (n_ω)	1.767–1.765	1.774–1.772	1.768
R.I. (n_e)	1.758	1.765–1.763	1.760
Birefringence	0.007–0.009	0.008–0.009	0.008
S.G.	3.98	3.97–4.01	4.02
Fluorescence to LWUV	Inert or weak orange	Inert	"Apricot" red
Fluorescence to SWUV	Inert or very weak orange	Inert	"Apricot" orange
Reference	Present study	Coldham (1985)	Gunawardene and Rupasinghe (1986)

Two- and Three-Phase (Primarily Liquid) Inclusions. These could be divided into two major types. In both types, the inclusions consisted of two (gas-liquid) or three (a liquid, a gas, and a small crystal) phases. Two-phase inclusions were much more common than three-phase ones. Crystal phases were uncommon, but those present were easily seen in polarized light.

The first type consists of large inclusions with an irregular, elongate form located along planes perpendicular to the seed and running along planes parallel to one pair of the prismatic *a* faces (figure 11). We believe that these are primary (see, e.g., Roedder, 1984), formed when a small portion of growth solution was trapped under a crystal face during growth. These inclusions were apparently captured in flattened depressions on the surface of the growing crystal. Such depressions are typical of hydrothermal crystals grown on a seed (Smirnov, 1997). They were observed in only two faceted stones and a few crystals, which were blue, yellow, and colorless.

The second type are typical "fingerprints" (figure 12), with regular to irregular patterns confined to healed fractures, and therefore are secondary (see, e.g., Roedder, 1984). They also form perpendicular to the seed plate and extend in both directions. "Finger-

prints" were found in many faceted stones and in most of the crystals, in samples of almost all colors.

Crystalline Inclusions. Almost all of the green-to-blue samples examined contained crystalline inclusions. In some cases, these were single crystals that could be resolved only with high magnification and immersion. Other samples contained abundant inclusions in the form of small, flake-like aggregates of tiny crystals (figure 13); these inclusions could be clearly seen with a hand loupe. In some cases, when examined with bright, fiber-optic, oblique illumination, most of these crystalline inclusions appeared to have a metallic luster. With high magnification, they appeared to be opaque isometric grains a few micrometers in diameter. Because the growth process used Cu-containing oxygen buffers, it is likely that this metallic phase is copper.

Other crystals in these aggregates were transparent, colorless or near-colorless, and isotropic with an octahedral shape (figure 14). Because the individual crystals were so small (less than about 12 μm), we could not determine their composition with the available instrumentation. However, our recent experiments have revealed that the addition of a small amount of Mg to an alumina-bearing solution leads to the formation of spinel ($MgAl_2O_4$) crystals. Trace amounts of Mg could occur as an impurity in the charge used for the autoclave, so we suggest that these octahedra are spinel crystals.

Another type of transparent crystal was seen in the green synthetic sapphires. These crystals appeared as isolated platelets with regular hexagonal outlines and no apparent color (figure 15). The optical properties of these crystals suggest that they are gibbsite.

Optical Inhomogeneities and Color Zoning. We observed characteristic optical inhomogeneities—swirl- and chevron-like patterns—in all the greenish blue and green specimens, rough as well as faceted (figure 16). These terms commonly refer to wavy or angular features inside synthetic or natural crystals.

The swirl-like patterns resemble textures that can be seen in artificial glass. When the faceted samples were examined face up, these patterns appeared as very faint, contrasting wavy lines. Chevron patterns were seen in the same samples, but at an angle to the table plane. These swirls and chevrons were much more visible in the darker samples than in the lighter ones. They were less distinct in the pinkish orange (padparadscha type) syn-
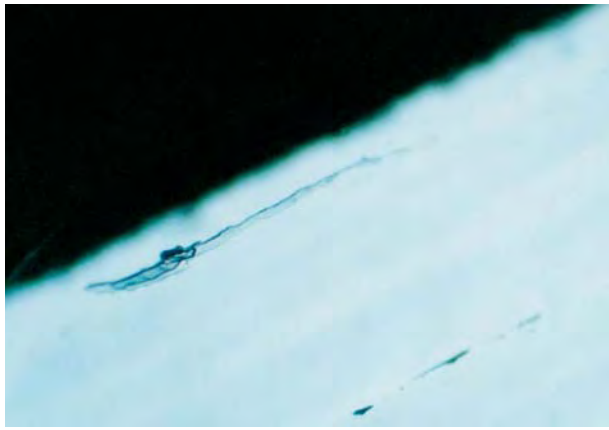
Figure 11. Irregular, elongate fluid-and-gas inclusions were found in some blue, yellow, and colorless Tairus synthetic sapphires, located along crystallographically oriented planes. Photomicrograph by S. Z. Smirnov; magnified 100×.
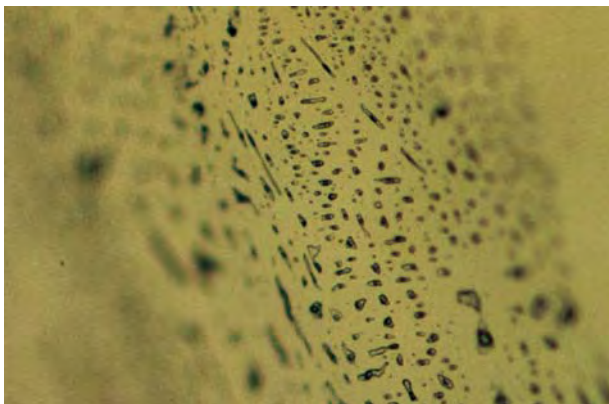

Figure 13. Flake-like crystalline inclusions are abundant in many of the green-to-blue Tairus hydrothermal synthetic sapphires. Photomicrograph taken by S. Z. Smirnov, with sample between crossed polarizers, immersed in methylene iodide, magnified 25×.

thetic sapphires and were not observed at all in the yellow or light pink samples.

Our studies revealed that the swirls and chevrons were typically seen in those samples that were grown on a seed plate with planar surfaces cut so as to be oriented at an angle to actual crystal faces (i.e., on a nonsingular crystal surface). They were found to represent boundaries between growth sectors of subgrains that formed on the seed plate as the crystal grew. Thus, the appearance of these patterns will be affected by the orientation of the table of a faceted stone. They are distinctly different from the angular growth zones found in natural and in flux-grown synthetic sapphires. Nor do they resemble the curved growth zoning usually seen in Verneuil-grown synthetic sapphires.

In several cross-sections of greenish blue Tairus

Figure 12. "Fingerprints" are common in the Cr- and Ni-doped Tairus synthetic sapphires. Photomicrograph by S. Z. Smirnov; magnified 100×.

samples, we observed color zoning parallel to the plane of the seed plate. The portion of the crystal nearest the seed plate was yellow, while the rest was greenish blue. This thin (about 0.5 mm) sharp zone is usually cut away during pre-forming, so it is seen only rarely in faceted stones.

Infrared Spectroscopy. Hydrothermally grown crystals commonly contain water in different forms. This is also true for corundum, both natural (see Smith, 1995, and references therein) and hydrothermal synthetic stones (Peretti and Smith, 1993). In rare cases, traces of water as OH^- groups may be found in Verneuil-grown crystals (Volynets et al., 1974; Beran, 1991). The form of water incorporation into sapphire and ruby has been the focus of many studies, because it can help clarify the genesis of the gem. Today it is generally accepted, on the basis of infrared spectroscopy, that water as OH^- groups enters the corundum structure as a compensating charge due to either the doping of the corundum with divalent cations or the formation of Al vacancies in the structure (Muller and Gunthard, 1966; Volynets et al., 1974; Beran, 1991). To examine this issue and also further distinguish the Tairus synthetic sapphires from their natural and other synthetic counterparts, we conducted an IR-spectroscopic study of the Tairus Ni- and Cr-doped hydrothermal synthetic sapphires.

The IR spectra of the greenish blue and green synthetic sapphires (samples 1 and 9, respectively, in table 1) are similar in the 4000-1600 cm^{-1} region (figure 17). This region is characterized by an intense wide band, with a maximum at 2980 cm^{-1}; a narrow peak at 2750 cm^{-1}; and five narrow peaks in
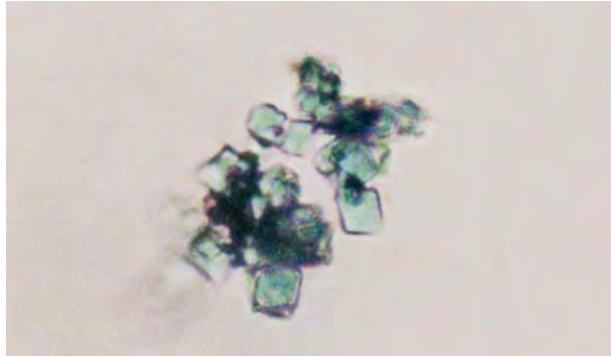
Figure 14. At high (500×) magnification, small transparent octahedral crystals (possibly spinel) can be seen inside some of the aggregates in greenish blue sapphires shown in figure 13. Photomicrograph by S. Z. Smirnov.

Figure 15. In the green hydrothermal synthetic sapphires, the transparent crystals appeared to be anisotropic hexagonal platelets, which may be gibbsite. When viewed between crossed polarizers, they showed a bright interference color. Photomicrograph by S. Z. Smirnov; magnified 500×.

the region between 2500 and 2000 cm^{-1}. In the spectrum of the greenish blue sapphire (A), there is a shoulder near 3300 cm^{-1}. In the spectrum for the green sample (B), two narrow peaks are superimposed on the wide band at 3400 and 3310 cm^{-1}.

The presence of an intense wide band near 3000 cm^{-1} is attibuted to OH^- groups contained in aluminum oxides. It is observed in the IR spectra of diaspore (AlOOH; Ryskin, 1974) and in the spectra of natural corundum containing divalent cations (Muller and Gunthard, 1966; Eigenmann and Gunthard, 1971; Volynets et al., 1974). The IR spectra of the Tairus Ni-doped synthetic sapphires (see figure 17) are similar to those for Ni-containing corundum grown by the Verneuil method in a reducing, hydrogen atmosphere (Eigenmann and Gunthard, 1971). Following these authors, we believe that the 2980 cm^{-1} band is the absorption band of OH^- groups that compensate the charge for the $Al^{3+}+O^{2-} \rightarrow Ni^{2+}+(OH)^-$ replacement.

The narrow peaks observed between 3600 and 3000 cm^{-1} are also related to the absorption of OH^- groups which compensate for charge deficiency due to the formation of cation vacancies. These peaks have been reported both for natural (Smith, 1995, and references therein) and synthetic corundum (Belt, 1967; Eigenmann and Gunthard, 1971; Volynets, 1974; Beran, 1991; Peretti and Smith, 1993, 1994). The peaks at 3310 and 3400 cm^{-1}, observed in the infrared spectrum of our green sample (see figure 17), were also reported earlier (Smith, 1995).

Peaks near 2000 cm^{-1} may be observed in the IR spectra of other OH^- containing aluminum oxides. However, the peaks at 2114 and 1984 cm^{-1} that are present in the spectrum of diaspore (Ryskin, 1974; Smith, 1995) were absent from the spectra of our hydrothermal synthetic sapphires. Therefore, we believe that the bands near 2000 cm^{-1} in our samples are not related to diaspore inclusions, especially as the samples studied were free of inclusions (at 100× magnification). The IR absorption lines for CO molecules may occur between 2133 and 2148 cm^{-1} (Hallam, 1973). Wood and Nassau (1967) observed the absorption bands related to CO_2 molecules in beryl structure channels at 2354 cm^{-1}. Because the Tairus crystals grew in carbonate solutions of complex composition, the incorporation of CO, CO_2, CO_3^{2-}, and other forms of carbon oxides into the growing crystal is very likely. Thus, we believe that the narrow bands at 2460, 2400, 2264, 2136, and
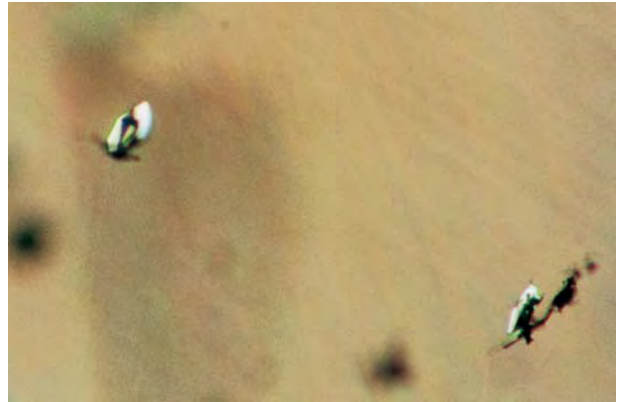
Figure 16. Swirl-like and chevron patterns were commonly seen in the Tairus synthetic green-to-greenish blue sapphires. Immersed in methylene iodide, magnified 100×; photomicrograph by S. Z. Smirnov.

2016 cm^{-1} could be related to the C–O bond in different carbon oxides that were incorporated into the sapphire crystals. Strong pleochroism is another feature of these bands, which suggests that these C–O bonds are part of the corundum structure and are not caused by separate carbon oxide species (e.g., CO or CO_2 in fluid inclusions).

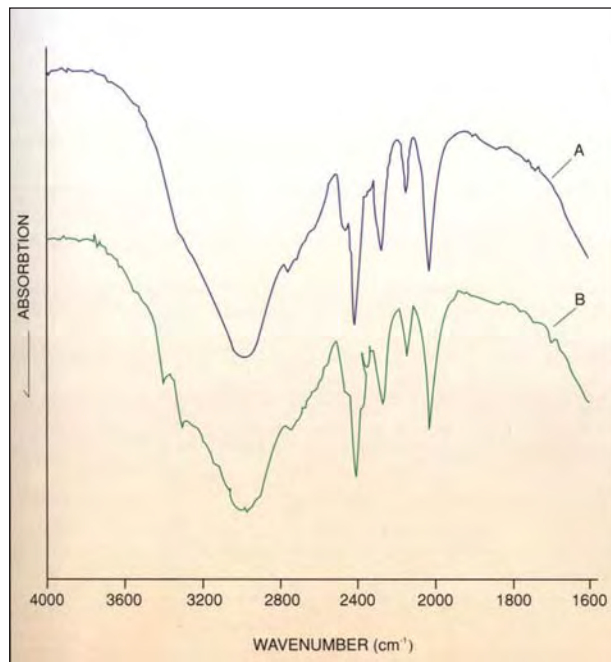These bands were also reported for Tairus hydrothermal synthetic rubies by Peretti and Smith. (1993). We have not found a description of such bands in the literature for natural and other synthetic sapphires. Therefore, we believe that the five narrow peaks between 2500 and 2000 cm^{-1} are characteristic of Tairus synthetic sapphires.

IDENTIFYING CHARACTERISTICS OF TAIRUS HYDROTHERMAL SYNTHETIC SAPPHIRES

Previously, blue, green, and yellow sapphires were grown only by flux- or melt-growth techniques, but the synthetic sapphires studied for this article more closely resemble their natural counterparts because they have been grown from a hydrothermal solution, as takes place frequently in nature. Nevertheless, there are a number of features by which an experienced gemologist can separate these sapphires from their natural counterparts and other synthetic sapphires:

1. The swirl-like patterns observed in Tairus synthetic sapphires are common to most synthetic crystals grown on seed plates under hydrothermal conditions and are rare for natural stones.
2. The red reaction to UV radiation of the greenish blue synthetic sapphires containing Cr is different from that of most natural and other synthetic sapphires.
3. The crystalline copper inclusions and flake-like aggregates seen in the Tairus synthetics are not present in natural sapphires. Metallic inclusions are common in melt- and flux-grown synthetics, but they usually consist of platinum-group metals.
4. Ni, an important chromophore in the Tairus synthetic sapphires, is not found in natural sapphires or most synthetic ones.
5. The absorption spectra of the greenish blue Ni-doped Tairus synthetic sapphires differ from those of natural blue sapphires, which owe their color to Fe and Ti. The spectrum (in unpolarized light) of a greenish blue Tairus synthetic sapphire includes three intense bands—at 377, 599, and 970 nm—and two weak bands, at 435 and 556 nm.
6. Five narrow peaks between 2500 and 2000 cm^{-1} in the infrared spectra of Tairus synthetic sapphires clearly separate them from their natural and other synthetic counterparts.

CONCLUSION

The technology to manufacture synthetic sapphire in a wide variety of colors by means of hydrothermal growth has been developed by researchers of the Tairus joint venture. This was achieved by doping synthetic corundum with different amounts of Ni^{2+}, Ni^{3+} and Cr^{3+}. Specific colors are also produced by controlling the oxidation-reduction environment. Although these colors overlap those of most natural and other synthetic sapphires, the Tairus synthetic sapphires can be readily identified on the basis of their distinctive internal features (swirl-like patterns and copper inclusions), visible-range and infrared spectra, and the presence of Ni as a trace element.

To date, thousands of hydrothermal synthetic sapphires have been grown at the Tairus factory in

Figure 17. The infrared absorption spectra of greenish blue (A) and green (B) Tairus synthetic sapphires are very similar (they are shown here offset for purposes of comparison). The curves have been corrected for a spurious absorption attributed to CO_2.

Novosibirsk (Russia) and cut at the Pinky Trading Co. facilities in Bangkok. Greenish blue, pinkish orange, and yellow sapphires are commercially available as cut stones up to 4 ct.

REFERENCES

Belt R.F. (1967) Hydrothermal ruby: infrared spectra and X-ray topography. *Journal of Applied Physics*, Vol. 38, No. 6, pp. 2688–2689.

Beran A. (1991) Trace hydrogen in Verneuil-grown corundum and its color varieties: an IR spectroscopic study. *European Journal of Mineralogy*, Vol. 3, No. 6, pp. 971–975.

Boksha O.N., Grum-Grzymailo S.V., Pasternak L.B., Popova A.A., Smirnova E.F. (1970) Synthesis and optical spectra of corundums doped with transition elements. In S.V. Grum-Grzymailo, B.S. Skorobogatov, P.P. Feofilov, and V.I. Cherepanov, Eds., *Spectroscopy of Crystals*, "Nedra," Moscow, pp. 295–302 (in Russian).

Burns R.G. (1981) Intervalence transition in mixed-valence minerals of iron and titanium. In G.W. Wetherill, A.L. Albee, and F.G. Stehli, Eds., *Annual Review of Earth and Planetary Sciences*, Vol. 9, Annual Reviews Inc., Palo Alto, CA, pp. 345–383.

Catalogue of Colored Glasses (1967). "Mashinostroenie," Moscow (in Russian).

Coldham T. (1985) Sapphires from Australia. *Gems & Gemology*, Vol. 21, No. 3, pp. 130–146.

Crowningshield R. (1983) Padparadscha: What's in a name? *Gems & Gemology*, Vol. 19, No. 1, pp. 30–36.

Eigenmann K., Gunthard Hs.H. (1971) Hydrogen incorporation in doped α-Al_2O_3 by high temperature redox reactions. *Chemical Physics Letters*, Vol. 12, No. 1, pp. 12–15.

Feklichev V.G. (1989) *Diagnostic Constants of Minerals*. "Nedra," Leningrad (in Russian).

Furui W. (1988) The sapphires of Penglai, Hainan Island, China. *Gems & Gemology*, Vol. 24, No. 3, pp. 155–160.

Gem Reference Guide (1995) Gemological Institute of America, Santa Monica, CA, 270 pp.

Goldschmidt V. (1916) *Atlas der Krystalformen*. Carl Winters Universtatsbuchhandlung, Heidelberg.

Gübelin E. (1982) New synthetic rubies made by Professor P.O. Knischka. *Gems & Gemology*, Vol. 18, No. 3, pp. 165–168.

Gunawardene M., Rupasinghe S. (1986) The Elahera gem field in central Sri Lanka, *Gems & Gemology*, Vol. 22, No. 2, pp. 80–95.

Hallam H.E. (1973) Molecules, trapped in low temperature molecular matrices. In Hallam H.E., Ed., *Vibrational Spectroscopy of Trapped Species: Infrared and Raman Studies of Matrix-Isolated Molecules, Radicals and Ions*, Wiley-Interscience, London-New York, pp. 68–132.

Kammerling R.C., Koivula J.I., Fritsch. E. (1994) An examination of Chatham flux-grown synthetic pink sapphires. *Journal of Gemmology*, Vol. 24, No. 3, pp. 149–154.

Kane R. (1982) The gemological properties of Chatham flux-grown synthetic orange sapphire and synthetic blue sapphire. *Gems & Gemology*, Vol. 18, No. 3, pp. 140–153.

Kuznetsov V.A., Shternberg A.A. (1967) Crystallization of ruby under hydrothermal conditions. *Soviet Physics-Crystallography*, Vol. 12, No. 2, pp. 280–285.

Laudise R.A., Ballman A.A. (1958) Hydrothermal synthesis of sapphire. *Journal of the American Chemical Society*, Vol. 80, pp. 2655–2657.

Minomura S., Drickamer H.G. (1961) Effect of pressure on the spectra of transition metal ions in MgO and Al_2O_3. *Journal of Chemical Physics*, Vol. 35, No. 3, pp. 903–907.

Muller R., Gunthard Hs.H. (1966) Spectroscopic study of the reduction of nickel and cobalt ions in sapphire. *Journal of Chemical Physics*, Vol. 44, No. 1, pp. 365–373.

Peretti H.A., Smith C.P. (1993) A new type of synthetic ruby on the market: Offered as hydrothermal rubies from Novosibirsk. *Australian Gemmologist*, Vol. 18, No. 5, pp. 149–157.

Peretti H.A., Smith C.P. (1994) Letters to the editor. *Journal of Gemmology*, Vol. 24, No. 1, pp. 61–63.

Platonov A.N., Taran M.N., Balitsky V.S. (1984) *The Nature of Gemstone Colors*. "Nedra," Moscow, 196 pp. (in Russian).

Roedder E. (1984) Fluid inclusions. *Reviews in Mineralogy*, Vol. 12, 644 pp.

Ryskin Ya.I. (1974) The vibration of protons in minerals: Hydroxyl, water and ammonium. In Farmer V.C., Ed., *The Infrared Spectra of Minerals*, Mineralogy Society Monograph, London, pp. 137–181.

Smirnov S. (1997) The inclusions of mineral-forming media in synthetic and natural gemstones (formation mechanisms and genetic application). Ph.D. diss., Novosibirsk (in Russian).

Smith C.P. (1995) A contribution to understanding the infrared spectra of rubies from Mong Hsu, Myanmar. *Journal of Gemmology*, Vol. 24, No. 5, pp. 321–325.

Smith C.P., Kammerling R.C, Keller A.S., Peretti A., Scarratt K.V., Nguen Dang Khoa, Repetto S. (1995) Sapphires from Southern Vietnam. *Gems & Gemology*, Vol. 31, No. 3, pp. 168–188.

Volynets F.K., Sidorova E.A., Stsepuro N.A. (1974) OH^- groups in corundum crystals which were grown with the Verneuil technique. *Journal of Applied Spectroscopy*, Vol. 17, No. 6, pp. 1626–1628.

Wood D.L., Nassau K. (1967) Infrared spectra of foreign molecules in beryl. *Journal of Chemical Physics*, Vol. 47, No. 7, pp. 2220–2228.

Wright W.D. (1964) *The Measurement of Colour*, 3rd ed. Van Nostrand, New York, 291 pp.

Yakubova V.V. (1965) Corundum. In F.V. Chukhrov and E.M. Bornschted-Kupletskaya, Eds., *Minerals*, Nauka, Moscow, pp. 63–75 (in Russian).

MULTICOLORED BISMUTH-BEARING TOURMALINE FROM LUNDAZI, ZAMBIA

By Mary L. Johnson, Cheryl Y. Wentzell, and Shane Elen

Tourmalines from an alluvial deposit near Lundazi in Zambia consist of color zoned pink/colorless/yellow-green "watermelon" nodules; many fashioned stones contain patches and blends of all three colors. Although these elbaite tourmalines are unusually rich in bismuth (up to 0.49 wt.% Bi_2O_3), the presence of bismuth apparently has no effect on their gemological properties. Approximately 10,000 carats of fashioned stones are known to have been produced from October 1996 to mid-1997.

At the 1997 Tucson show, one of the authors (CYW) saw some unusual tourmalines that were reportedly from recent workings in Zambia. Marc Sarosi Co., of Los Angeles, was marketing this material as "mixed-color" tourmaline: Colors available include light-to-medium-toned desaturated pink, orange, green, and yellowish green (see, e.g., figure 1), as well as colorless, and individual fashioned stones frequently contain regions of two or more of these colors. Coincidentally, we found that the chemistry of these tourmalines was unusual, with elevated contents of bismuth (Bi). The purpose

of this article is to report on this new deposit and to document the unusual composition and other properties of this Bi-bearing elbaite.

LOCATION AND ACCESS

The multicolored tourmalines described in this report were found in a field in the Kalungabeba area of the Lundazi district (figure 2), about 16 km (10 miles) southwest of Lundazi itself, according to Mr. Sarosi, who visited the site in early 1997. The stones were originally discovered by a person who was digging a hole for an outhouse.

A rough dirt road leads to this site from Lundazi; it is best traveled by four-wheel-drive vehicle. During the rainy season, from about late December until March, the area is often inaccessible.

GEOLOGY

The geologic feature known as the Mozambique Belt forms a triangular area bounded by the Luangwa valley (eastern Zambia), the Zambezi valley (in northern Mozambique), and Lake Malawi (in Malawi; again, see figure 2). The main rock units in the belt are high-grade gneisses and granitic rocks of

ABOUT THE AUTHORS

Dr. Johnson is manager of Research and Development, and Ms. Wentzell is staff gemologist, at the GIA Gem Trade Laboratory, Carlsbad, California. Mr. Elen is a research gemologist in GIA Research, Carlsbad.

Please see acknowledgments at end of article.

Figure 1. This 9.44 ct pink elbaite tourmaline and its 11.48 ct yellow-green companion are among the thousands of carats of gem tourmaline that have been fashioned from material recovered recently from a deposit near Lundazi, Zambia. Note the distinctive "checkerboard" cut. Courtesy of Marc Sarosi; photo © GIA and Tino Hammid.

the 2.05–2.68 billion-year-old Basement Complex, as well as metacarbonates, schists, metavolcanics, and quartzites of the 1.35–2.05 billion-year-old Muva Supergroup (Kamona, 1994). The gneisses and schists are intruded by later granitic pegmatites, which commonly have quartz cores and outer zones of microcline feldspars. Muscovite is usually concentrated at the contact between these zones, and aquamarine may occur in either zone. The pegmatites may also contain gem tourmaline, as well as concentrations of rare elements (Nb, Ta, Li, Cs, Y, La, and U). The Mozambique Belt also hosts gold mineralization, in sheared quartz veins occurring in schists and metavolcanics of the Muva supergroup; bismuth minerals (bismuthinite, bismutite) are found in this gold ore.

Tourmaline has been mined in at least three areas in eastern Zambia (figure 2): Lundazi, at the northeast end of the Belt (e.g., the Aries deposit: Kamona, 1994); Chipata, in the center of the belt (see, e.g., Schmetzer and Bank, 1984a and b); and Nyimba, in the south (e.g., the Hofmeyer deposit: Kamona, 1994). The Chipata area is known to produce "intense" yellow tourmalines, (Schmetzer and Bank, 1984a and b; Koivula, 1985); red to brownish red tourmalines (Koivula and Fryer, 1985); and

brownish orange and brownish green stones (mentioned by Koivula and Kammerling, 1991). The Hofmeyer pegmatite near Nyimba is the source of tourmaline varieties rubellite and green "emeraldolite" (Kamona, 1994). Bank (1982) described yellow-green, green, red, brown, and violet tourmalines from Zambia, but he provided no specific information about their source. The bicolored tourmaline mentioned by Thomas (1982) may have come from Lundazi or Nyimba.

MINING AND PRODUCTION

The Kalungabeba deposit is alluvial, and the tourmaline-bearing gravels also contain spessartine, aquamarine, and dispersed quartz. Both pink and "multicolored" tourmalines have been found, the former occurring in a variety of crystal shapes, but the latter always as nodules; all show wear from alluvial transport. At the time of Mr. Sarosi's visit, there were no known gem-bearing outcrops in the immediate vicinity of this field, although Mr. Sarosi reports that subsequent mining has unearthed spessartine garnet–bearing pegmatites.

Production at this locality started in October 1996. At the time of Mr. Sarosi's visit in early 1997, about 90% of the tourmaline was coming from a

Figure 2. A new deposit of multicolored tourmalines has been found in a field in the Kalungabeba area of Zambia's Lundazi district, about 16 km southwest of the city of Lundazi.

single pit measuring about 12 m (40 feet) in diameter and 6 m (20 feet) deep. Approximately 700 unlicensed miners worked the deposit during the initial "rush"; after five died, the Ministry of Mines closed the area and then issued a number of licenses (around May 1997). At present, approximately 60 miners are working the deposit by hand, hauling loads of gravel to an adjacent water-filled depression, where wet-sieving is done to recover the gem rough. About 100 kg of facet-quality rough (and several tons of lower-quality material) had been recovered as of June 1997. By this time, Mr. Sarosi, who believes he purchased most of the available multicolored rough, had fashioned some 10,000 carats of goods, ranging up to 20 ct.

MATERIALS AND METHODS

Nineteen faceted stones (3.04 to 11.48 ct) and 10 nodules (10.28 ct [9 × 11 × 14 mm] to 20.61 ct [12 × 14 × 15 mm]) were examined; these were chosen to represent the variety of material on hand. The faceted stones consisted of six pink, five yellow-green, and eight multicolored samples; the rough nodules were all multicolored green and pink. We looked at the rough samples with diffuse transmitted illumination to characterize the color zoning,

but we did not test these further gemologically.

Gemological characterization of the fashioned samples was performed as follows on all 19 faceted stones, except where noted. We observed the face-up colors using daylight-equivalent fluorescent light sources. Polarization behavior was noted using a GIA GEM Instruments Illuminator polariscope, and we determined pleochroism using a dichroscope and the polariscope light source. The colors seen with a "Chelsea" filter were noted for 13 of the 19 faceted stones, and we measured refractive indices for these same 13 stones using a Duplex II refractometer with a sodium-equivalent light source and a polarizing eyepiece. Specific gravities were determined by hydrostatic weighing (13 stones). Fluorescence was observed in a darkened room using a controlled viewing environment and a GIA GEM short-wave/long-wave ultraviolet lamp. Absorption spectra were noted with a Beck spectroscope in a desk-model configuration and transmitted light. Microscopic properties were observed with a gemological microscope (Reichert Stereo Star Zoom) equipped with polarizing plates.

We investigated trace-element chemistry by qualitative energy-dispersive X-ray fluorescence (EDXRF) spectroscopy, using a Tracor Xray (now

Spectrace Instruments) Spectrace 5000 instrument with a rhodium-target X-ray tube. Complete spectra were acquired for six faceted stones, including a bicolored stone for which both pink and green regions were analyzed. It is unusual to see bismuth in tourmaline (Paraíba stones being a notable exception; see, e.g., Fritsch et al., 1990), and we were quite surprised to see evident Bi peaks in the EDXRF spectra of the first stones we examined. Therefore, for eight other stones, data were collected only in the bismuth region (8–18 keV) of the EDXRF spectrum.

Electron microprobe analyses were obtained and processed at the University of Manitoba, Canada, for three samples (3 points each on a 9.44 ct pink cut stone and an 11.48 ct yellow-green cut stone, and 8 points in a traverse along a polished slice from a multicolored nodule). The following elements were quantitatively measured: Na, Mg, Al, Si, P, F, K, Ca, Ti, V, Cr, Mn, Fe, Zn, and Bi (Bi_2Se_3 was used as a Bi standard for analyses, and the detection limit was 0.17 wt.% Bi_2O_3). The analytical conditions and methods for calculating the tourmaline formulas are given in Burns et al. (1994).

APPEARANCE AND GEMOLOGICAL PROPERTIES

Visual Appearance. *Rough Material.* The nine rough samples (some of which are illustrated in figure 3) seemed typical for tourmaline, showing three-sided symmetry in cross-section. The rounded top and bottom surfaces showed conchoidal fracture, creating an overall nodular shape. Some parallel striations were evident on the sides of the nodules, which is also typical for tourmaline; however, all samples showed worn surfaces.

With diffuse transmitted light, we saw that the rough was zoned "watermelon" fashion, typically with pink triangular cores and green rinds that approached hexagons in outline. Paler (green to colorless) zones were sometimes evident between the pink cores and green rinds (again, see figure 3).

Cut Stones. We examined one round, one cushion, two rectangular, four square, and 11 oval cut stones, all modified brilliants (see, e.g., figure 4). All of the fashioned stones had been modified so that the crown area was covered with many facets ("checkerboard" cut). The colors of these samples are summarized in table 1. Color distribution ranged from even through uneven to multicolored. Most of the multicolored stones were fashioned to
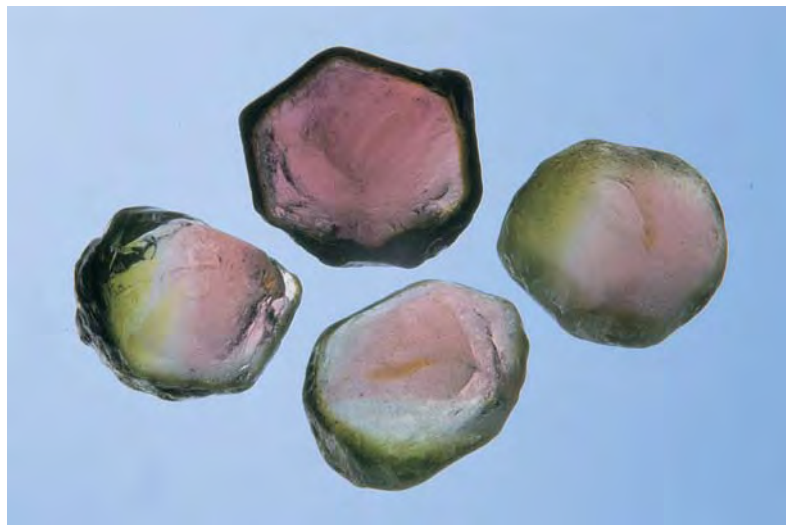
Figure 3. These four tourmaline nodules from the new Lundazi deposit show "watermelon" color zoning. Total weight is 55.73 ct, with the largest stone measuring about 15 × 14 × 12 mm. Courtesy of Marc Sarosi; photo by Maha DeMaggio.

show patches of color throughout (figure 5), rather than the regular bars of color that are commonly seen in a bicolored or tricolored tourmaline.

According to Mr. Sarosi, this "mixed-color" tourmaline presents some unusual challenges to the gem cutter. To obtain the desired multicolored appearance, Mr. Sarosi noted, the green rind on the rough must be retained in the faceted stone. In addition, the rind also seems to impart physical stability to the stone; if all of it is removed, the stone often breaks during fashioning. Regardless, the tourmaline rough cracks into pieces if sawn. A larger than expected number of stones break during faceting, and a few have even broken after cutting was completed. Because of this, the largest fashioned stones have only reached 20 ct in size, and the rough has a yield of about 20% (in comparison to an expected yield of 30%–33%). Mr. Sarosi finds that the "checkerboard" cut (again, see figure 1) works best to minimize breakage during cutting.

Physical and Optical Properties. Since we might expect the physical and optical properties of tourmaline to vary with color, we arranged the data into three classes: pink (including red), yellow-green, and multicolored stones. The properties for each of these groups are summarized in table 1. A desaturated "blend" of pleochroic colors was seen in some of the multicolored stones. All 13 stones on

Figure 4. The multicolored tourmalines are fashioned as either a single color or as a mixture of colors in a single stone. These four elbaite tourmalines, which range from 3.38–8.14 ct, were part of the study sample. Courtesy of Marc Sarosi; photo by Maha DeMaggio.

which refractive index readings were taken had R.I.'s in the range of n_ε = 1.619–1.620 and n_ω = 1.637–1.639, with birefringences of 0.018–0.020. None of the stones tested showed any reaction to UV radiation. These properties are not unusual for tourmalines of these colors.

Spectroscopy. The samples showed typical spectra for tourmalines of similar colors (again, see table 1).

Microscopy/Inclusions. The main inclusions seen with magnification were: "pinpoints" (very small minerals), growth tubes (figure 6) or needles, and fractures. All of these inclusions are common in tourmaline, regardless of its source, and there was no indication of possible included bismuth minerals (e.g., metallic bismuthinite or native bismuth, or high-relief near-colorless bismutite). Small opaque reddish orange spheres were noted in the ends of

TABLE 1. Gemological properties for various colors of Lundazi tourmaline.

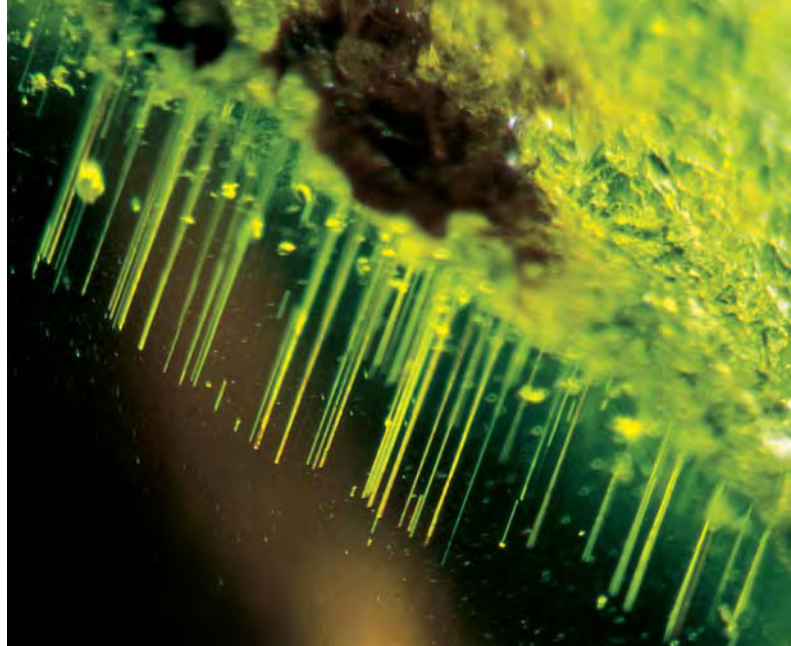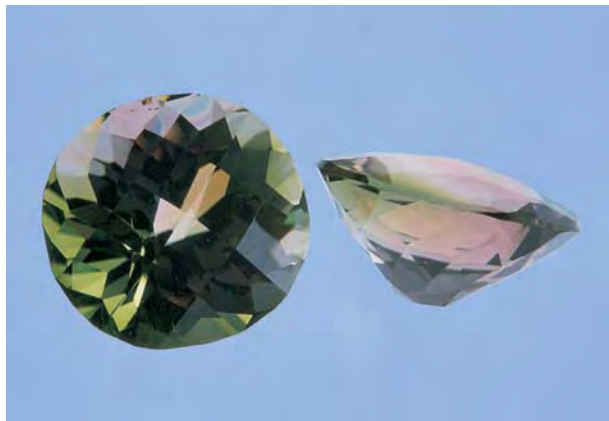| Property	Pink	Yellow-green	Multicolored
Weight	3.04–9.44 ct	4.75–11.48 ct	3.38–8.14 ct
Color	Purplish pink to red-purple to orangy red	Yellowish green to greenish yellow	Pink and yellowish green
Pleochroism	Purplish red to red—orangy red to yellow	Yellowish green to green—yellow to green to green-brown	Mixtures of the colors seen in the pink and yellow-green stones
Optic character	Uniaxial	Uniaxial	Uniaxial
Color-filter reaction	Gray-green	Slightly grayish green to green	Gray-green to grayish green
R.I. (n_ε)	1.619–1.620	1.619–1.620	1.620
R.I. (n_ω)	1.637–1.638	1.638–1.639	1.639
Birefringence	0.018	0.018–0.020	0.019
Specific gravity	3.041–3.043	3.040–3.049	3.045–3.055
Reaction to long- and short-wave UV	Inert	Inert	Inert
Absorption spectrum	Lines at 451 and 458 nm, weak group of 4 or 5 lines to 500 nm; 535 nm line, 490–540 nm band, absorption below 415 nm	One stone: lines at 460 and 500 nm, general absorption above 640 nm. The rest: weak general absorption below 500 nm, faint to weak diffuse 500 nm line	Mixture of pink and yellow-green spectra
Inclusions	"Pinpoints" of tiny colorless crystals, parallel growth tubes, one small transparent plate; filled growth tube	Clean, or scattered "pinpoints" only; "pinpoints" lying in growth planes; thin growth tubes near perimeter of stone	Curved or planar clouds of "pinpoints"; growth tubes, primarily in green areas; filled growth tubes
Growth structures	Minimal to angular	Wavy and/or angular	Straight, wavy, and/or angular

growth tubes in four samples.

The prominent growth features we identified were growth bands—sharp boundaries between regions of slightly different refractive index, similar to the graining seen in diamonds. These bands were straight, angular, or wavy. Angular growth bands were seen in pink, yellow-green, and multicolored stones; wavy growth bands in combination with angular growth bands were seen in yellow-green and multicolored stones; and straight growth bands in combination with angular growth bands were seen in multicolored stones. In one pink stone, we saw only minimal growth banding. The growth bands were pronounced (eye-visible) in nearly all stones; however, no strain was obvious in any stone when viewed between crossed polarizers.

CHEMICAL ANALYSIS

EDXRF. We performed EDXRF analyses on six of the faceted tourmalines: two pink, one yellow-green, two multicolored (analyzed without regard to color orientation), and one pink-and-yellowish green bicolor in which both color regions could be separately examined. Selected-energy-region EDXRF analyses for bismuth were performed on eight additional stones—three pink, two yellow-green, and three multicolored. These analyses could be roughly quantified on the basis of the microprobe results (see below). We found major amounts

Figure 6. Some of the growth tubes in the green rind of this 12.02 ct multicolored tourmaline nodule are partially filled with an orange material. Photomicrograph by John I. Koivula; magnified 20×.

(greater than 1 wt.% oxide) of Al and Si, and minor (greater than 0.1 wt.% oxide) Ca and Mn. The Fe content could be classified as major, minor, or trace (less than 0.1 wt.% oxide) in these stones, depending on color: The amount of absorption due to Fe is appreciably greater in the spectra of yellow-green stones (or regions) than in those of pink stones (or regions). Bismuth occurred at minor to trace levels. Trace amounts of Cu, Zn, Ga, and Ge were found in all the EDXRF spectra. Ti was seen in the yellow-green region of one multicolored stone and in another multicolored stone at the trace level. Pb was detected in one multicolored stone.

Each of the eight spectra taken using conditions to detect only Bi revealed relatively high amounts of that element (i.e., at the minor-element level), regardless of the color of the material. Raw counts in the EDXRF analyses suggest that more Bi is present in the early-forming pink zones (i.e., the cores of the multicolored nodules) than in the later-forming yellow-green rinds.

Electron Microprobe. Three samples were examined in more detail using an electron microprobe (the two cut stones shown in figure 1 and the multicolored nodule shown in figure 7); the results are given in table 2. The compositions indicate that these tourmalines are all elbaite, the sodium-, lithium-, and aluminum-rich species in the tourmaline mineral group. As with the EDXRF analyses, the green rind of the tourmaline nodule showed less bismuth

Figure 5. The multicolored nature of the fashioned stones comes from the cutter's incorporation of the different color zones in the original tourmaline rough. Attractively mixed in the face-up view of this 5.87 ct Lundazi tourmaline, the color zones are clearly evident in the side view of a 4.94 ct Lundazi stone. Photo by Maha DeMaggio.

than the pink core. The most bismuth (0.49 wt.%) was found in the pink stone.

DISCUSSION

The gemological properties of the Zambian tourmalines we studied are consistent with those of the tourmalines from the Lundazi area described by Thomas (1982). One reason for extensive past interest in Zambian tourmalines was the possibility that specimens from the Chipata area might have been the hypothetical manganese-rich species tsilaisite, although none proved to be so (see, e.g., Schmetzer and Bank, 1984a and b; Shigley et al., 1986). All the stones examined for the present study have low Mn contents.

The unusual feature of these elbaites is their high Bi contents. Traces of Bi are sometimes found in rocks crystallized from late-stage silicic melts (i.e., in granitic pegmatites: see, e.g., Mintser, 1979); in Zambia, a possible source for this element is the nearby gold deposits (Kamona, 1994). However, bismuth does not readily substitute for common elements in silicates (see, e.g., Kupčík, 1972), so its presence in tourmaline is unexpected.

Figure 7. Microprobe analyses across the primary color zones—pink and green—in this Lundazi tourmaline nodule showed higher Bi contents in the pink core. Courtesy of Marc Sarosi; photo © GIA and Tino Hammid.

TABLE 2. Electron microprobe data for three Lundazi tourmalines.

Oxide (wt.%)	Pink (3 points)	Yellow-green (3 points)	Multicolored nodule Green rind (4 points)	Multicolored nodule Pink core (4 points)
SiO_2	38.00–38.50	38.00–38.90	38.00–39.10	38.60–39.10
TiO_2	nd[a]	0.03–0.05	0.05–0.34	nd–0.02
Al_2O_3	41.00–41.30	39.20–40.60	37.10–40.00	41.30–41.90
V_2O_3	nd–0.01	nd–0.02	nd	nd
Cr_2O_3	nd–0.05	nd–0.12	nd–0.09	nd–0.12
Bi_2O_3	**0.34–0.49**	**nd–0.13**	**nd–0.02**	**0.16–0.25**
MgO	nd	0.04–0.07	0.21–0.61	nd
CaO	0.51–0.58	0.51–1.07	0.09–0.34	0.38–0.47
MnO	0.18–0.26	0.30–0.48	0.36–0.91	0.26–0.38
FeO	nd–0.07	0.69–0.84	1.70–4.19	0.03–0.13
ZnO	nd–0.02	0.01–0.03	nd–0.05	nd
Na_2O	1.66–1.74	1.74–1.83	2.03–2.49	1.70–1.82
K_2O	nd–0.01	0.01–0.02	nd–0.02	nd–0.01
P_2O_5	nd–0.01	nd	nd–0.01	nd–0.03
Li_2O[b]	2.14–2.19	2.04–2.31	1.80–2.16	2.11–2.27
F	0.01–1.12	0.88–1.00	0.95–1.12	0.85–1.07
B_2O_3[c]	11.03–11.13	11.03–11.09	10.87–11.19	11.18–11.25
H_2O[c]	3.30–3.84	3.35–3.39	3.29–3.40	3.37–3.46
-O=F	(-0.47)–nd	(-0.42)–(-0.37)	(-0.47)–(-0.40)	(-0.45)–(-0.36)
Total	99.01–99.84	99.39–100.09	100.06–101.15	100.27–101.39

[a]nd=none detected.
[b]Determined by assuming there are 3 Y cations per formula unit, among them Ti, Al, V, Cr, Mg, Mn, Fe, Zn, and Li (see Burns et al., 1994).
[c]Determined from tourmaline stoichiometry: 3 B per formula unit, 4 (OH + F) per formula unit.

Examples of Bi-bearing tourmaline are relatively uncommon. In an exhaustive literature search, Dietrich (1985) noted trace amounts of Bi in dravite-uvite and schorl tourmalines, but not in elbaites. Peretyazhko et al. (1991) described rubellites (elbaites) from miarolitic granitic pegmatites in the Malkhan Range in Central Transbaikalia, Russia, that contained both Bi (up to 0.55 wt.% Bi_2O_3) and lead. The elbaites from São José da Batalha, Paraíba, Brazil, are best known for their copper contents, but they also contain up to 0.83 wt.% Bi_2O_3 (on the basis of microprobe analyses by Fritsch et al., 1990; Henn et al., 1990; and Rossman et al., 1991). In addition, according to unpublished microprobe data, a color-change tourmaline from East Africa (described by Koivula and Kammerling, 1991) contained trace amounts of Bi.

One reason for the paucity of information on bismuth in tourmaline is that most modern analyses are performed with the electron microprobe, which has a relatively high detection limit (e.g., 0.17 wt.% Bi_2O_3 in our analyses; however, EDXRF is considerably more sensitive for Bi. Further, unless bismuth is looked for in microprobe analyses, it will

not in general be found. We would not be surprised if tourmalines from other localities are also found to contain significant amounts of bismuth.

It is not apparent what effect, if any, bismuth has on the gemological properties of tourmaline. Bismuth is not a chromophore (see, e.g., Kupčík, 1972). As a heavy element, its presence should increase both specific gravity and refractive index (see, e.g., Bloss et al., 1983), but neither of these properties appears to have been affected at the concentration levels noted in our samples.

CONCLUSION

Significant amounts of tourmaline from a new alluvial deposit in the Lundazi area of Zambia are now available. These attractive tourmalines are notable for their chemical composition (Bi-bearing elbaite) as well as for the unusual "mixed-color" appearance of the faceted stones, a consequence of the durability problems inherent in the rough. About 10,000 ct of faceted stones are now available, and tons of lower-quality material have been mined.

Bismuth is not usually present at detectable levels in gem tourmaline. In the Lundazi stones,

more Bi was measured in the pink cores than in the green rinds, and individual analyses give concentrations of up to 0.49 wt.% Bi_2O_3. Nevertheless, the presence of Bi in these tourmalines does not appear to influence their gemological properties. The most distinctive property of these stones is the growth zoning; otherwise, the gemological properties are consistent with those recorded for elbaites of similar colors from other localities.

REFERENCES

Bank H. (1982) Turmaline diverser Grün- und Rottöne aus Sambia. *Zeitschrift der Deutschen Gemmologischen Gesellschaft*, Vol. 31, No. 1/2, pp. 91–92.

Bloss F.D., Gunter M., Shu C.S., Wolfe H.E. (1983) The Gladstone-Dale constants: A new approach. *Canadian Mineralogist*, Vol. 21, No. 1, pp. 93–99.

Burns P.C., MacDonald D.J., Hawthorne F.C. (1994) The crystal chemistry of manganese-bearing elbaite. *Canadian Mineralogist*, Vol. 32, No. 1, pp. 31–41.

Dietrich R.V. (1985) *The Tourmaline Group*. New York, Van Nostrand Reinhold Co., 300 pp.

Fritsch E., Shigley J.E., Rossman G.R., Mercer M.E., Muhlmeister S.M., Moon M. (1990) Gem-quality cuprian-elbaite tourmalines from São José da Batalha, Paraíba, Brazil. *Gems & Gemology*, Vol. 26, No. 3, pp. 186–205.

Henn U., Bank H., Bank F.H. (1990) Transparent bright blue Cu-bearing tourmalines from Paraiba, Brazil. *Mineralogical Magazine*, Vol. 54, pp. 553–557.

Kamona A.F. (1994) Mineralization types in the Mozambique Belt of eastern Zambia. *Journal of African Earth Sciences*, Vol. 19, No. 3, pp. 237–243.

Koivula J.I. (1985) Gem news: Tucson 1985. *Gems & Gemology*, Vol. 21, No. 1, p. 60.

Koivula J.I., Fryer C.W. (1985) Interesting red tourmaline from Zambia. *Gems & Gemology*, Vol. 21, No. 1, pp. 40–41.

Koivula J.I., Kammerling R.C. (1991) Gem News: Tourmaline with unusual "color change." *Gems & Gemology*, Vol. 27, No. 3, pp. 184–185.

Kupčík V. (1972) Bismuth: Crystal chemistry. In K. H. Wedepohl, Ed., *Handbook of Geochemistry*, Vol. II/1, Springer-Verlag, Berlin, pp. 83-B-1-83-M-1, 83-O-1.

Mintser E.F. (1979) The geochemical properties of the behavior of bismuth in hypogenic processes. In E.E. Angino and D.T. Long, Eds., *Benchmark Papers in Geology*, Vol. 49: *Geochemistry of Bismuth*, Dowden, Hutchinson & Ross, Stroudsburg, PA, pp. 268–327.

Peretyazhko I.S., Zagorskiy V.Ye., Bobrov Yu.D. (1991) First find of bismuth- and lead-rich tourmaline. *Doklady Akademii Nauk USSR, Earth Sciences Section*, Vol. 307, No. 1–6, pp. 175–179 [In Russian].

Rossman G.R., Fritsch E., Shigley J.E. (1991) Origin of color in cuprian elbaite from São José da Batalha, Paraíba, Brazil. *American Mineralogist*, Vol. 76, pp. 1479–1484.

Schmetzer K., Bank H. (1984a) Crystal chemistry of tsilaisite (manganese tourmaline) from Zambia. *Neues Jahrbuch für Mineralogie Monatshefte*, No. 2, pp. 61–69.

Schmetzer K., Bank H. (1984b) Intensive yellow tsilaisite (manganese tourmaline) of gem quality from Zambia. *Journal of Gemmology*, Vol. 19, No. 3, pp. 218–223.

Shigley J.E., Kane R.E., Manson D.V. (1986) A notable Mn-rich gem elbaite tourmaline and its relationship to "tsilaisite." *American Mineralogist*, Vol. 71, pp. 1214–1216.

Thomas A.E. (1982) Zambian tourmaline. *Journal of Gemmology*, Vol. 18, No. 1, pp. 4–6.

DIAMOND

Cabochon Cut

Black opaque materials, usually fashioned as cabochons or beads, are submitted regularly to the Gem Trade Laboratory for identification; many require advanced testing (see, e.g., M. L. Johnson et al., "Some Gemological Challenges in Identifying Black Opaque Gem Materials,"*Gems & Gemology*, Winter 1996, pp. 252–261). Nevertheless, the identity of the two black cabochons shown in figure 1 came as quite a surprise to us.

The refractive index was over the limits of a standard refractometer, and the specific gravity, measured by the hydrostatic method, was 3.44. With magnification, the cabochons showed a poor polish and an aggregate structure, with several transparent-to-translucent, near-colorless areas seen on the base of each piece (figure 2). The near-colorless areas showed weak yellow fluorescence to long-wave ultraviolet radiation, but the rest of each cabochon was inert. These properties suggested that the material was diamond, so we performed a hardness test on an inconspicuous portion of the basal edge of each piece, by rubbing it against a faceted piece of synthetic corundum and observing the result at 10∞ magnification. Together, the high degree of friction between the two materials, plus the scratch produced on the synthetic corundum, indicated a hardness of 10—and confirmed the

Figure 2. Fiber-optic illumination revealed the aggregate nature of the cabochons shown in figure 1, as seen here through the base of one of them. Magnified 15×.

identification of these cabochons as diamond.

We have reported on many unusual diamond cuts in this section, but these are the first diamonds we have seen fashioned as cabochons. We noted that the transparent areas on the bottoms of the two pieces were similar in size, shape, and placement. When we asked our client (who actually cut these gemstones) about this, he told us that the rough material had been shaped first into a bead, then sawed in half to make the two cabochons.

IR

Figure 1. Unlike most black opaque materials, these cabochons (3.55 and 3.56 ct, approximately 9.26 mm in diameter and 4.56 mm in depth) did not require advanced testing for identification because standard gemological tests proved them to be diamond.

Figure 3. This 5.54 ct Fancy Vivid orange diamond is rare for its intensity of color. Diamonds in the orange hue range are typically darker, less saturated, and often modified by brown.

Rare Fancy Vivid Orange

In the Fall 1996 issue (pp. 206–207), we reported on a diamond of rare color: a 3.40 ct heart shape that was graded Fancy Intense pinkish orange. At that time, we noted the unusual hue as well as an exceptionally strong saturation. A 5.54 ct cushion-shaped diamond (figure 3), which was recently submitted to the East Coast lab, shared certain gemological properties with that heart shape and gave us an opportunity to expand our reporting of rare colors.

The current stone was more saturated and more of a "pure" orange than the previously described heart shape; it received a color grade of Fancy Vivid orange. While we encounter diamonds in the orange hue range from time to time, we seldom encounter one that we can describe simply as "orange," with no modifiers. The intensity of the stone's color also adds to its rarity. In the system used by the GIA Gem Trade Laboratory to describe colored diamonds, the Fancy Vivid grade represents those light- to medium-toned diamonds of the strongest saturation range (if the stone was darker in tone, the description would be Fancy Deep).

The rough was reported to be of South African origin and to have appeared predominantly brown, with only a hint of orange. Like the Fancy Intense pinkish orange diamond described earlier, this stone also proved to be a type IIa diamond (as determined by infrared spectroscopy). The diamond fluoresced moderate yellow to long-wave UV radiation and moderate orange to short-wave UV.

John King and TM

With Surface Droplets of Filling Material

The most prominent visual feature of most fracture-filled diamonds—the brightfield and darkfield flash-effect colors—should be familiar to *G&G* readers (see, e.g., R. C. Kammerling et al., "An Update on Filled Diamonds: Identification and Durability," *Gems & Gemology*, Fall 1994, pp. 142–177; and S. F. McClure and R. C. Kammerling, "A Visual Guide to the Identification of Filled Diamonds," *Gems & Gemology*, Summer 1995, pp. 114–119 plus chart). In recent months, however, staff members in both the East and West Coast laboratories have seen fracture-filled diamonds in which these flash-effect colors were less pronounced. Examples from the East Coast lab were shown in the Spring 1997 Lab Notes section (pp. 56–57). More recently, the West Coast lab examined a fracture-filled near-colorless marquise brilliant (0.49 ct) that had extremely subtle flash colors—and surface features that provide a plausible explanation for this subdued appearance.

With magnification, one surface-reaching "feather" in the stone showed low relief over most of its extent, with extremely subtle yellow and purple flash colors (figure 4). However, a portion of this fracture near the surface of the stone had very high relief, with no evidence of filling material. Transparent droplets were visible on the surface of the diamond near this apparently "unfilled" portion of the feather (figure 5). The use of energy-dispersive X-ray fluorescence (EDXRF) spectroscopy confirmed the presence of lead (Pb) in this stone, which we have found in all effective diamond-filling materials that we have tested to date. In fact, we would not expect EDXRF to detect Pb in a gem diamond of this appearance unless some sort of filler was present.

In the Fall 1994 article by Kammerling et al. (cited above), we reported that heating a fracture-filled diamond could cause the flash-effect colors to be more subdued. The features we observed in this stone might well have been created if the diamond had been heated with a torch after it was filled. Although the filling material deep within the fracture probably was damaged by heating, the filling material nearer the surface of the stone had actually boiled out and then condensed as small droplets.

MLJ and SFM

Figure 4. The yellow darkfield (left) and purple brightfield (right) flash-effect colors in this fracture-filled 0.49 ct marquise brilliant are very subtle, as is typically seen in a filled diamond that has been subjected to heat. Magnified 30×.
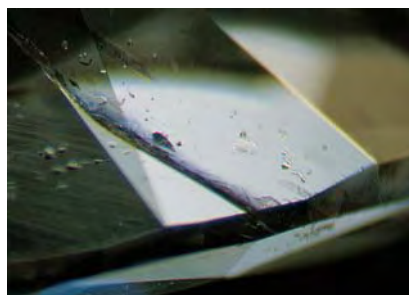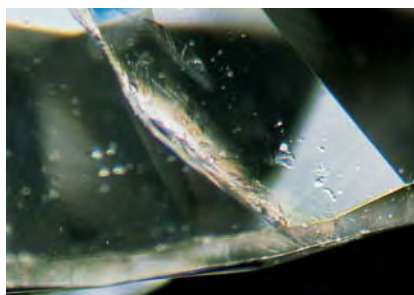
Figure 5. Small droplets on the surface of the filled diamond in figure 4 are probably condensed filler material that boiled out of the filled fracture when the stone was heated. Magnified 40×.

A Faceted Cat's-Eye EMERALD

Most chatoyant stones are fashioned as cabochons. In general, the cat's-eye phenomenon is due to the presence of parallel bands of included materials (or hollow tubes) in a stone that has been shaped so that light is concentrated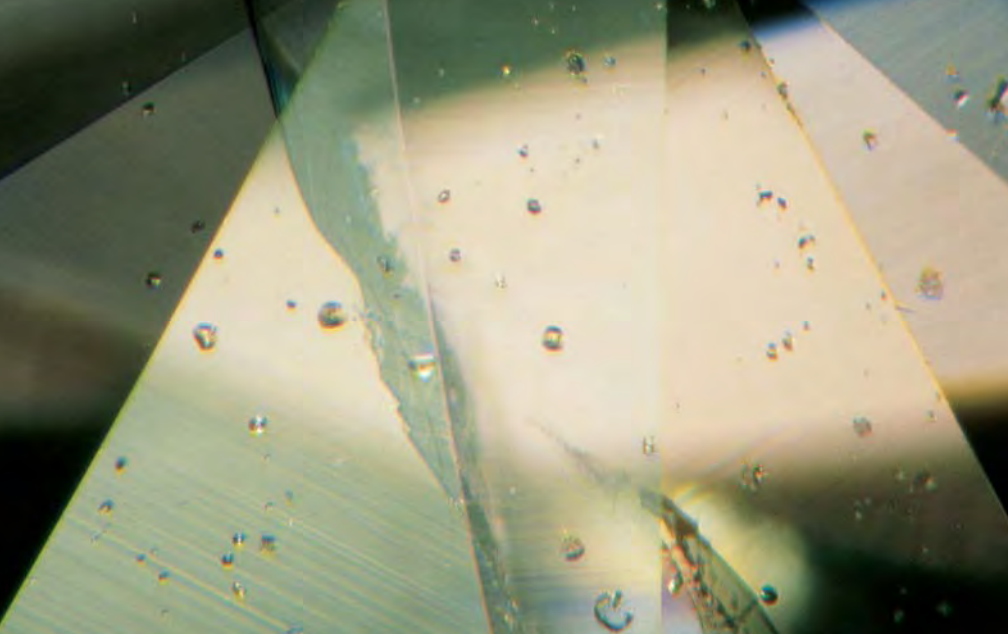 along a line perpendicular to these parallel bands. In the rare cases where a potentially chatoyant stone has been fashioned as something other than a cabochon, or with the long axis of the cabochon oriented parallel to the inclusions, the result may be an overall sheen, but it is usually not a sharp "eye."

In summer 1997, a 3.19 ct semi-transparent green stone was submitted to the West Coast lab for identification. Although faceted, the stone showed an obvious and sharp "eye" (figure 6). The gemological properties of this emerald-cut stone were consistent with emerald, including: R.I.'s of 1.570–1.578, an S.G. of 2.68 (measured with a DiaMension noncontact measurement system, manufactured by Sarin Technologies Ltd.), and typical "chrome lines" seen with a desk-model spectroscope. It was inert to both long- and short-wave UV radiation. With magnification, we could see small, dark, opaque crystals—probably chromite—as well as fractures and curved bands of parallel white fibrous inclusions resembling the "silk" commonly seen in rubies and sapphires. These inclusions confirmed the identification of the stone as a natural emerald, and no evidence of clarity enhancement was present.

The observations through the microscope also made it clear that the orientation of the white fibers was responsible for the chatoyancy. The curvature of the "silk" itself—not of the stone's surface—and the orientation of the curve to the table of the stone concentrated the light into a sharp "eye." Although cat's-eye emeralds are known from both Colombia (see Winter 1996 Gem News, pp. 284–285) and Brazil (see, e.g., Gem News: Spring 1992, p. 60; Spring 1995, pp. 60–61; and Fall 1995, p.

Figure 6. This 3.19 ct (11.05 × 10.73 × 3.69 mm) faceted emerald shows a sharp "eye."
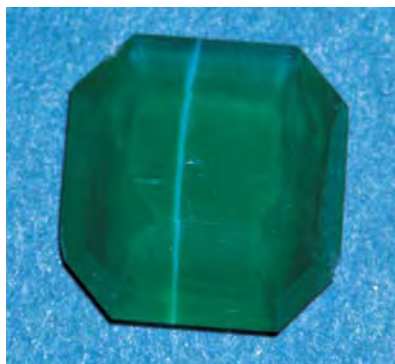
206), this is the first faceted cat's-eye emerald we have seen.

MLJ, Dino DeGhionno, and Philip Owens

JADEITE JADE

Impregnated, with Exceptional Transparency

Polymer impregnation in jadeite jade is an identification challenge frequently encountered at the GIA Gem Trade Laboratory. While we rely on infrared spectroscopy for conclusive evidence of impregnation, standard gemological testing can reveal features suggestive of this treatment. These features have been documented in the article "Identification of Bleached and Polymer-Impregnated Jadeite" (Fritsch et al., *Gems & Gemology*, Fall 1992, pp. 176–187) and in a number of Lab Notes (e.g., Spring 1995, p. 55).

An 8.25 ct variegated green-and-white carving was submitted to the East Coast laboratory for identification. Standard gemological testing revealed properties typical of jadeite jade, particularly a refractive index of 1.66 by the spot method, and the presence of chromium lines in the spectroscope (which also indicates natural green color). The bulk of the carving was inert to both long- and short-wave UV.

Usually, a distinctive surface texture is the first indication of impregnation; in this case, however, it was the unusual internal structure that initially raised our suspicions. The carving had near-colorless areas of exceptional transparency surrounding isolated green grains of jadeite (figure 7). Although untreated jadeite is often variegated green-and-white, it is quite rare to see the "white" areas with this degree of transparency (see, however, Gem Trade Lab Notes, Summer 1995, pp. 123–124). When we examined the piece further, we discovered residual polymer, most noticeably in a drilled hole (figure 8), but also in depressed areas of the carving. These areas fluoresced strong yellow to long-wave UV

Figure 7. The "white" areas in this polymer-impregnated green-and-white jadeite jade carving were extremely transparent. Magnified 20×.

Figure 8. Excess polymer is visible in this hole drilled in the carving shown in figure 7. Magnified 20×.

radiation, while the rest of the piece remained dark. Visible outlines of grain boundaries in both the white and green areas further supported our suspicion that the piece had been impregnated; this was subsequently confirmed by infrared spectroscopy.

The infrared spectrum revealed yet another unusual feature in this thin (and apparently very heavily impregnated) carving: The polymer peaks were so strong that the typical jadeite spectrum was dwarfed in comparison, and the absorption peaks typical of jadeite were not recognizable until the spectrum was greatly magnified. *Elizabeth Doyle*

Resembling Nephrite Jade

One of the unavoidable temptations for any gemologist is the "Sight ID": the identification of a stone without the use of a refractometer, a spectroscope, a microscope, or any other instrument. In many cases, the materials to be identified are indeed what we suspected them to be, which raises the risk of increasing our hubris to unacceptable levels; then another, more challenging sample arrives to restore necessary humility.

In spring 1997, the West Coast laboratory examined a sample that illustrates the hazards of attempting instrument-free identifications. The pierced and carved lid (to an urn that was not submitted) measured 97.8 × 97.7 ∞ 49 mm. The carving was translucent, with a glassy luster and a

mottled brownish green color. Perhaps a better descriptive term than "mottled" for the distribution of color might be "cloudy" (nebulous), since the color patches appeared to have diffuse margins, and there were no strongly saturated areas. At this point, the practitioner of the "Sight ID" technique would have proclaimed it to be nephrite on the basis of its luster, diaphaneity, and desaturated color.

Gemological properties immediately confounded this expectation: We obtained an R.I. of 1.66; observed a line at 437 mm (characteristic of jadeite) and chrome lines with the

Figure 9. Jadeite "phantom" crystals, with translucent green cores and near-colorless rims, were seen with low magnification in this carved lid. The center crystal measures about 0.5 mm across.
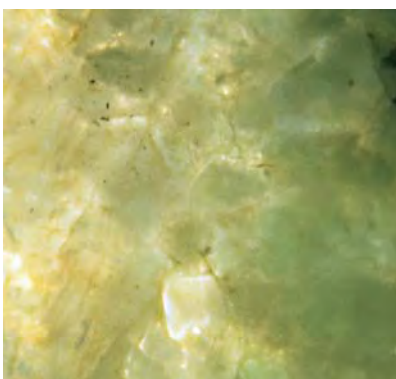
spectroscope; and resolved an aggregate optic character with the polariscope—as expected for jadeite, nephrite, and many other aggregates and rocks. The piece was inert to both long- and short-wave UV radiation; it was too large for us to obtain specific-gravity measurements.

With magnification, we observed features expected for jadeite, not nephrite, as well as the reason for the nephrite-like appearance. Jadeite jade and nephrite jade, both aggregate materials, owe their toughness to different microstructures: In jadeite, the material consists of intergrown blocky jadeite crystals with interfingering margins; whereas nephrite is a felted (compressed and intertwined) aggregate of actinolite-to-tremolite amphibole fibers. This lid was carved from material consisting of rather large (millimeter-size) jadeite grains with translucent-to-semitranslucent green cores and near-colorless transparent margins (figure 9); such cloudy-cored "phantom" jadeite crystals were new to our experience. The appearance of the overall piece was due in part to the green cores, as well as to the thin, iron-stained fractures throughout it. As with all jadeite jades, we checked this piece for polymer impregnation using Fourier Transform infrared spectroscopy (FTIR); no absorptions indicative of impregnation were seen.

MLJ

Synthetic Green PERICLASE

In the Spring 1996 Gem Trade Lab Notes (pp. 48–49), we reported on a 5.49 ct colorless periclase that might have been confused with grossular garnet. At the end of that entry, we noted that green synthetic periclase, as reported in the literature, might cause even more concern because of its resemblance to green garnet.

As fate would have it, the West Coast laboratory was recently asked to identify the 115.32 ct transparent yellowish green piece of rough shown in figure 10, which had been represented as a natural periclase from

Figure 10. The shape of this 115.32 ct piece of rough synthetic periclase was dictated by well-developed cubic cleavage.

Ghana. Gemological properties were: R.I.—1.736; S.G.—3.59; optic character—singly refractive with weak anomalous double refraction; no fluorescence (inert) to either long- or short-wave UV radiation; and no absorption features seen with the handheld spectroscope. When a strong parallel beam of light was directed into the piece from a fiber-optic light source, we saw strong red transmission. With magnification, we noted numerous blocky crystals in addition to well-developed cleavage along cube planes. This cleavage actually dictated the shape of the rough (and proved that the piece could not be grossular garnet, since garnets do not show cleavage in any direction). Chemical analysis by EDXRF spectroscopy showed a high magnesium content, with small amounts of chromium, calcium, and iron; this confirmed the identity of the material as periclase (pure periclase is magnesium oxide, MgO).

Periclase has not been reported as occurring in nature in anything close to this size as facetable single-crystal material. In fact, we could not find any reference to a known natural faceted periclase of any size (we could not conclusively identify the emerald-cut stone described in the Spring 1996 issue as natural or synthetic)—or to natural periclase colored green by chromium. However, large transparent pieces of synthetic periclase have been reported as by-products of the manufacture of refractory magnesia by a company in Australia (see G. Browne, "Australian Synthetic Periclase," *Australian Gemmologist*, November 1993, pp. 265–269). This process uses magnesite nodules—magnesium carbonate—from the Kunwarara deposit near Rockhampton, Queensland, which are crushed and heated to produce calcined magnesia. This material can then be electrofused to form ingots of fused synthetic periclase. These ingots have a 2-m-diameter central core of cryptocrystalline synthetic periclase, which is surrounded by two rims of differing structure. The inner rim, where the gem-quality crystals form, is approximately 10 cm wide. One of the habits of these crystals, as described by Browne, is "pseudocubic masses bounded by cleavage planes," which exactly describes the rough we examined.

The process for producing synthetic periclase differs greatly from all other known growth processes for synthetic gems, and the internal characteristics generated by electrofusion are not well documented. Square, plate-like negative crystals were observed in some samples of known synthetic periclase seen in the Gem Trade Laboratory in 1969, a material marketed under the name Lavernite ("Developments and Highlights at the Gem Trade Lab in Los Angeles," *Gems & Gemology*, Spring 1969, p. 22.) However, since natural periclase is so rarely found in gem-quality crystals of any size, the inclusions we observed could not assist in identifying this piece as natural or synthetic. In this instance, we reasoned that since the size and color of this specimen were so far removed from any periclase that has been found in nature, this item must be synthetic. As discussed in the earlier entry, we have not found definitive criteria to establish whether a smaller faceted piece of such material would be natural or synthetic.

*Maha DeMaggio
and SFM*

Editor's note: An 18.98 ct yellowish green pear-shaped brilliant, examined in the East Coast lab at press time, also turned out to be synthetic periclase. It had the same R.I., S.G., and chemical constituents described above; was inert to long-wave UV, but fluoresced an extremely weak orangy yellow to short-wave UV radiation; and showed weak red transmission to the fiber-optic light. With magnification, we saw a pinpoint cloud and a small round bubble.   *IR*

QUARTZ

Quench-Crackled and Dyed to Imitate Amethyst

Last winter, a client called the East Coast lab to ask us about an alleged new treatment that uses lasers to induce a purple color in rock crystal. The client stated that this treated material had been offered for a price even lower than that of synthetic amethyst. Although we were aware that radiation might be able to intensify the purple color in amethyst (G. R. Rossman, "Color in Gems: The New Technologies," *Gems & Gemology*, Summer 1981, pp. 60–71), we did not know of any mechanism whereby a laser could induce purple color in near-colorless quartz. At our request, then, the client sent us two beads for examination (figure 11).
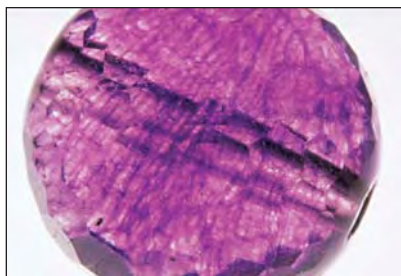
The beads were light to medium purple, but even to the unaided eye the color looked uneven. With magnification, we observed that the material was fractured throughout, with the purple color concentrated in these fractures (figure 12). Small flat surfaces on the beads allowed us to measure the refractive indices at 1.54 and 1.55, indicating quartz. When the

Figure 11. These purple beads, each about 10 mm in diameter, were offered as amethyst. They are actually colorless quartz that has been quench-crackled and dyed purple.

beads were exposed to both long- and short-wave UV radiation, the fractures fluoresced a weak to medium orange, whereas the solid areas of the material were inert. The mid-infrared spectrum showed several overlapping peaks between 3000 and 4000 cm^{-1}, which are seen in all varieties of quartz, plus additional structure around 2900 cm^{-1}, which is similar to the absorptions seen in polymer-impregnated materials. These properties led us to the conclusion that the beads had been quench-crackled and dyed. The pervasive cracks effectively hid any other internal features, so we could not determine whether the starting material was natural or synthetic quartz.

Over the years, we have reported on quench-crackled quartz in both green and red, imitating emerald and ruby (see, for example, Winter 1981 Lab Notes, pp. 229–230, and Gem News: Winter 1989, p. 247, and Fall 1992, pp. 205–206). However, this is the first time we have seen quartz dyed purple to simulate amethyst.

IR

Figure 12. Magnification readily revealed the extensive network of fractures and the concentration of purple color in the fractures of the beads shown in figure 11. Magnified 10×.

TOPAZ

Fashioned to Imitate Diamond Rough

In the hands of a clever lapidary, almost any near-colorless rough material can be fashioned into an object resembling a diamond crystal. We have reported on a number of cubic zirconia imitations of diamond rough (see Lab Notes, Winter 1988, pp. 241–242, and Fall 1996, p. 205; and Gem News, Spring 1994, p. 47). The high refractive index of cubic zirconia results in a good-looking imitation, but such pieces feel suspicious in the hand because of their high specific gravity. Recently we reported on an imitation made from topaz (Lab Notes, Spring 1997, p. 57). With a specific-gravity range that includes the value for diamond, such an imitation has the appropriate heft, but the lower refractive index gives a suspect appearance.

In late spring 1997, the East Coast lab received two specimens for identification, both of which appeared to be diamond rough in the form of distorted octahedra with characteristic dodecahedral grooves. The larger (63.65 ct) "crystal" was near-colorless, while the smaller (26.88 ct) stone had numerous dark inclusions and an uneven light blue color (see figure 13). The stones did not have an adamantine luster, but they did show a greasy-looking patina similar to that sometimes seen in waterworn diamond crystals. Although the specific gravities, measured hydrostatically, were 3.55 and 3.54, respectively, none of the other properties was consistent with those of diamond.

In fact, the optical and physical properties revealed that the true identity of these two specimens was topaz. Both were doubly refractive, and we found a biaxial optic figure in the larger piece. Although the roughened surfaces were not ideal for R.I. measurement, we obtained values of 1.60 and 1.61 by the spot method. Both pieces showed weak yellow fluorescence to long-wave UV radiation and no reaction to short-wave UV. Hardness tests on discreet areas of each piece of rough showed them to

Figure 13. These two "crystals," fashioned to look like diamond rough, were identified as topaz. They weighed 63.65 and 28.88 ct.
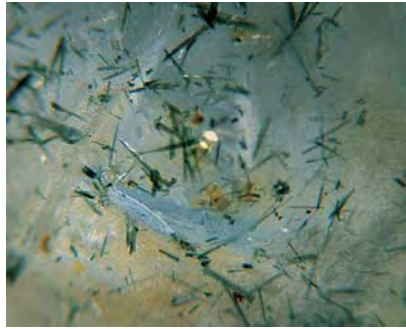
Figure 14. The many long, narrow inclusions in this topaz are tourmaline and chlorite crystals. They give an overall blue color to the otherwise near-colorless topaz host. Magnified 15×.

Figure 15. The shape, orientation, and raised relief of the "trigons" on this fashioned topaz do not reproduce the appearance of actual trigons on diamond crystals. Magnified 5×.

be between 7 and 9 on the Mohs scale. Neither piece showed any features in the hand spectroscope.

Using magnification, we identified the dark inclusions in the smaller piece by their crystal habit and blue, gray, and green colors as tourmaline and chlorite (figure 14), which are not known to occur in diamond. When this same stone was examined with diffused light, it was apparent that most areas were near-colorless and the overall blue color was caused by the inclusions. The trigons on both pieces also showed a number of characteristics that are not seen in diamond: They were raised above the surface rather than depressed into it, were different in shape from the faces on which they occurred, and (as shown in figure 15) were not inverted (as described for natural diamond in Y. L. Orlov, *The Mineralogy of the Diamond*, John Wiley and Sons, New York, 1973, especially pp. 72–106). In reflected light, we saw weak polishing lines on some areas of the 26.88 ct piece, which proved that these surfaces were not naturally occurring.

It is evident that a great deal of lapidary artistry was used to manufacture these specimens. They serve to remind us that a gemologist must never be swayed by the "obvious" appearance of an unknown specimen before reaching a conclusion.

GRC and IR

DIAMONDS

Extreme wear on diamonds. A turn-of-the-century brooch was brought to one of the contributing editors (EF) by M. Bouchet—a Nantes, France, jeweler who specializes in estate pieces—to confirm that the gems in the piece were indeed diamonds. The brooch contained several near-colorless round brilliants, all of which showed extreme wear on the facet junctions surrounding their tables. Using a thermal probe diamond tester, Drs. Fritsch and B. Lasnier, of the University of Nantes, easily proved that all the stones were natural diamonds. The center stone, unmounted, is shown in figure 1. This stone is even more damaged than the one mentioned in the Fall 1983 Gem Trade Lab Notes (p. 172). Note that the wear is much greater on one side, where it extends almost halfway down the star facet. Most remarkably, all the stones in the brooch showed the same pattern of abrasion, with the most abraded parts of each in the same orientation relative to the brooch. Damage was also visible on the tables of most of the stones as scratches, nicks, and small feathers extending into the diamonds. The worn-down surfaces were quite smooth.

The jeweler told Dr. Fritsch that sometime after the purchase the customer had returned the brooch, claiming that the stones were not diamonds and asking to be reimbursed. The customer had shown the piece to another jeweler, who stated that faceted stones with so much wear could not possibly be diamonds, but were most likely zircon imitations. Aside from the issue of hardness, the abraded edges along the table of the diamond in figure 1 make it difficult to discern the table reflections in this stone. Thus, the important visual "test" for diamonds—that is, that many diamond imitations do not "look right" because the reflection of the table in the pavilion facets is the wrong size (for stones with different refractive indices) or even doubled (in most orientations of birefringent materials, such as zircon)—would not be reliable in this instance.

The reason for this extreme wear remains a mystery, as no information was available on the history of the brooch.

How many diamonds are there in Arkansas? Professor A. A. Levinson, of the University of Calgary, Alberta, Canada, has provided the following analysis of developments at the Crater of Diamonds State Park, near Murfreesboro, Arkansas.

Although diamonds were found in a pipe near Murfreesboro in 1906, various attempts to mine them from 1907 to 1932 always ended in financial loss. In 1972, the locality became the Crater of Diamonds State Park, a tourist attraction where members of the public could keep all the diamonds they found. Over the past 20 years, about two stones—with an average weight of approximately 0.2 ct—have been found daily (see, e.g., "Arkansas's Diamond Park: Challenge of the Hunt versus Chance for Big Profits" by R. Shor, *Jeweler's Circular-Keystone*, November 1993, pp. 56–57). In this era of frantic exploration for new diamond deposits, it was therefore natural to reconsider the Murfreesboro lamproite pipe for its economic potential. However, there had never been a reliable estimate of the ore grade (carats per ton) of the pipe, nor an accurate determination of the value of the stones.

In 1987, the Arkansas state legislature passed a law allowing commercial mining at the site. In September 1996, after approval was received from the U.S. National Park Commission, and after the failure of litigation by various third parties seeking to halt the project, a group under the auspices of the State of Arkansas Department of Parks and Tourism began to collect an approximately 10,000 ton bulk sample of the lamproite for evaluation of the ore. The final results of this evaluation were given in an Ashton Mining of Canada Inc. press release dated February 10, 1997.

Citing information that was provided in this and previous press releases, Professor Levinson noted that the bulk sample was collected from 18 trenches in those parts of the pipe that were the historical sources of most of the recorded diamonds. From a total of 8,819 tons of ore, 207 diamonds were recovered (total weight 45.75 ct, for an average weight per stone of 0.22 ct). This calcu-

lates to an average diamond content of 0.005 carat per ton of ore.

These results fall significantly short of the diamond content required to support a commercial mining operation (e.g., typical economic kimberlite pipes average 0.3–0.5 ct/ton). Clearly, this pipe can remain a tourist attraction without the complication of concurrent mining.

Professor Levinson suggests that the tourists are mining more diamonds than the bulk sample indicates the source should provide naturally. From the information given, he notes, about 0.40 ct of diamonds are recovered daily by tourists. This is equivalent to the diamond content of 80 tons(!) of lamproite at this deposit (i.e., 0.40 ct divided by 0.005 ct/ton), leading to an interesting question as to how some of these diamonds reached the site.

COLORED STONES AND ORGANIC MATERIALS

Prospecting for beryl in Saudi Arabia. There are many instances in the Arabic literature of emeralds and other beryls being found in Saudi Arabia; these were compiled in a 1989 report by B. A. Al-Fotawi ("A Brief Review of the Mines and Mineral Occurrences in the Arabian Peninsula (Hamad Al-Jasear)," Saudi Arabian Ministry for Mineral Resources Open File Report DGMR-of-09-18, Kingdom of Saudi Arabia, 19 pp.). While working for the Ministry of Petroleum and Mineral Resources, Faisal M. Allam investigated some of these occurrences, and reported his findings to the Saudi Arabian government in 1992 ("Gemological Investigation for Gemstone—Emerald/Aquamarine in the Arabian Shield," Technical

Figure 1. Note the extreme and uneven wear on this diamond (about 4.5 mm in diameter), which was the centerpiece of a brooch in which all the diamonds showed similar abrasion. Photo by Bernard Lasnier.

Report DGMR-TR-91-9 of the Ministry of Petroleum and Mineral Resources). Mr. Allam recently became a GIA student, and generously agreed to share the results of this hard-to-find report with our readers.

Mr. Allam studied the Hadiyah area, which reportedly was a site of ancient emerald mining; however, the only green mineral he found was epidote, not emerald. Other varieties of beryl had been described from 12 localities (pegmatite dikes) in the Precambrian Arabian Shield rocks in Saudi Arabia between Riyadh and the Red Sea; these localities were explored in more detail. Although none showed potential for large-scale gem mining, some gem-quality aquamarine was obtained from the Karath Well pegmatite, and small faceted aquamarines could be fashioned from gemmy crystals (up to 8 cm long by 1.5 mm wide) found at Jabal Tarban. Specimen-quality aquamarine crystals may be recovered from both of these sites, as well as from Sarat Bishah and Jabal al Hawshah. Two other sites had smaller or scarcer beryl samples, while no beryl was found in the remaining six historic occurrences. Three good-quality aquamarines in the 1–2 ct range were cut from Karath Wells material.

Lab Alert: Radioactive cat's-eye chrysoberyls. Several hundred carats of radioactive cat's eye chrysoberyl are being offered on the Bangkok market, according to Kenneth Scarratt, president of the Centre for Gemstone Testing (the successor of the AIGS Laboratory) in that city. The material was discovered in late August 1997, when a Bangkok dealer (J. Bergman, of Gem Essence Co.), requested that some brown cat's-eye chrysoberyl be tested for radioactivity.

The Centre for Gemstone Testing examined one 3.5 ct stone and found it to be highly radioactive, with an activity level of 52 nCi/g. This is significantly higher than the legal release levels set by the relevant authorities in the United States (1.0 nCi/g), United Kingdom (2.7 nCi/g), and Asia (2.0 nCi/g). Using a Geiger-Mueller counter, Mr. Scarratt found that the stone had a contact radiation level of about 11 milliroentgens per hour. Subsequent tests showed that it had a half-life of approximately 103 days, indicating that this particular stone would not reach the legal release level in Asia before January 1999. Until then, it must be kept in a properly shielded radioactive materials storage container.

The chrysoberyl in question was described as having an "unusual dark brown" color (figure 2), which was found to be stable to a quick "fade test"—heating in the well of a microscope (until too hot to hold) for a period of one hour. The original material reportedly came from Orissa, India, and Mr. Scarratt believed that it was bombarded with neutrons in a nuclear reactor somewhere in Asia and then released illegally. According to one source with whom Mr. Scarratt spoke, "hundreds" of these stones have been available in Indonesia since April 1997, and by early September still more material had changed hands at the gemstone marketplace in Chantaburi,

Figure 2. Material similar to the pale green cat's-eye chrysoberyl on the left was irradiated to produce the 3.5 ct radioactive dark brown cat's-eye chrysoberyl on the right. Photo courtesy of Kenneth Scarratt.

Thailand. Robert E. Kane, director of the Gübelin Gemmological Laboratory in Lucerne, Switzerland, reported seeing several examples of this material at the September 1997 Hong Kong Show. Mr. Scarratt advised that members of the gem trade immediately check all cat's-eye chrysoberyls of an unusual dark brown color for excessive radioactivity.

Demantoid garnets from Russia . . . The greater availability of fine Russian demantoid was described by W. R. Phillips and A. S. Talantsev in the Summer 1996 *Gems & Gemology* ("Russian Demantoid, Czar of the Garnet Family," pp. 100–111). The editors saw an excellent demonstration of the return of this material earlier this year. Bear and Cara Williams of Bear Essentials, Jefferson City, Missouri, showed us several bright green demantoids that were reportedly from the Bobravka River, near Nizhniy Tagil. These stones had been fashioned in the nearby Ekaterinburg region. We borrowed two stones,

weighing 1.34 and 1.18 ct (figure 3), for gemological characterization.

Gemological properties were as follows (largest stone first, where different): shape—oval brilliant, oval mixed cut; color—yellowish green; color distribution—even; pleochroism—none; optic character—singly refractive; Chelsea color filter reaction—deep orangy red, weak orangy red; R.I.—greater than 1.81; S.G.—3.87, 3.86; inert to both long- and short-wave ultraviolet radiation; no visible luminescence ("transmission luminescence"); absorption spectrum—460 nm cutoff, 620 nm line, 638 nm line, weak 690 nm line (difficult to see in the large stone), 680 nm cutoff (large stone only); inclusions—"horsetails" (both stones), fractures (both stones), large cavity on girdle (large stone only). An energy-dispersive X-ray fluorescence (EDXRF) spectrum taken on the largest stone showed major Si, Fe, and Ca, minor Cr, and trace V.

. . . . and from Namibia. A number of people have brought to our attention the fact that demantoid garnets—long thought to occur almost exclusively in Russia (see, e.g., the Phillips and Talantsev article cited in the previous entry)—are now commercially available from a new locality in the southern African nation of Namibia. Contributing editor Henry Hänni first brought these stones to our attention. In spring 1997, he received two demantoid garnet crystals that were reportedly from a new source in Namibia; they were sent by Mr. Hilmar Bosch, Hilton, Natal, South Africa. The two crystals weighed 13.52 and 3.87 ct (Mr. Bosch reported seeing crystals as large as 30 ct). They had the following properties (largest first, where different): shape—both were partial rhombic dodecahedra (figure 4); surface texture—stepped growth in small steps, with features resembling slight corrosion; color—light yellowish green,

Figure 3. These two demantoid garnets, 1.18 and 1.34 ct, were recently recovered from Russian deposits. Stones courtesy of Bear Essentials; photo by Maha DeMaggio

Figure 4. These two crystals (3.87 and 13.52 ct) are demantoid garnets from a new locality in Namibia. Photo courtesy of Henry Hänni.

grayish green (both resembling peridot in color); color distribution—yellower at the core (in the first stone), even (in the second); absorption spectrum—sharp band at 425; reaction to Chelsea filter—reddish. With magnification, we saw open fissures in both crystals and some tiny fluid inclusions in the smaller piece; however, no "horsetail" inclusions were seen in either crystal. EDXRF spectroscopy gave Si, Ca, and Fe—consistent with andradite—but very little chromium (the green chromophore), which was estimated at 0.05 wt.% Cr_2O_3. An article by Thomas Lind et al. in a recent issue of the *Zeitschrift der Deutschen Gemmologischen Gesellschaft* ("Neues Vorkommen von Demantoid in Namibia," Vol. 46, No. 3, 1997, pp. 153–160) reported between 0.02 and 0.13 wt.% Cr_2O_3 in this material.

Marc Sarosi, a gem dealer in Los Angeles, California, shared seven fashioned demantoids (0.71–3.42 ct), two small demantoid crystals (8.91 and 9.54 ct), and one 1.11 ct yellowish brown andradite from this locality with the Gem News editors (some of these stones are shown in figure 5). Gemological properties of the fashioned demantoids were as follows: color—green to yellowish green;

refractive index—over the limits of our standard refractometer (greater than 1.81); optic character—singly refractive with strong anomalous double refraction; inert to both long- and short-wave ultraviolet radiation; Chelsea filter reaction—orange to red; specific gravity—3.83–3.85; absorption spectrum (using a handheld spectroscope)—band at 445 nm, general absorption below 450 nm, and (one stone only) diffuse 580 and 630 bands. Magnification revealed strong dispersion, "fingerprints," crystals (some of which could be resolved as prismatic in shape), a negative crystal with a two-phase inclusion, and needles in two samples. No sample contained "horsetail" inclusions, although the 1.11 ct yellowish brown andradite contained yellow needles (some of which curved slightly); Lind et al. also found no "horsetails" in the Namibian demantoids they examined. The stones showed pronounced angular or straight transparent growth zoning, and, in one case, iridescence along the growth planes (so-called "rainbow graining"). EDXRF analysis of the green fashioned stones revealed major Ca, Fe, and Si, and minor Mn and Cr. The two rough specimens we examined showed parallel growth of smaller crystals, with smooth dodecahedral faces and etched trapezohedral faces; one piece had grown on a 5 mm white "scepter" quartz crystal.

A published report in *Jewellery News Asia* (August 1997, p. 36) states that the source for these demantoids and other andradites is the Usakos mine in Namibia, and that the largest stone fashioned to date weighs 9.89 ct. The deposits are reportedly alluvial in nature.

A gem-quality ettringite group mineral, probably sturmanite. Each February, the gem and mineral shows in Tucson provide many interesting, sometimes important, gemological discoveries. Although some of these are relatively easy to analyze and describe, others are much more

Figure 5. The newly discovered Namibian deposit reportedly produced these rough and fashioned demantoids and yellowish brown andradite from the new find in Namibia. The largest crystal (right) measures 13.91 × 12.06 × 7.27 mm, and the largest pear-shaped demantoid weighs 1.95 ct. Stones courtesy of Marc Sarosi, Los Angeles, CA; photo by Maha DeMaggio.
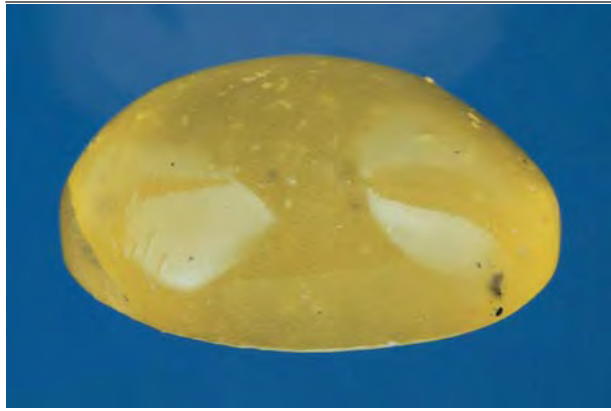
Figure 6. This 3.82 ct yellow cabochon is a mineral in the ettringite group, probably sturmanite. Photo by Maha DeMaggio.

challenging. Such was the case with the 3.82 ct bright yellow translucent oval cabochon shown in figure 6.

The original 10.12 ct piece of rough came from Kevin Lane Smith, a Tucson gem and mineral dealer. Mr. Smith also had a fist-size, highly translucent piece of this material; a large, well-polished translucent cabochon; and a small faceted stone. The material was reportedly from the Kuruman District in South Africa, and it was represented as ettringite, a member of the mineral group of the same name. Ettringite-group minerals are hydrous mixed sulfates/carbonates/borates/hydroxides of calcium and other elements (e.g., Al, Cr, Fe, Mn, and Si); identifying specific minerals in this group is difficult, so many specimens are simply labeled "ettringite group." Thus, we thought that gemological identification of this material would be a good exercise in gem-testing technique.

Gem Trade Lab staff gemologist Phil Owens fashioned the rough into a 14.00 × 10.22 × 5.12 mm oval cabochon (figure 6); he commented that the material was very soft (ettringite has a hardness of 2–2.5) and difficult to polish. In part, this latter difficulty was caused by numerous inclusions of tiny, transparent-to-translucent, near-colorless crystals, which were appreciably harder than the host material. As a result, the softer mineral undercut around the surface-reaching inclusions.

The basic gemological properties obtained from the cabochon were of little help in determining whether it was ettringite or sturmanite. The spot R.I. reading of 1.50 was consistent with a reading for either mineral. The specific gravity, determined by the hydrostatic method, was 1.86, slightly higher than the 1.847 value for sturmanite (see D. R. Peacor et al., "Sturmanite, a Ferric Iron, Boron Analogue of Ettringite," *Canadian Mineralogist*, Vol. 21, 1983, pp. 705–709) and considerably higher than the 1.77 value for the type specimen of ettringite. The slightly elevated value (relative to sturmanite) could be caused partly by the many tiny inclusions previously mentioned, which contributing editor Dino De-Ghionno—using X-ray powder diffraction analysis—identified as calcite.

EDXRF analysis, performed on the finished cabochon by former GTL Research Technician Dijon Douphner, showed that the yellow material contained Al, Ca, Fe, Mn, and S, with possible traces of As, Cu, Pb, K, and Sr. The iron and manganese content appeared too high for ettringite, which nominally does not contain these elements. (Note that GIA's EDXRF system does not detect oxygen, hydrogen, or boron.) However, the qualitative chemistry fit very well with the chemical formula for sturmanite.

A small powder sample, scraped from the rough by Mr. DeGhionno, was used for X-ray powder diffraction analysis. The pattern that we obtained matched the line positions and relative intensities listed for sturmanite more closely than it matched those for the mineral ettringite.

Thus, much of our data pointed to sturmanite as the correct identity of this bright yellow cabochon. However, because the ettringite group is a solid solution (as is, for example, garnet), the chemistry and nature of the material can vary significantly, even within a single sample. Consequently, our conclusion on a GTL report would read: "A member of the Ettringite mineral group, probably Sturmanite."

Bicolored grossular-andradite garnets from Mali. When "Gem-Quality Grossular-Andradite: A New Garnet from Mali" (M. L. Johnson et al., Fall 1995 *Gems & Gemology*) was written, we had seen these garnets in three color types: orange to brown, somewhat desaturated yellow-green, and bright green (see the cover of the Fall 1995 issue for examples). In 1996, Bank et al. ("Gemmologie Aktuell," *Zeitschrift der Deutschen Gemmologischen Gesellschaft*, Vol. 45, No. 1, pp. 1–4) predicted that bicolored yellowish green and dark brown grossular-andradite garnets were also possible. Coincidental with the publication of that article, in fact, two bicolored emerald-cut grossular-andradite garnets from Mali were loaned to the Gem News editors by David Knecht of RKG, Minneapolis, Minnesota. The larger, 2.57 ct, stone was a "classic" bicolor—brownish yellow on one side and greenish yellow on the other. The smaller, 1.22 ct, stone had a yellowish green core (figure 7) surrounded on all sides by green-yellow garnet; the core was especially distinct in polarized light. The gemological properties were (larger stone first, where different): optic character—singly refractive, with medium-order (2.57 ct) or high-order (1.22 ct) strain; color-filter reaction—brownish red, none; R.I.—1.770 (2.57 ct stone, greenish yellow region), 1.768 (2.57 ct stone, brownish yellow region), 1.761 (1.22 ct stone); S.G.—3.66, 3.64; fluorescence—inert to both long- and short-wave UV; absorption spectrum—415 nm cutoff, 440–450 nm band, faint absorption at 500 nm (2.57 ct stone); faint 415 nm band, 440–450 nm band (1.22 ct stone). According to EDXRF results, both stones contained Al, Si, Ca, Fe, Ti, Cr, and Mn. Green cores (like the one in the 1.22 ct stone) also have been seen in

Figure 8. The tubular structures did not disturb the play-of-color in this rough opal from Shewa Province, Ethiopia. Photomicrograph by John I. Koivula; magnified 15×.

some near-colorless grossular garnets from Asbestos, Quebec (see, for instance, W. L. Roberts, G. R. Rapp Jr., and J. Weber, *Encyclopedia of Minerals*, 1st ed., Van Nostrand Reinhold Co., New York, 1974, plate 60).

More on opal from Shewa, Ethiopia. Dr. Don Hoover (formerly of the U.S. Geological Survey) recently shared with us two samples of Ethiopian opals that have somewhat unusual properties, as compared to other opals and especially to those described in the Johnson et al. article on this locality (*Gems & Gemology*, Summer 1996, pp. 112–120). As illustrated in figure 8, thin "tubes"—such as the ones shown in figure 10 of the 1996 paper—pervaded the approximately 2 cm chunk of rough opal. The tubes occupied the same volume as patches of play-of-color in this opal; however, the play-of-color regions did not appear to be bounded, warped, or disturbed in any way by the presence of the tubes. This relationship implies that the tubes were older than the final aggregation of opal spheres into organized regions that caused the play-of-color diffraction effect.

The second piece, an approximately 5 ct chunk of white opal that also showed play-of-color, was interesting because of its very low apparent density. However, the specific gravity could not be measured by standard hydroscopic techniques, as the material rapidly took up water. With Dr. Hoover's permission, we attempted to slice a cube of the material in order to determine density by direct comparison of weight and volume (weight divided by volume equals density). Although the material crumbled while being sliced, we ended up with four fairly regular pieces of 1.90, 0.88, 0.45, and 0.41 ct. GTL weights-and-measures coordinator Christopher Lewis then ran each piece on the Sarin DiaMension, a noncontact measurement device (used for determining the proportions of

Figure 7. This 1.22 ct garnet from Mali has an intense yellowish green core. Photo by Maha DeMaggio.
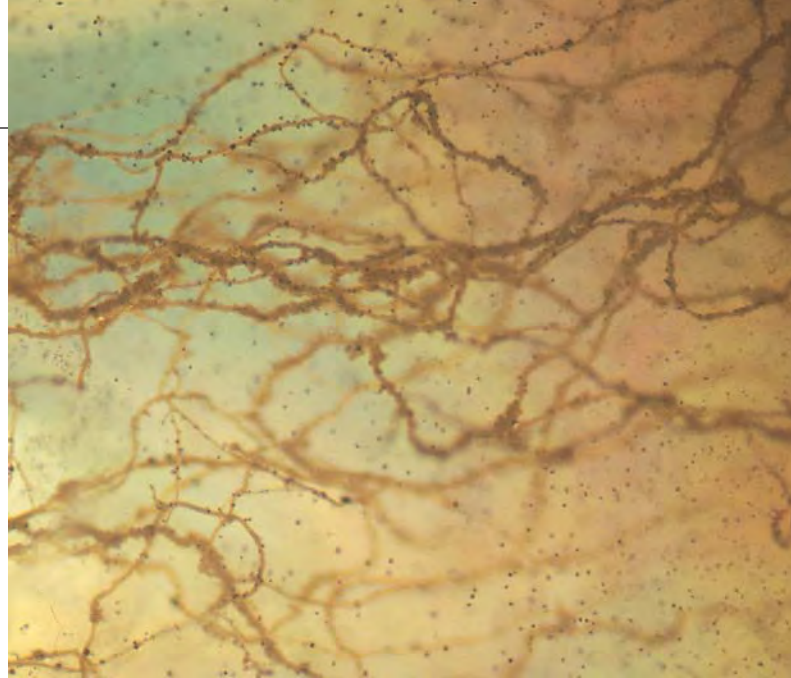
faceted diamonds) that can calculate the volume of any appropriately sized sample having a fairly simple convex shape (that is, one having no holes or dimples; for instance, a heart-shaped brilliant is not convex). The four pieces had calculated densities of 0.81, 0.79, 0.68, and 0.67 grams per cubic centimeter. Such low densities have not been recorded for gem opals, but they have been seen in "tabasheer," opaline siliceous material formed in the stems of bamboos and other grasses (see, e.g., C. Frondel, *The System of Mineralogy of James Dwight Dana* [etc.], 7th ed., Vol. 3, 1962, pp. 287–306). The 0.45 ct piece was then placed in a beaker of water to see whether it sank or floated: It floated for about 30 seconds, then sank rapidly in a cloud of small bubbles. The piece became somewhat more translucent and grayer after half an hour in water, but it maintained its play-of-color and was not damaged by its soaking. It reverted to "normal" once it dried out.

Gem rhodonite from Australia. Many minerals have very similar gemological properties, and can only be separated with great difficulty. Examples include: the rare mineral genthelvite, which requires X-ray diffraction or chemical analysis to distinguish it from pyrope-almandite garnet (Fall 1995 Gem News, pp. 206–207); members of the amphibole group, which often cannot be distinguished from one another even with X-ray diffraction and EDXRF analysis; and members of the tourmaline group, which are usually identified simply as "tourmaline" instead of by the species name of elbaite, dravite, liddicoatite, and the like, because of the difficulty of separating the various species.

In August 1997, Randy Polk of Phoenix, Arizona, sent *Gems & Gemology* editor Alice Keller a parcel of both rough and fashioned examples of an intense pink

Figure 9. These rough and fashioned pieces of rhodonite from the Woods mine in Australia illustrate the range of color in this material. The largest piece measures 66.0 × 58.0 × 19.0 mm. Photo by Maha DeMaggio.

material (figure 9). This material came from the Woods mine in a remote area of New South Wales, Australia. When it was last seen on the market, about the early 1970s, it was believed to be rhodonite. However, in the past 20 years, new minerals have been characterized—including marsturite, nambulite, and natronambulite—which can be separated from rhodonite only with difficulty. In addition, certain previously identified minerals (pyroxmangite, bustamite) were commonly mistaken for rhodonite, or believed to be varieties of rhodonite, in the past. Thus, the question arose as to whether this material—especially the fine-grained crystalline aggregate (figure 10) constituting the darker pieces—was actually rhodonite or some other mineral nearly indistinguishable from it. Adding impetus to our examination was a statement from Mr. Polk that this material had been analyzed and tentatively identified as natronambulite.

Staff gemologist Philip Owens determined gemological properties for six (3.01–7.78 ct) cabochons. All six stones were translucent pink; four were evenly colored, and two (4.69 and 7.78 ct) were mottled with paler pink regions. All showed an aggregate optic character, and all were inert to the color filter. The four evenly colored stones had R.I. values of 1.73 (1.728 on a flat face of a rose cut stone) and S.G.'s between 3.41 and 3.72. The two mottled stones had spot R.I.'s of 1.54 and S.G. values of 3.00 and 3.17 (such low S.G. values are typical of massive rhodonite, which can have a significant admixture of quartz). The six stones were inert to both long- and short-wave UV, and they showed no luminescence to visible light ("transmission luminescence"). Five of the six stones showed absorption bands at 420 and 548 nm, as well as weaker bands at 440 and 455 nm; in the sixth, the 455 nm band was not observed. All of these properties were consistent with the material being rhodonite.

With magnification, all six stones showed a mottled texture, consisting of fine to medium grains. Shiny (sul-

fide?) and black opaque (manganese oxide?) patches were observed on one sample. Brown stains between grains were observed in two samples. The largest and most transparent crystals were found in a 3.01 ct pear-shaped cabochon (again, see figure 9), which was chosen for further testing. (This sample also had the highest specific gravity.) EDXRF revealed major Mn, Si, and possibly Ca; minor Sr and Ba; and traces of Zn and possibly Ni. An X-ray diffraction powder pattern was an excellent match to our rhodonite standard pattern (a sample from Australia, pattern measured in 1971) and also to JCPDS pattern 13–138, a rhodonite from Franklin, New Jersey. The latter was important because the sample that provided our rhodonite standard pattern also might have come from the Woods mine.

Figure 10. With magnification, it is evident that the dark samples in figure 9 are an aggregate of fine-grained deep pink crystals, showing random orientation. Photomicrograph by John I. Koivula; magnified 15×.

Although we are confident that the sample we tested is rhodonite (based on the relative intensities in its diffraction pattern), there is no guarantee that all of the material in this deposit is rhodonite.

Mr. Polk is the exclusive agent for this handsome pink material, which is being mined by John and Alex Taggart. Large quantities are available: About six tons of various qualities is expected to be on the market soon, and Mr. Polk tells us that at least two solid pieces weighing 2 tons each have been found. Mr. Polk and his colleagues have graded the material into several categories based on transparency and depth of color. "Pencil-sized" unterminated crystals have been found, and some of the material may be suitable for mineral specimens. Mr. Polk informs us that the Woods mine has produced several additional unusual minerals; the mineralogy of this deposit warrants further study.

TREATMENTS

"Pink geuda" sapphires from Vietnam and their treatment. Ted Themelis (Gemlab Inc., Athens, Greece) has provided the following information to the Gem News editors. During a March 1997 visit to Vietnam, he noted the abundance of geuda-type sapphires, locally referred to as "white sapphires," that had a very pale pink overtone. These reportedly are found in the Hoang Lien Son area, Lao-Cai Province, of northwest Vietnam. Most of the stones were opaque and cloudy, with pronounced milkiness; they ranged in size to a little over five grams. Rutile silk was seen in all specimens, either concentrated in patches or irregularly distributed throughout the stone. Some specimens were reminiscent of Sri Lankan geuda. Mr. Themelis observed that the milkier or more included the stone was originally, the more intense was the color produced by treatment.

Mr. Themelis performed three heat-treatment experiments on rough samples of this Vietnamese "pink geuda." First, he heated 118 pieces at 1650°C for five minutes in air, followed by rapid cooling (30°C/minute). Of these, 31 pieces turned blue, ranging from light to very dark; 54 developed patches or zones of blue; 21 turned pink or purple; and 12 pieces turned very light pink. Although the treatment noticeably improved the diaphaneity of all of these samples, they were still semi-translucent to opaque, suitable for cutting only as cabochons.

In a second experiment, Mr. Themelis heated 58 pieces of Vietnamese "pink geuda" that had a more noticeable pink tinge and obvious milkiness, at 1675°C for 10 minutes in pure oxygen, again followed by rapid cooling. Of these stones, 28 pieces turned medium-to-intense pink, with improved diaphaneity and luster (although still of cabochon quality); 13 pieces turned medium blue (also cabochon quality); and 17 pieces showed a shift in color from light purple in fluorescent light to very light pink under incandescent light (with improved diaphaneity, but still semi-translucent to opaque).

Last, Mr. Themelis heated 86 pieces of the Vietnamese "pink geuda" at 1700°C for 10 minutes in a reducing atmosphere, again followed by rapid cooling. Of these stones, all still opaque, 51 turned very dark blue, almost black; 23 turned purplish blue to blue; and 12 pieces turned mottled blue, with concentrated patches of blue color all over their surfaces. He believes that these newly discovered Vietnamese "pink geuda" sapphires show potential for commercial heat treatment, as a good percentage of the treated material is suitable for cutting low-quality cabochons.

SYNTHETICS AND SIMULANTS

Change-of-color synthetic sapphires represented as yet another "new find." The range of colors seen in most change-of-color synthetic sapphire is quite distinctive (described as "greenish blue in fluorescent or natural light and pinkish purple in incandescent light"; see, e.g., Gem Trade Lab Notes, Summer 1995, p. 127), and usually the material is represented to the unwary as alexandrite. However, the distinctive set of colors of these synthetic sapphires may cause suspicion in the mind of an experienced gemologist who sees such a stone, regardless of what it is stated to be.

The three synthetic sapphires in figure 11 were part of a lot of six samples (weighing from 1.32 to 2.28 ct) purchased from Afghani "freedom fighters"; these supposedly were natural sapphires from a new locality in the region. The "native cut" faceting they had undergone added to their air of authenticity. Examination with a microscope and a diffused transmitted light source quickly confirmed the suspicions of contributing editor Shane McClure: Curved striae were present in all three

Figure 11. These three "native cut" synthetic sapphires (weighing 2.03 to 2.28 ct) were represented as change-of-color sapphire from a new locality in or near Afghanistan. Courtesy of Dr. Horst Krupp, Firegems, La Costa, CA; photo by Maha DeMaggio.

Figure 12. These five samples of gadolinium gallium garnet (2.41–2.75 ct) were fashioned from material reportedly produced in a military facility in Russia. Photo by Maha DeMaggio.

stones. The source of our information, Dr. Horst Krupp, told us that clean pieces of rough as large as 40 grams were said to be available; no doubt larger pieces would have resembled their parent boules too closely for effective deception.

GGG from Russia. The Spring 1995 Gem News section (p. 70) contained an entry on a number of synthetic and imitation gem materials that were available at the 1995 Tucson show. These included materials being offered by the Morion Co. of Cambridge, Massachusetts; among those mentioned in that entry, but not described, was gadolinium gallium garnet (GGG) in a range of colors. The material was being sold primarily as unpolished disks about 80 mm in diameter by 5 mm thick. When asked why the material had been pre-formed in this fashion, the firm's president, Dr. Leonid Pride, stated that he purchased them in this shape from a factory in Russia that originally grew the crystals for use in electronic memory elements for military applications.

Since 1995, additional colors of GGG have become available. For instance, in September 1997 rough was available in: "intense pink, pink, light pink, almandine [red?], green-blue, aquamarine blue, sky blue, intense blue, raspberry, and lilac," according to Dr. Pride. The Morion Co. also has had a small number of faceted samples available at the annual Tucson shows; five of these (ranging in weight from 2.41 to 2.75 ct; figure 12) were obtained for characterization. We determined the following properties: color—various (see table 1); body color distribution—even; diaphaneity—transparent; R.I.—over the limits of the standard refractometer (greater than 1.81); S.G. (four of the five samples)—7.11 to 7.14, dark blue stone 6.64 (see below); singly refractive; pleochroism—none; magnification—no inclusions noted. Luminescence to ultraviolet radiation, Chelsea filter reaction, and the spectrum seen with the handheld prism spectroscope depended on the color of the stone (again,

see table 1). On the basis of its appearance and these properties, GGG is easily separated from any natural gem materials.

EDXRF analysis showed that the dark blue specimen contained calcium and zirconium in addition to gadolinium and gallium. This detectable difference in chemistry most likely accounts for the significantly lower S.G. All of the specimens showed X-ray diffraction patterns consistent with GGG.

MISCELLANEOUS

***Gems & Gemology* author wins European cutting competition.** Arthur Lee Anderson of Speira Gems, Ashland, Oregon, recently won first prize in the gemstone cutting competition, the "28th German Award for Jewellery and Precious Stones Idar Oberstein 1997." Held every three years, the competition draws entries from all over the world and is juried by members from the European gemstone and jewelery industry. Mr. Anderson's winning entry was a 21.70 ct "Webbed Pear Cut" citrine (figure 13), a design that he developed over the past year. To create this design, Anderson employed several different cutting techniques, as well as the use of optics and reflections in the citrine. Mr. Anderson described some of his fashioning techniques in the article "Curves and Optics

TABLE 1. Color-dependent properties of five samples of GGG produced in Russia.

| Color | UV fluorescence | | Chelsea filter | Absorption spectrum (nm) |
	Long-wave	Short-wave		
Purple	Weak orangy red	Weak orangy red	No reaction	Weak absorption at 500–520 and 530–550, strong bands at 570–580 and 610–620, 650 cutoff
Purplish pink	Weak orangy red	Weak orangy red	No reaction	Sharp lines at 465, 485, 515, 520, 540; weak 550; doublets at 530, 570, 580 and 590
Orangy red	Very weak red	Weak red	Red	Vague absorption at 400–440 and 500–600; 690 cutoff
Green-blue	Inert	Inert	No reaction	Weak 540 band; moderate bands at 570 and 620; 650 cutoff
Blue	Inert	Inert	Red	Weak 440 and 455 bands; 460–470, 590–620, and 640–690 bands

Figure 13. This 21.70 ct "Webbed Pear Cut" citrine brought gem cutter Arthur Anderson top honors in the 28th German Award for Jewellery and Precious Stones. Photo by Manfred Grebel.

in Nontraditional Gemstone Cutting," which appeared in the Winter 1991 issue of *Gems & Gemology* (pp. 234–239).

Standards issued for the jewelry industry in China. The Chinese State Bureau of Technological Supervision (CSBTS) issued three national standards for the jewelry industry on October 7, 1996; they went into effect throughout China on May 1, 1997. The three documents defining these standards (*GB/T 16552-1996 Gems —Nomenclature, GB/T 16553-1996 Gems— Testing, and GB/T 16554-1996 Diamond Grading*) were drafted by the National Gemstone Testing Center in Beijing, and are written in Chinese; research associate Yan Liu of GIA Research provided us with the following summary.

The first, *GB/T 16552-1996 Gems—Nomenclature*, specifies the rules for naming gemstones. This standard is usable for identifications, as well as for descriptions used for imports and exports, insurance, and the trade. The term *gems* refers to both natural and manufactured gem materials. Natural gems include single-crystal (or twinned) gem materials ("natural gemstones"); natural aggregate and amorphous materials, including jadeite, nephrite, chalcedony, opal, serpentine, and natural glass (all of these are included in the heading "natural jades," which could confuse Western purchasers); and "natural organic substances." Manufactured materials—including single-crystal synthetics, assemblages, "reconstructed stones," and imitations—are placed in the category of "artificial products." Enhancement is also defined, as are optical phenomena. The Chinese standard was created with AGTA, CIBJO, and All Japan Gem Society standards taken into consideration, and the document includes a table translating between English and Chinese gem names.

The second document, *GB/T 16553-1996 Gems— Testing*, provides terminology and methods for gem identification, and can be used as a gem identification manu-

al. It contains identification criteria for 49 natural gemstones, 31 natural aggregate or amorphous materials, eight natural organic substances (including petrified wood, but not ivory), and 17 "artificial stones." Enhancements described include heating, bleaching, waxing, the use of colorless and colored oils, filling and impregnation, dyeing, irradiation, laser drilling, coating, and surface diffusion.

The last standard, *GB/T 16554-1996 Diamond Grading*, is a manual for the grading of the color, clarity, cut, and weight of a faceted diamond. This standard is only suitable for grading natural colorless to light yellow (or light brown, or light gray) diamonds of 0.20 ct or larger. Twelve color grades are used (D through N, and below N), and master stones are used to judge color and fluorescence. Clarity is evaluated under a 10× loupe, using "European" terminology: LC (loupe clean), two grades of VVS, two grades of VS, two SI grades and three P (piqué) grades. There are three cutting grades based on diamond proportions. The standard also specifies notation for diamond plots and explains how to grade mounted diamonds.

The term *natural jades*, used in the first two standards to classify aggregate or amorphous materials, requires some additional discussion. The Chinese term *yu*, although often considered equivalent to the English *jade*, in fact might be better translated throughout Chinese history as "most resistant carvable stone." Although many of the aggregate materials included in this classification might only cause puzzlement in the overseas gem trade if they were described as "natural jades" (for instance, turquoise or rhodochrosite), the description as "natural jade" of some materials discussed in these standards (e.g., serpentine, quartzite, aventurine quartz) could generate considerable, and potentially expensive, confusion. To prevent misuse of this term, the Nomenclature standard puts further restrictions on the use of "yu" or "jade" to describe materials. No material—even nephrite or jadeite—can be called simply

"jade" or "jade rock;" thus, nephrite is "nephrite jade"—but serpentine is also "serpentine jade." Materials cannot be described by their shapes: "round jade" is not an acceptable definition. Except for specific, well-defined materials cited in the standard, place names are not acceptable in jade descriptions. Hence, "Yunnan jade" is not a valid term. (One exception to the "no place names" rule is "Dushan jade," which is the accepted name in these Chinese standards for a specific zoisite/plagioclase feldspar rock.)

ANNOUNCEMENTS

Dates set for February 1998 Tucson shows. The American Gem Trade Association (AGTA) GemFair will run from Wednesday, February 4, through Monday, February 9, 1998, at the Tucson Convention Center. Following that show at the Convention Center will be the Tucson Gem and Mineral Society show from February 12 to 15. At the Holiday Inn City Center (Broadway), from February 4 to 11, will be the Gem & Lapidary Dealers Association (GLDA) show. The Gem and Jewelry Exchange (GJX) show will run from February 5 to 12, across Grenada Street from the Holiday Inn City Center. Other show venues featuring gem materials include the: Pueblo Inn, Rodeway Inn, Tucson Showplace, Sonoran Desert Marketplace, Discovery Inn, Holiday Inn Express, Quality Hotel and Suites, Tucson Scottish Rite Temple,

Howard Johnson's, Tucson East Hilton & Towers, La Quinta Inn, The Windmill Inn, Southwest Center for Music, Holiday Inn Palo Verde/Holidome, and Days Inn. Times and dates of shows vary at each location. Consult the show guide, which will be available at the different Tucson venues, for further information.

Visit *Gems & Gemology* in Tucson. *Gems & Gemology* Editor Alice Keller and Senior Editor Brendan Laurs will be staffing the *Gems & Gemology* booth in the Galleria section (middle floor) at the Tucson Convention Center for the duration of the AGTA show, February 4–9. Stop by to ask questions, share information, or just say hello. Many back issues will be available.

International Society of Appraisers. The 19th Annual International Conference of the International Society of Appraisers (ISA) will be held March 22–25, 1998, in San Diego, California. The ISA is a multidiscipline professional association, with members in the United States, Canada, and other countries; it is dedicated to advancing the theory, principles, techniques, and ethics of appraising personal property. Founded in 1979, it is the largest association of its kind. At the upcoming 19th program, concurrent programs will focus on gems and jewelry, antiques and residential contents, as well as fine art. Further information about this conference is available on the internet at http://www.isa-appraisers.org.

1997

CHALLENGE WINNERS

Proving once again that Gems & Gemology *readers are dedicated to their education and knowledge of the field, almost 400 people particpated in the 1997* Gems & Gemology *Challenge. Entries came from all over the world, as readers tested their knowledge on the questions from the Spring 1997 issue. Those who earned a score of 75% or better received a GIA Continuing Education Certificate recognizing their achievement. Those listed below received a perfect 100% score. Congratulations!*

USA: Alabama *Guntersville*: Cindy K. Fortenberry; *Mobile*: Lori Bryant • **Alaska** *Craig*: Deborah Anne Welker • **Arizona** *Flagstaff*: Robert Brent Fogelberg; *Fountain Hills*: Hank Wodynski; *Scottsdale*: Kenyon V. Painter, Norma B. Painter; *Tucson*: Dave Arens, Luella Dykhuis, Geraldine Alex Towns • **California** *Burlingame*: Sandra MacKenzie-Graham; *Carlsbad*: Jan L. Arnold, Marla Belbel, Lori J. Burdo, Carl Chilstrom, Diane Flora, Brian I. Genstel, Becka Johnson, Mark S. Johnson, Douglas Kennedy, Wendi Mayerson, Jana E. Miyahira, Kyaw Soe Moe, David Peters, Diane Saito, Jim Viall, Melissa Watson-Lafond, Michael Wobby, Philip G. York; *Carmel*: Douglas R. Mays; *Chino Hills*: Virgilio M. Garcia, Jr.; *Elk Grove*: Michael Pace; *Los Angeles*: Todd Buedingen, Grace Lee; *Los Gatos*: G. Donald Eberlein; *Mill Valley*: Susan Bickford; *Oceanside*: LaVerne M. Larson; *Palo Alto*: Joyce Henderson; *Penn Valley*: Nancy Marie Spencer; *Sacramento*: J. Marlene White; *San Diego*: Tracy Nuzzo; *San Jose*: Willard C. Brown; *San Rafael*: Robert A. Seltzer; *Santa Clarita*: Beverly Nardoni-Kurz; *Santa Cruz*: Tony Averill, Linda M. Bork; *Santa Rosa*: Keith M. Davie; *Santa Ysabel*: Glenn Shaffer; *Tustin*: Alvin Ip; *Ukiah*: Charles "Mike" Morgan; *Walnut Creek*: Michael W. Rinehart; *Watsonville*: Janet S. Mayou; *West Hills*: Bradley A. Partington • **Colorado** *Colorado Springs*: Molly K. Knox; *Crested Butte*: Nancy Y. Blanton; *Denver*: Alan J. Winterscheidt • **Connecticut** *Essex*: Nancy N. Richardson; *New Haven*: Matilde Paolini McAfee; *Rockville*: Barbara A. Orlowski; *Simsbury*: Jeffrey A. Adams; *Westport*: William A. Jeffery, Mary B. Moses • **Florida** *Cape Coral*: Jeffrey R. Hicks; *Deland*: Sue Angevine Guess; *Hollywood*: Barry Belenke; *Indialantic*: Luis Angel Magana; *Miami Beach*: Pinchas Schechter; *Naples*: Michael J. McCormick; *Palm Harbor*: Timothy D. Schuler; *Plantation*: Garrett Walker; *Satellite Beach*: Consuelo Schnaderbeck; *West Palm Beach*: Mathew Mooney • **Hawaii** • *Maui, Makawao*: Alison Hutchison-Fahland; • *Oahu, Honolulu*: Brenda K. Reichel; *Mililani*: Abe L. Wilson • **Illinois** *Bloomington*: Anne Blumer; *Geneseo*: Mark O. Arnold; *Geneva*: Lori M. Mesa; *Normal*: William A. Lyddon; *Springfield*: Pat Pikesh; *Troy*: Bruce Upperman • **Indiana** *Brownsburg*: Charles Robert Scanlan; *Indianapolis*: Mark Ferreira, Mary Wright; *Jeffersonville*: Seth Christian Simpson • **Iowa** *Fairfield*: Richard C. Kurka • **Kansas** *Topeka*: John C. Goldsmith • **Maine** *Portland*: Arthur E. Spellissy, Jr. • **Maryland** *Davidsonville*: Helen Serras-Herman; *Temple Hills*: William R. Mann • **Massachusetts** *Attleboro*: Jeff Wong; *Braintree*: Alan R. Howarth; *Brookline*: Martin Haske; *Lynnfield*: John A. Caruso; *Milton*: Beth I. Fleitman; *Norwood*: Edward F. McDonough • **Michigan** *Bay City*: Bradley J. Payne; *Escanaba*: Laurence Bell • **Missouri** *Jefferson City*: Margaret A. Gilmore; *Kansas City*: Greg Nedblake, J. Michael Tracy; *Perry*: Bruce L. Elmer • **Montana** *Great Falls*: Amy Wolfe-VanCleave • **Nevada** *Las Vegas*: Kelley E. Thomas; *Reno*: Terence E. Terras • **New Jersey** *Phillipsburg*: Robin A. Stokes; *Roselle Park*: Jo Anne M. Whitteaker • **New Mexico** *Albuquerque*: Susan M. G. Wilson • **New York** *Brooklyn*: Istvan Rudas; *Gansevoort*: Clifford H. Stevens; *New York*: Lisa H. Thierman, Brandon Tso; *Rye*: Gregory J. Cunningham • **North Carolina** *Advance*: Blair Tredwell;

Manteo: Eileen Alexanian; *Shelby*: Sue Whitaker; *Tryon*: Matthew Randolph; *Wilmington*: Ben H. Smith, Jr. ◆ **Ohio** *Akron*: Lynn L. Myers; *Dayton*: Stephanie M. Weber, Michael Williams; *Toledo*: Mary C. Jensen, Jack Schatzley ◆ **Oregon** *Beaverton*: Robert H. Burns; *Milwaukie*: Cinda V. di Raimondo; *Newport*: Richard Petrovic ◆ **Pennsylvania** *Jeffersonville*: Aurora A. Stuski-Ryley; *Womelsdorf*: Lori Perchansky; *Yardley*: Jon Barry Dinola, Peter R. Stadelmeier ◆ **South Carolina** *Sumter*: James S. Markides ◆ **Tennessee** *Coalmont*: Clayton Lee Shirlen ◆ **Texas** *Arlington*: A. Thomas Light; *Austin*: Corey Shaughnessy; *Dallas*: Ray Zajicek; *El Paso*: Jim Ferguson; *Flower Mound*: Elizabeth M. Roach; *Lamesa*: Fontaine Cope; *Richardson*: Becky Templin Shelton ◆ **Virginia** *Blacksbury*: Scott Steward; *Fredericksburg*: Ted Kowalski; *Hampton*: Edward A. Goodman; *Harrisonburg*: Daniel M. Scanlan; *Roanoke*: Stephen O. Phillips; *Springfield*: Robert G. Davis ◆ **Washington** *Bellingham*: D. Hurlbert; *Lakebay*: Karen Geiger ◆ **Wisconsin** *Beaver Dam*: Thomas G. Wendt; *East Troy*: William Bailey; *Mequon*: Kathleen J. Molter; *Racine*: Kathi Vallner-Villarreal ◆ **AFRICA Zimbabwe** *Harare*: Lesley Faye Marsh ◆ **AUSTRALIA** ● **New South Wales** *Concord West*: Steve John Puz; *Miranda*: C. V. Russell ● **Queensland** *Logan*: Ken Hunter ● **Western Australia** *Coogee*: Helen Judith Haddy ◆ **BELGIUM** *Brussels*: Jo Delcoigne, Léon Rubin; *Diegem*: Guy Lalous; *Hemiksem*: Daniel De Maeght; *Ruiselede*: Lucette Nols ◆ **BRAZIL** *Rio de Janeiro*: Luiz Angelo; *São Paulo*: Alejandro B. Ferreyra, Maria Amelia Franco ◆ **CANADA** ● **Alberta** *Calgary*: Diane Koke, Janusz

1997 CHALLENGE WINNERS

J. Meier ● **British Columbia** *Aldergrove*: Ron Plessis; *Chemainus*: Mark S. Curtis; *Delta*: Barbara Muir; *Vancouver*: Michael J. P. Cavanagh; *Victoria*: Fred G. Billcock, Anthony De Goutiére ● **Ontario** *Bobcaygeon*: David R. Lindsay; *Cookstown*: Michael Hyszka; *Etobicoke*: David N. Carabott; *St. Catharines*: Alice J. Christianson ● **Québec** *Laval*: Monique Savard; *Montréal*: Christiane Beauregard, Lina Massé, Yves Morrier ◆ **CHINA** *Fuzhou*: Tang Deping ◆ **ENGLAND** *Kent*: Linda Anne Bateley; *London*: P. D. Chib ◆ **FINLAND** *Kajaani*: Petri Tuovinen ◆ **FRANCE** *Herserange*: Frederic Pracucci; *Paris*: Marie-France Chateau, Stephen Perera; *St. Ismier*: Laurent Sikirdji ◆ **GERMANY** *Idar-Oberstein*: Josef Bogacz, Erik Vadaszi ◆ **HONG KONG** *Kowloon*: Edward Johnson ◆ **GREECE** *Athens*: Anna-Maria Falaga; *Thessaloniki*: Ioannis Xylas ◆ **INDIA** *Bangalore*: S. R. S. Murthy ◆ **INDONESIA** *Jakarta*: Warli Latumena, Sarono; *Jember*: Adi Wijaya ◆ **ITALY** *Ferrara*: Sonia Franzolin; *Florence*: Rita Parekh, Paolo Penco; *Genova*: Mafalda Pasqui; *Lucca*: Roberto Filippi; *Modena*: Apicella Tania; *Pordenone*: Barbara Pistuddi; *Porto Azzurro*: Diego Giuseppe Trainini; *Roma*: Andrea Damiani; *Sanremo*: Enrico Cannoletta; *Valenza*: Rossella Conti ◆ **NETHERLANDS** *Amsterdam*: P. Horninge; *Rotterdam*: E. Van Velzen; *Voorburg*: Wilma Van der Giessen ◆ **NEW ZEALAND** *Lower Hutt*: Dennis Blacklaws ◆ **PHILLIPINES** *Mandaluyong*: Mark Alexander B. Velayo; *Manila*: Colleen C. Mangun ◆ **POLAND** *Lublin*: Marek Prus ◆ **PORTUGAL** *Algarve*: Johanne C. Jack; *Viseu*: Rui P. Branco ◆ **SCOTLAND** *Edinburgh*: James W. M. Heatlie, Margery E. Watson ◆ **SPAIN** *Agramunt*: Santiago Escolà Villalta; *Madrid*: María Isabel Cereijo Hierro, José Antonio Gutiérrez Martínez, Ricardo García de Vinuesa; *P. P. Farnals*: Monika Bergel-Becker; *Puerto de Soller-Balears*: J. Maurici Revilla Bonnin; *Villauiciosa Asturias*: Claudio Argüelles Moris ◆ **SRI LANKA** *Kandy*: Senarath B. Basnayake ◆ **SWEDEN** *Järfallä*: Thomas Larsson; *Västerhaninge*: Peter Markstedt ◆ **SWITZERLAND** *Rodersdorf*: Heinz Kniess; *Wolfertswil*: Hedley Prynn; *Zollikon*: Adrian Meister; *Zürich*: Eva Mettler ◆ **TAIWAN** *Taichung*: Ho-Chi Yang ◆ **THAILAND** *Bangkok*: Patricia Goossens ◆ **TURKEY** *Istanbul*: Mehmet Celal Yahyabeyoglu ◆ **VIRGIN ISLANDS** *St. Thomas*: Nancy L. Fernandes

Challenge Answers (see pages 71–72 of the Spring 1997 issue for the questions): (1) a, (2) c, (3) c, (4) b, (5) b, (6) b, (7) c, (8) a, (9) b, (10) d, (11) d, (12) c, (13) b, (14) b, (15) a, (16) d, (17) c, (18) d, (19) c, (20) a, (21) b, (22) c, (23) a, (24) c, (25) d

BIRTHDAY BOOK OF DIAMONDS

Photos by Harold and Erica Van Pelt, 112 pp., illus., publ. by Harold & Erica Van Pelt, Los Angeles, CA, 1997. US$19.95.*

The crisp, perfect color photographs of Harold and Erica Van Pelt, no less than 54 in number and all full page, depict an astonishing variety of loose diamonds as well as jewels and watches set with diamonds and other gems. Some of the diamonds are very famous indeed, such as the Hope, the Eugénie Blue, the Dresden Green, and the Star of the East. Other spectacular pieces include the Cullinan blue-and-white diamond necklace, the diamond-studded Order of the Golden Fleece, and the Marie Antoinette earrings. It is amazing that these earrings, set with large and fine diamonds, descended unharmed from the French queen's jewel case after she met her death at the guillotine in 1793 (they are now in the collection of the Smithsonian Institution).

Although diamonds and diamond-set jewels dominate the illustrations, a number of other gems are included to illustrate the gemstone for each month. A nice touch is also provided by heading each month with a crystal drawing of one of the forms diamond crystals take in nature.

As mentioned in the foreword by Richard T. Liddicoat, Chairman of the Board at GIA, the *Birthday Book of Diamonds* indicates the dates for each month, but not the specific days of the week. Consequently, it is "perfect for noting birthdays, anniversaries, and other special occasions that repeat from year to year." Although the pages assigned to this purpose are the functional aspect of the book, the illustrations and their captions (the latter by Alice Keller) provide valuable facts about these notable jewels and gems, many of which appear in print here for the first time.

The *Birthday Book* is strongly and handsomely bound. With a little

BOOK Reviews

SUSAN B. JOHNSON AND JANA E. MIYAHIRA, EDITORS

care in making the entries neatly, it will become a lasting treasury of references and reminiscences.

JOHN SINKANKAS
Peri-Lithon Books
San Diego, California

RUBY & SAPPHIRE

By Richard W. Hughes, 511 pp., illus., publ. by RWH Publishing, Boulder, CO, 1997. US$98.00.*

This is Mr. Hughes's second book on ruby and sapphire. The first, titled *Corundum*, was published by Butterworth-Heinemann in 1990. *Ruby and Sapphire* is self-published by the author, which allows him full freedom in his writing. Tasteful advertisements, placed at the end of some chapters, helped fund the publishing costs. I did not find the ads disruptive and, in fact, believe they will be useful to some readers.

On opening the book, I found a bookmark on which Mr. Hughes warns the reader about his parochial writing style. Mr. Hughes makes no apologies for this style; rather, he states his desire to create a complete, factual book in which he interjects his opinions and observations for entertaining and stimulating reading. I personally enjoyed this style very much. While all of the factual information was at my fingertips, Mr. Hughes's personal interjections kept the reading lively. I think anyone involved in the gem trade will find these insights enlightening, if sometimes irreverent.

The first chapter presents the history of rubies and sapphires. Chapters 2 through 9 cover chemistry and crystallography, properties, color,

spectra and luminescence, inclusions, treatments, synthetics, assembled stones, and fashioning. In chapter 2, the text and diagrams that describe the morphology of ruby and sapphire from various sources provide information that is often difficult for the gemologist to find. The following chapters (3–6) supply the kinds of details that many gemologists will find useful for identifying corundum and its treatments. Inclusions are explained in general in chapter 5, whereas inclusions specific to treatments, synthetics, and particular sources are found in those respective chapters (6, 7, and 12). I would have enjoyed more of the excellent photomicrographs of inclusions categorized by source.

Chapter 10 discusses the grading and valuation of ruby and sapphire, as well as the world market. Although Mr. Hughes does not give a pricing breakdown that uses a colored stone grading system, he does explain the fundamentals of modern colored stone grading, along with how to judge the quality of these gem varieties of corundum. Quality ranking by source is also discussed. A section of this chapter is devoted to famous rubies and sapphires, with a summary of these magnificent stones listed together with auction prices where applicable.

Chapter 11 covers the geology of ruby and sapphire, and chapter 12 is entirely devoted to world sources. With in-depth information on the location and history of individual sources, as well as the characteristics of the corundum produced in each, chapter 12 is also a remarkable reference.

The book is lavishly illustrated with color photos, and each chapter ends with a detailed bibliography for further research. This book is the most in-depth publication on ruby and sapphire I have seen. I highly rec-

ommend it to anyone involved in the buying, selling, grading, identifying, or appraising of rubies and sapphires.

ANDREW LUCAS
Gemological Institute of America
Carlsbad, California

THE NATIONAL GEM COLLECTION

By Jeffrey Post, 144 pp., illus., publ. by Harry N. Abrams, Inc., New York, 1997. US$39.95.*

The heralded redesign of the famous gem and mineral hall of the National Museum of Natural History at the Smithsonian Institution (Washington, DC) has been completed. To celebrate the recent opening of the new hall, Dr. Jeffrey Post, Curator of Gems and Minerals, describes the fabulous collection—arguably the finest on public display in the world—in this new book.

Dr. Post has provided an attractively presented and entertaining short course on the world of gems, in conjunction with brief histories of some of the major items in the collection. Although the Hope diamond is the best-known piece, the collection has many other unique stones and famous jewelry pieces that are beautifully portrayed in the book. Among the remarkable gems are the Rosser Reeves star ruby; the Hooker,

Mackay, and Chalk emeralds; and the Logan sapphire. Historically significant jewelry—such as the Napoleon diamond necklace, the Marie Antoinette earrings, and the Spanish Inquisition necklace—add breadth to the appeal. In the nearly four decades since Mr. Winston donated the Hope diamond to the Smithsonian Institution, many important gifts have helped build the collection.

Excellent photography by Chip Clark and quality color printing add the necessary element to make Jeffrey Post's effort a superb coffee table book on gems.

RICHARD T. LIDDICOAT
Gemological Institute of America
Carlsbad, California

CLASSICAL LOOP-IN-LOOP CHAINS AND THEIR DERIVATIVES

By Jean Reist Stark and Josephine Reist Smith, 190 pp., illus., publ. by Chapman and Hall, New York, 1997. US$44.95.*

Loop-in-loop chains are some of the oldest forms of jewelry known. In fact, they were the principal types of chains fabricated from the Bronze Age through the Middle Ages. This book is a comprehensive instruction manual for making these elegant chains,

written for the person with experience working at the jeweler's bench.

Developed over many years of practical instruction, the text is extraordinarily detailed, well organized, and clear. It is the authors' stated intention that the book be sufficient by itself as a guide to making these chains, and in this they have succeeded. The hands-on portion of the book contains 34 projects. It begins with simpler chains (such as single loop-in-loop chains) and then moves, chapter by chapter, through chains of increasing complexity. It ends with multiple woven loop-in-loop chains. Each chapter is accompanied by high-quality drawings and photos of the finished chains, as well as by numerous excellent working drawings. There are also sections dealing with history, hand tools and equipment, metals, clasps and terminations, and much more. In addition, the book includes an appendix, a glossary, and an index.

Although there are other books on chain-making—and numerous books on jewelry-making that contain information on fabricating chains—*Classical Loop-in-Loop Chains* is the definitive work on the subject.

STEPHEN B. WORKMAN
Gemological Institute of America
Carlsbad, California

CALL FOR POSTERS

The Gemological Institute of America will host the International Gemological Symposium in San Diego, California on June 21–24, 1999. More than 2000 people are expected to attend this pivotal event. The symposium program—with the theme "Meeting the Millennium"—will feature technical sessions and panel discussions on a variety of topics of vital interest to all members of the gem and jewelry industry. In addition, there will be an open Poster Session featuring original presentations on such topics as new gem materials, synthetic gem materials, treatments, gem identification and grading, instrumentation and techniques, gem localities, gem exploration, jewelry manufacturing, and jewelry design.

Contributions are being solicited for this Poster Session. To be considered for this important event (space is limited), please submit a preliminary abstract (no more than 250 words) to one of the Poster Session organizers by October 1, 1998. For further information on the Poster Session, contact Dr. James Shigley at 760-603-4019 (Fax: 760-603-4021, or e-mail: jshigley@gia.edu) or Ms. Dona Dirlam at 760-603-4154 (Fax: 760-603-4256, or e-mail: ddirlam@gia.edu). For information on the International Gemological Symposium, contact Carol Moffatt at 760-603-4406 (cmoffatt@gia.edu) or write to any of these individuals at GIA, 5345 Armada Drive, Carlsbad, CA 92008.

GEMOLOGICAL ABSTRACTS

C.W. Fryer, Editor

DIAMONDS

Argyle Diamonds' pink diamond tenders (1985–1996). *Australian Gemmologist*, Vol. 19, No. 10, 1997, pp. 415–418.

Pink diamonds, and other fancy colors such as purplish red, have been marketed by Argyle Diamonds in a tender process since 1985. This article describes these stones year-by-year, through 1996, noting individual sizes, important stones, and other interesting facts. During this period, nearly 650 faceted stones were offered, weighing almost 550 carats.

The annual offerings have ranged from 33 to 88 stones. In general, the stone sizes (carat weight) have increased over the years. The first stones over 3 ct were offered in 1989; only eight stones over 3 ct (the largest at 3.66 ct) have ever been tendered.

Traditionally, the collection is viewed in Geneva, but in recent years Tokyo and Hong Kong have become established venues. The 1996 tender of 47 stones was purchased by 13 individual dealers and jewelers for a per-carat price of over $100,000. However, on at least three previous occasions (the last in 1993), the entire collection was sold to a single bidder, Geneva-based Robert Mouawad. *AAL*

Ashton finds diamonds in Alberta kimberlites. *Diamond Intelligence Briefs*, June 6, 1997, p. 1523.

Ashton Mining of Canada Inc. has found diamonds in kimberlites in yet another Canadian province, Alberta.

Kimberlite pipe K12 (also reported as K14), in the Buffalo Hills, has yielded 11 diamonds 0.5 mm or larger in maximum dimension, as well as 139 smaller "micro-diamonds"; two other pipes, K2 and K4, have returned "very low" diamond counts. Exploration continues. *MLJ*

Automation v cheap labour. J. Lawrence, *Diamond International*, No. 44, November-December 1996, pp. 87–88.

About 50% of India's diamond-cutting workforce are contract workers who are paid $1 for each small diamond that they polish. This price is the "base cost" for the Indian cutting center and has been constant for the past two decades, primarily because of the gradual decline in the rupee's value relative to the dollar (about 12 to the dollar in 1976 and about 33 to the dollar when the article

---

was written). In the highly competitive world of diamond fashioning, the article asks: "Will a centre with a stable $1 base charge prove unassailable by new technology?" In other words, can new technology negate the competitive advantage enjoyed by India because of its low wages, and enable diamond-cutting centers to be established elsewhere?

When considering automation, additional manufacturing costs must be factored in, such as for capital equipment, amortization, and the salaries of people needed to operate small, semi-skilled production lines. To balance these extra costs, one needs added value in terms of better yields and polished make. Such advances require equipment that is technically feasible but not presently available, equipment that probably would be expensive to develop.

After presenting several scenarios, the authors conclude that automation would only boost yield by one or two percent over that achievable by India's good artisan workforce. *AAL*

Dia Met developments. *Mining Journal, London*, March 7, 1997, p. 184.

Between 1988 and 1995, small-scale operations recovered more than 250,000 carats of diamonds from a 3225 hectare area at Salvación in Venezuela. Dia Met Minerals (of Canada) signed a letter of intent with Cooperativa La Salvación (CS), a Venezuelan corporation, to exploit this deposit. Diamonds recovered to date have come from alluvial workings, but these are believed to have originated from kimberlite dikes on the property. Dia Met plans to explore the kimberlites while CS continues to mine the alluvial sources. *MLJ*

Diadem touts California's first diamond pipe since 1849. *The Diamond Registry*, Vol. 29, No. 6, 1997, p. 5.

Macro- and micro-diamonds of unspecified sizes have been found in 11 holes drilled in the 1120 acre Leeks Springs, California, property held by Diadem Resources Inc. The source rock is apparently olivine lamproite breccia and agglomerate. *MLJ*

Diamond—Birthstone for April. H. Bracewell, *Australian Gold, Gem & Treasure*, Vol. 12, No. 4, April 1997, p. 24.

Hylda Bracewell's series on birthstones concentrates on their lore rather than their gemological properties. We learn that diamond is a "help to lunaticks," that a person wearing a red diamond will achieve heroic deeds, but a black diamond will attract misery. Diamonds with black spots, "bubbles," or "lines" in them are eunuchs and should be avoided. Much of this lore is very old, and all of the above apparently came from Camillus Loenardus's *Speculum Lapidum Venice* (1502). Another tidbit from that work: "the Diamond is a most precious Stone of the colour of polished iron. . . ." Some modern lore is included, such as what personality type should wear which dia-

mond shapes. According to Ms. Bracewell, round brilliants should be worn by the home loving, pears by extroverts, marquise cuts by the emotional, ovals by the enterprising, emerald cuts by the logical, and heart shapes by the romantic. *MLJ*

Diamonds from the deep. M. D. Riley, *American Jewelry Manufacturer*, Vol. 41, No. 11, November 1996, pp. 18, 20, 22, 24.

Diamond exploration has surged worldwide, especially since 1990. This article reviews marine exploration, particularly marine diamonds off the shores of Namibia.

At the time this article was written, about 35% of Namibian diamond production, almost all of which is gem quality, was being recovered from the sea by De Beers Marine, operating as a contractor to Namdeb (an equal partnership between De Beers and the Namibian government). Several other companies also recover diamonds from the sea, but these are smaller operations and closer to the shore. Onshore reserves in Namibia are nearing depletion, but increased marine production is offsetting that decrease. Similar marine deposits, although not yet as significant as those off Namibia, are successfully being mined off South Africa's west coast.

With Namibian offshore deposits as a model for the origin and occurrence of marine diamonds, exploration has been under way in recent years offshore of Kalimantan (Borneo), Western Australia (Bonaparte Gulf and Cambridge Gulf), Canada (Coronation Gulf in the Beaufort Sea), northern Russia, and Sierra Leone. To date, none of these exploration projects has found an economically viable diamond deposit. *AAL*

India's eximports: Gems & jewellery exports record downtrend in 1996–97. *Diamond World*, Vol. 24, No. 3, 1997, pp. 41–42.

Diamonds constitute more than 90% of India's gem and jewelry exports. For many years, cut and polished diamonds led exports, both in value and carat weight. However, the financial year 1996–1997 (ending March 31, 1997) was the first exception in the long trend of continually increasing exports—diamonds led a decline. Polished diamond exports decreased by 9.16% on a value basis (to $4,235 million), and by 1.72% on a carat weight basis (to 18.88 million carats), compared to 1995–1996.

Other export items also decreased in 1996–1997 because of lackluster overseas markets. These included cut and polished colored gemstones (-5.89%), pearls (-35.89%), costume jewelry (-91.96%), and synthetic gems (-96.06%).

One of the few bright spots in export figures was gold jewelry, which increased 25.24% to $713 million. *AAL*

Japan holds the key. M. Cockle, *Diamond International*, No. 45, January-February 1997, pp. 41–44.

Since 1980, the world's retail diamond jewelry sales have increased more than 2.5 times (to about $52.7 billion in

1995). The U.S. and Japan are the mainstays of the industry. Interestingly, De Beers has had to raise its estimate of annual retail sales for the U.S. by about 6% for the past decade. It was discovered that jewelry containing inexpensive (predominantly Indian-cut) diamonds had not been included in previous surveys.

The two major markets have not grown equally since the late 1980s. Monetary factors, primarily, have weakened the Japanese market. (The yen depreciated 15% against the dollar in 1995 alone.) Because Japan accounts for about one-third of the world's retail sales, sluggish performance in that market affects the entire industry. Conversely, any growth in the world market is dependent on Japan's recovery.

This article reviews the history of De Beers's involvement in the Japanese diamond jewelry market from 1966 (when that retail market was $255 million) to 1996 (when retail sales totaled about $17 billion—a 66-fold increase in 30 years). Marketing campaigns and the appreciation of the yen (until recent years) are the main factors behind the spectacular rise in popularity of diamond jewelry in Japan. In addition, recent growth of the Japanese market is attributed to: (1) an increase in the size of the average engagement-ring stone (from 20 points in 1980 to 40 points in 1995); and (2) the development of the "single-woman market," so that today over 60% of single Japanese women own a diamond. This latter market has been incredibly successful: Three out of 10 unmarried Japanese women buy diamond jewelry once a year.

Clearly, such achievements cannot be repeated *ad infinitum*. In fact, there is evidence of a change in attitude among younger Japanese women toward jewelry consumption in general, and the diamond engagement ring in particular. Some young people do not want to spend three months' salary on a ring. Further, there is a trend toward less expensive weddings, and Japanese tourists find that they can buy costly items, such as jewelry, more cheaply overseas.

This paper contains the most up-to-date (through 1995) statistical compilations for the retail diamond jewelry business worldwide. These compilations include world retail diamond jewelry sales for 1980–1995, retail sales by country, average price paid for jewelry, and number of pieces sold.   *AAL*

Kensington considers Chinese diamonds. *Mining Magazine*, Vol. 176, No. 2, February 1997, p. 119.
Canadian diamond mining company Kensington Resources has optioned a 50% share in a diamond mine 300 km south of Beijing. This [name unspecified] mine currently produces 40,000–45,000 carats per year, with a "measured and indicated" resource believed to be 2 million carats (ore grade 1.17 ct/ton) to 300 m deep in the mine; an additional one million carats may be found at greater depth (to 600 m) at a lower ore grade (0.77 ct/ton). Kensington has also signed joint-venture agreements for two diamond prospects nearby.   *MLJ*

Lac de Gras revision. *Mining Journal, London*, February 14, 1997, p. 130.
BHP delivered the final feasibility study for the BHP/Dia Met Lac de Gras project in Canada's Northwest Territories; the study covers 17 years' worth of planned operations. The Panda, Misery, Koala, and Fox pipes will be developed. One change from preliminary plans is that the Sable pipe, with a value of US$63/ton, will be developed during the first 17 years, and the Leslie pipe, with a value of $28/ton, will not. Capital cost estimates remain unchanged, at C$900 million to bring the mine into production and another C$300 million for expansion in the 10th year of operations. Two additional pipes (plus Leslie) may prove economic, and another five await large-diameter drill core sampling for evaluation purposes.   *MLJ*

Mwadui diamonds again flow from Williamson mine. *In-Sight—The CSO Magazine*, Winter 1996–97, p. 11.
The Mwadui mine (originally known as the Williamson mine) is the world's largest economic kimberlite pipe (146 hectares in surface area). *[Abstracter's note: From 1958 until 1973, it produced over 500,000 carats annually.]* After Tanzania became independent, production declined as the mine fell into disrepair. In 1994, production ceased entirely.

Recently, De Beers and Tanzania agreed to rejuvenate the mine, with De Beers getting a 75% stake and Tanzania, 25%. *[Abstracter's note: De Beers will invest $16 million to refurbish the mine with new infrastructure and equipment. Limited mining resumed in October 1996 (16,000 carats were produced that year).]* Open-pit mining of the kimberlite pipe will begin in about two years, and is projected to last for another seven years. More than 3,000 tons daily (about 1 million tons a year) will be processed. *[Abstracter's note: Annual caratage would be about 200,000 if published reports are correct that the kimberlite yields 0.2 ct of diamonds per metric ton.]* Clearly, the Mwadui mine is poised to regain much of its former glory.

De Beers has a license to explore a large area (23,000 km^2) around the Mwadui mine. Already, some 60 previously unreported kimberlites have been discovered.
                                                      AAL

New company to develop diamond pipes . . . *Mining Journal, London*, July 25, 1997, p. 65.
Russian diamond producer Almazy Rossii Sakha (ARS or Alrosa) has formed a joint-stock mining company to develop the Botuobinskaya and Nyurbinskaya kimberlite pipes in the Nakyn region of the Nyurba district in western Sakha (Yakutia). The new company, Alrosa-Nyurba, has a charter capital of 20 billion rubles (about US$3.5 million); development of the two pipes is expected to cost $350 million. The mine life for both pipes is estimated at 25 years; they could produce about $900 million of diamonds annually within five years.   *MLJ*

New diamond targets in Mali. *Mining Journal, London*, May 16, 1997, p. 392.

Several kimberlite "targets," some containing diamonds, have been discovered at the Kenieba project in Mali. Nine areas have chromites with chemical compositions matching those found in diamondiferous kimberlites; 23 areas show "anomalous" indicator minerals, and some contain macro diamonds. Thirty magnetic targets have been found. So far, at least two kimberlite pipes are known, the 19 hectare Cirque pipe and the 4 hectare Sekonomala pipe. A 70.62 ct diamond found in a "paleo placer" in late April 1997 originally may have come from the Cirque pipe.   *MLJ*

New facility helps Finnish diamond search. *Diamond News and SA Jeweller*, February 1997, p. 13.

A pilot-scale plant that uses flotation technology for concentrating small diamonds has been developed at the Outukumpu laboratory of VTT Chemical Technology–Mineral Processing in eastern Finland. Plant capacity is about five tons of ore per hour.

Flotation depends on the separation between water and hydrophobic materials (substances that repel water, either naturally or through chemical treatment). In this concentration technique, small hydrophobic particles—in this case, diamonds—are gathered in the froth that forms as air bubbles rise through a tank containing water, carefully ground ore, and (sometimes) additives. Although flotation is a common technique for concentrating certain metal ores, its application to diamond recovery is unexpected.   *MLJ*

Redaurum finds diamonds in Colorado. *Diamond Intelligence Briefs*, July 30, 1997, p. 1546.

Redaurum has found two more large diamonds—28.2 ct and 16.3 ct—at the Kelsey Lake mine near Fort Collins, Colorado. The former is the sixth largest stone found to date in North America. A 28.3 ct stone found last year sold for $90,000.   *MLJ*

Russian diamond pipe tender. *Mining Journal, London*, May 30, 1997, pp. 425–426.

Russia is seeking foreign participation to develop the Lomonosova kimberlite pipe, in the Zolotitsa kimberlite field on the edge of the Arctic Circle in northern Russia, about 90 km north of Archangelsk. Lomonosova, a large pipe, has an estimated grade of 0.3 ct per ton; Russian press reports indicate a potential output of 3–6 million carats (Mct) for 30–40 years, or possibly even more than a total of 250 Mct. Their possible worth could be in excess of US$12 billion. The state enterprise Severalmaz holds the official license to develop the Lomonosova pipe.

Russia's diamond production is now dominated by Almazy Rossii Sakha (ARS), which operates large mines in Sakha (Yakutia). Annual production is currently running about 13 Mct, with stones averaging US$90 per ct. Eighty-five percent of this production presently comes from the Udachny open pit. Total ARS rough diamond production in 1996 was worth about US$1.35 billion.
                              MLJ

Scandinavian progress for Cambridge. *Mining Journal, London*, November 15, 1996, pp. 393–394.

Cambridge Resources has been looking for diamonds in the Alno and Kalix permit regions in Sweden; the area is adjacent to the Baltic-Bothnian megashear, a large tectonic feature similar to that in Canada's Northwest Territories. Sixty magnetic anomalies were found in the 1996 prospecting season, and five "areas of particular interest" have been defined—based on the presence of heavy minerals (e.g., diamond- and kimberlite-indicator minerals) and topographic depressions.   *MLJ*

Statistical survey Belgian diamond sector 1996. *Diamant*, Vol. 38, No. 390, February-March 1997, pp. 6–8, 10, 26.

By importing over 210 million carats (Mct) of rough during 1996, Antwerp further solidified its reputation as the world's largest diamond supply center. Of these, 130 Mct (62%) were gem or near-gem and 80 Mct (38%) were industrial.

The import figures are truly staggering, considering that only about 113 Mct of rough diamonds were mined worldwide in 1996. Two factors explain the discrepancy between the 210 and 113 Mct figures. First, there were significant "double counts" (e.g., sight goods were sent from the CSO in London for sorting in Antwerp; these were sent back to London, then returned later to Antwerp, and they were counted both times they entered Belgium). Second, diamonds were sent to Antwerp from the Russian stockpile.

Diamonds entering Belgium from the CSO constituted 33% of the rough, while those from the outside market constituted 67%. In addition to Russia, outside goods primarily came from Zaire and other west and central African countries via Liberia and Congo-Brazzaville. Since mid-1996, diamonds from Australia's Argyle mine also have been part of the outside market.

Most (79%, or 92.5 Mct after deduction of double-counts) of Belgian rough gems and near-gems exported in 1996 went to India. This 12% increase over 1995 clearly points to more lower-quality goods entering the market. Little is cut locally in Belgium.

Antwerp's imports of polished diamonds are also impressive: They reached 6.8 Mct in 1996 (an 18% increase over 1995), with most coming from India (36%), Russia (10%), the U.S. (10%), and Israel (8%). The re-export of almost 7 Mct of polished goods primarily went to the U.S. (24%), Hong Kong (14%), Israel (9%), Switzerland (8%), and Japan (7%). Of the major markets for polished goods exported from Belgium, Japan suffered the most severe year-to-year decline (-19% in U.S. dollars), which was attributed to continued recession there.
                              AAL

Supply set to be outstripped by demand. L. Rombouts, *Diamond International*, No. 45, January-February 1997, pp. 57–59, 61, 62, 64.

Diamond mining, with few exceptions, is very profitable. As a result, particularly since 1990, it has attracted many mining companies that previously showed little interest. Recent statistics and economic studies show a growing demand for diamonds and a shortfall in better-quality goods in a few years—because of the gradual depletion of reserves at existing mines.

This article reviews worldwide diamond mining and exploration for 1996. New mine supply is estimated at 111 million carats [Mct], valued at $6.44 billion. Russian stockpile contributions to world supplies in 1996 were 12.3 Mct, so world rough supplies for the year totaled 123.3 Mct (a decrease of about 6.7 Mct over 1995).

Mine production in each major source country is reviewed. Key facts include:

- By the year 2000, Botswana's Orapa mine will be the world's second largest (after Argyle), with production of 12–13 Mct annually.
- Eighty-five percent of Russian production comes from the Udachny mine, which is reaching its limit of profitability as an open-pit mine.
- Production declined markedly in 1996 at the (now underground) Finsch mine in South Africa.
- Production levels remain at about 5.5 Mct at the Mbuji-Mayi mine in Zaire, despite generally chaotic conditions in that country.
- Offshore production in Namibia (about 550,000 carats) now accounts for about 45% of that country's total.

Worldwide, diamond exploration activity costs about $350 million per year. Much of it is centered in Canada, Russia (especially in the Arkhangelsk region), Finland, Australia, Angola, Botswana, Zimbabwe, and other parts of Africa (e.g., Sierra Leone, Tanzania).   *AAL*

"A testing time" in diamond jewelry production. *Mazal U'Bracha*, Vol. 13, No. 83, October 1996, pp. 73, 76, 77.

The largest diamond-jewelry exporters are Italy, Hong Kong (including mainland China), Thailand, and India, according to Harry Garnett, director of the De Beers CSO Marketing Liaison Department. However, this has not always been the case. Labor costs, particularly those associated with setting loose stones in jewelry, are a major factor in jewelry manufacturing, so the relative importance of each center has changed over time.

Hong Kong was the main supplier of low-cost jewelry to the U.S. in the 1970s. By the early 1980s, this role had shifted to Thailand. More recently, India became the main supplier. That country has an almost inexhaustible supply of cheap labor (average labor costs per worker are about $80–$180 per month).

The 1990s have been a "testing time" for the diamond jewelry industry, with lower margins, more contract workers, tighter inventory control, and a move toward last-minute buying of polished goods. This competitive market has also resulted in the use of lighter gold settings, lower-quality diamonds, and more colored stones to meet lower price points.

The U.S. jewelry manufacturing industry has become more specialized and service oriented; the Japanese have become more insistent on higher design and quality standards; and the Italian industry has retained its position as the world's leading manufacturing country in terms of size, creativity, and flexibility. The article's prognosis is that changes will continue in the diamond jewelry manufacturing industry, with continued pressure on profitability and efficiency. This will lead to a more compact pipeline, in which both polished-goods and jewelry wholesalers will play less important roles.

AAL

GEM LOCALITIES

Returning the deposed queen conch to royal status in Florida. *National Geographic*, Vol. 192, No. 1, July 1997, p. 145.

Queen conchs are desirable for their shells and meat, as well as for conch pearls. Florida populations had fallen drastically, by 1985, when the state banned conch harvesting. A hatchery began producing conch larvae on Long Key in 1990, and 5,000 young conch have been released offshore. They are monitored by means of a metal detector, which finds the aluminum tags attached to their shells; nearly 20% of the young have survived since their release at an unspecified date   *MLJ*

Emerald mineralization and metasomatism of amphibolite, Khaltaro granitic pegmatite–hydrothermal vein system, Haramosh Mountains, Northern Pakistan. B. M. Laurs, J. H. Dilles, and L. W. Snee, *Canadian Mineralogist*, Vol. 34, Part 6, 1996, pp. 1253–1286.

Emerald formation usually involves two different sources of materials: (1) ultramafic (dark) rocks that contain chromium, and (2) highly evolved rocks that contain beryllium. Most emerald deposits are associated with granitic pegmatites and hydrothermal quartz veins intruded into Cr-bearing schist; emeralds are usually found in the schist adjacent to the pegmatites. The Khaltaro deposit is geologically significant because emeralds formed within the hydrothermal veins and pegmatites, so Cr (generally an immobile element) must have migrated from the host rock during their formation.

The Khaltaro deposit is located at an elevation of nearly 4200 m, in a remote area of northern Pakistan. Small-scale mining by the Gemstone Corporation of Pakistan in 1985–1990 produced about 600 carats of gem-quality emerald from two small prospects. However, further exploitation has been discouraged by the fact that the emeralds are pale and fractured, as well as by the inaccessibility of the locale.

Emerald at Khaltaro occurs in two types of

hydrothermal veins—quartz and tourmaline-albite—and, less commonly, in the fine-grained outer zone of the pegmatites. Only rarely does it form in the altered amphibolite next to the veins. Emerald crystals up to 2.5 cm long were reportedly found by local miners in the tourmaline-albite veins. Aquamarine and colorless beryl are also found locally.

The emerald crystals examined were unmodified hexagonal prisms terminated by pinacoids, abundantly cracked and included. A few samples showed potential for chatoyancy, because of hollow tubes parallel to the c-axis. Microprobe analyses (some provided in the article) give 0.20–1.27 wt.% Cr_2O_3 and 0.62–0.89 wt.% Fe_2O_3. Khaltaro emeralds can be differentiated from other Pakistan emeralds by their cathodoluminescence emission spectra and chemistry (higher Si, Al, and Cs; and lower Mg, Na, Fe, and Sc).

Based on studies of trace elements and oxygen isotopes in whole-rock samples and individual minerals, the authors suggest that the Be from the pegmatite-hydrothermal vein system combined with Cr from the host rock when fluorine-rich hydrothermal fluids altered calcic amphibole and zoisite in the amphibolite. The released Cr migrated a short distance into the veins, where it combined with the crystallizing beryl to form emerald. *MLJ*

Characterization of alexandrite, emerald and phenakite from Franqueira (NW Spain). C. Marcos-Pascual and D. B. Moreiras, *Journal of Gemmology*, Vol. 25, No. 5, 1997, pp. 340–357.

Described are the occurrence and characteristics of the beryllium minerals emerald, alexandrite, and phenakite from Franqueira, Spain. The geologic conditions are similar in many ways to those of the well-known deposits of Tokovaja in the Ural Mountains of Russia; that is, Be and Cr were brought together when pegmatites and associated mobile elements (Be, B, P) were emplaced into Cr-bearing mafic rocks. The gem-bearing zone is only 3 m thick and crops out for 15 m, although it may extend further underground. The Franqueira minerals are similar to their counterparts from Tokovaja, as several comparative tables show. The authors present extensive chemical and physical data on the three minerals, along with discussion of their abundant inclusions. If the photos are representative, then the quality of color or clarity in these gems, unfortunately, is not high. *CMS*

Iberian emeralds. *Mining Journal*, *London*, December 20/27, 1996, p. 496.

The Franqueira deposit, in the Helena permit area of northwestern Spain, contains gem-quality emerald, alexandrite, and phenakite. It was found by geologists from Oveido University. The exploration permit for the 30 km^2 Helena permit area has been awarded to Cambridge Mineral Resources and will be managed locally by Stella Exploration Services. The largest emerald to date, 30 ∞ 10 cm, reportedly had good transparency and a dark green color. [*Abstracter's note: Although the article claims that this is the first documented deposit of gem-quality emerald and alexandrite in Western Europe, both Austria and Norway have produced gem-quality emeralds.*] *MLJ*

A new colour-change effect. A. Halvorsen and B. B. Jensen, *Journal of Gemmology*, Vol. 25, No. 5, 1997, pp. 325–330.

Chromium-bearing tourmalines from the Usambara region of Tanzania exhibit color variations from green through orange to red when viewed in transmitted light, depending on the thickness of the sample. Examination of pleochroism and spectral features indicates that the apparent color depends on the distance that light travels within a sample (path length). Faceted green gems display flashes of red when internally reflected light travels far enough within a sample to achieve the required selective absorption. The perceived difference in color was attributed to the "psycho-physical effect," as defined in a 1964 paper by C. P. Poole on color change in Cr compounds.

The authors propose the term "Usambara effect" for this color change that is due to path length. It would be interesting to try the authors' experiment (well illustrated in figure 3) on other types of gems, such as some malaia garnets, that also exhibit red flashes. The likelihood that path length accounts for these flashes has long been the subject of speculation, but it has never before been illustrated so conclusively.

Two issues of this journal later, in a letter to the editor, Dr. Kurt Nassau pointed out that the effect is well known in the field of organic dyes, where it has been called "dichroism." Thus, he argued, the new name proposed by Halvorsen and Jensen is misleading. Since *dichroism* is used differently in gemology, however, Dr. Nassau proposed the terms "concentration dichroism" and "thickness dichroism" as appropriate. *CMS*

A note on a new occurrence of vanadian grossular garnet from Madagascar. A. Mercier, B. Moine, J. Delorme, and M. A. F. Rakotondrazafy, *Journal of Gemmology*, Vol. 25, No. 6, 1997, pp. 391–393.

A new deposit of green grossular was discovered in late 1991 in the Gogogogo area of southwest Madagascar. Its pale yellowish green to dark green color is primarily caused by vanadium, as is the case with tsavorite from East Africa. Overall chemical and physical properties (as represented by a single dark green specimen) resemble those of similar material from East Africa and Pakistan, including an R.I. of 1.742 and S.G. of 3.62. *CMS*

Pailin's path to prosperity. S. Kanwanich and R. Saen-grungruang, *Bangkok Post*, June 1, 1997, p. 1 (Perspective section).

Pailin, a Cambodian border town with Thailand, has long been known for its gemstones. Although this natural

resource has always been exploited, trade—once banned by authorities—has recently received official recognition again. Most investors are Thai, and gem concessions are a major income source in Pailin.

The gem trade largely supports the free health care and education systems. Gem shops abound, and gem concessions are sold at rapidly inflating prices. Miners use heavy equipment to sift for gem minerals, but this is usually unproductive because most concessions were previously mined. Although gems are still abundant, they are buried deeper, requiring more-sophisticated machinery and extraction techniques.

This well-written article also looks at the history of the area and provides a fascinating, first-hand glimpse into the excitement and complex interaction of merchant and military in what is today a gem boomtown.

Alison Mader

Physicochemical structural characteristics of ambers from deposits in Poland. F. Czechowski, B. R. T. Simoneit, M. Sachanbỉnski, J. Chojcan, and S. Wolowiec, *Applied Geochemistry*, Vol. 11, No. 6, 1996, pp. 811–834.

Amber has been mined from, or known to occur at, over 600 localities in Poland. At present, the richest occurrence is being mined near Gdansk (on the Baltic Coast), particularly between the mouths of the Stogi and Vistula rivers. This paper compares physical and chemical properties of ambers from the Gdansk region with those from newly discovered occurrences in central Poland near Belchatów (associated with brown coal) and in southwest Poland near Jaroszów (associated with refractory clay). Very sophisticated analytical techniques (e.g., gas chromatography, nuclear magnetic resonance, positron annihilation spectroscopy, and nitrogen sorption) were used to make comparisons.

The results show that these ambers from distinctly different geological environments are similar in some respects, such as in their chemical character: They consist of mixtures of the same compounds, namely succinates and n-alkanes. However, relative proportions of these compounds differ in ambers from the three localities and even within the amber samples themselves (exterior versus interior zones). Similar variations are reported for other properties, such as porosity, reflectance, and solvent-extraction yields.

On the basis of the chemical similarities (particularly the succinates), the authors suggest that amber from all three areas is of similar origin and can be called "Baltic amber." The authors assume that all three ambers came from the same hypothetical conifer of the *Pinus succinifera* family.

AAL

A study of New Zealand Kauri copal. S. J. A. Currie, *Journal of Gemmology*, Vol. 25, No. 6, 1997, pp. 408–416.

Kauri copal, a resin produced by the long-lived Kauri pine,

has been "mined" for more than 150 years from New Zealand coal beds. Its interest to gemologists lies largely in its resemblance to amber, but this role pales by comparison to the almost half million tons once exported for use in varnishes and linoleum. Some fine varnishes still use it today. The Otamatea Kauri Museum in northern New Zealand preserves the material's history.

Twenty-five specimens of widely varying color (colorless to dark brown), diaphaneity (transparent to opaque), and age ("recent" to 40 million years) were studied by the author. The results are compiled in a comprehensive table that includes source, age, specific gravity (1.03–1.095), refractive index (1.540), solubility in ether and alcohol, fluorescence, and smell. Tests and observations, other than R.I. and S.G., showed a broad range of reactions, but fossil samples of copal could be distinguished from recent specimens in that the former are insoluble in alcohol. As such, the fossil samples are indistinguishable from most amber. Moreover, because the alcohol test is destructive, it has only very limited application in gemology. This article is a must-have reference on a poorly documented (yet abundant) gem material.

CMS

INSTRUMENTS AND TECHNIQUES

A Raman microscope in the gemmological laboratory: First experiences of application. H. A. Hänni, L. Kiefert, and J. P. Chalain, *Journal of Gemmology*, Vol. 25, No. 6, 1997, pp. 394–406.

The Swiss Gemmological Institute (SSEF) in Basel has found its recent acquisition of a Raman microscope well worth the investment, to judge by this excellent account of its initial applications at this laboratory. Much more accurate, easier to use, and considerably less expensive than its predecessors, the Renishaw Raman microscope at SSEF easily fits on a desktop. It has enabled SSEF staff members to identify CO_2 inclusions in sapphire that are diagnostic of heat treatment, detect and identify fracture fillings in emerald, easily identify mounted gemstones, and characterize specimens with irregular surfaces. It can also distinguish component minerals in many aggregates.

The method is nondestructive in all but a few well-documented conditions and works on all types of materials, except those having simple compositions and high symmetry, such as metals and alloys. Raman spectroscopy does require that the user be aware of its limitations and parameters; also, the lack of a large, published database means that each laboratory must obtain many of its own reference spectra from known samples. However, Raman spectroscopy clearly has earned a place of respect among the few high-tech laboratory techniques that have proved indispensable to gemological testing today.

CMS

JEWELRY RETAILING

Due to shortage, prices increase for Tahitian cultured black pearls. *National Jeweler*, July 1, 1997, p. 26.

Because of a pearl shortage, prices of Tahitian cultured black pearls jumped 7.9% during the first quarter of 1997 over the same period the previous year. The amount of pearls exported during that time decreased by 109 kg, according to customs figures provided by the Tahitian government.

The biggest export market for loose Tahitian pearls during the first quarter was Japan, although the volume (440.7 kg worth $7.8 million) was down this year from the first three months of 1996 (547 kg worth $9.7 million). The U.S. moved from fourth to second place, importing a total of 61.7 kg of Tahitian pearls, compared with 39.8 kg imported during the same period last year.

<div align="right">MD</div>

Top of the heap. *Retail Jeweller & British Jeweller*, July 10, 1997, pp. 10–11.

Christie's London jewelry sales in June 1997 brought in £7.03 million, a massive 61% increase over last year's June sales. The sale included the Hatot collection and an important privately owned European collection. About 30% of sales were to individuals from Asia and the Middle East.

The highlight of the sale was a spectacular fancy-colored diamond pendant/brooch that brought the top price of £441,500, almost double its pre-sale estimate. This pendant was purchased by an American dealer. In the Bijoux Français sale, a diamond pendant by Van Cleef & Arpels sold above estimate for £199,500 to a member of the British trade, while a private Hong Kong buyer paid £155,500 for a 1925 ruby-and-diamond necklace by Mauboussin, originally estimated at £60,000–£80,000.

At Sotheby's June 19 sale, diamonds took all the top prices. An arrow and quiver brooch—set with diamonds, emeralds, and rubies—sold for £25,300, much higher than a pre-sale estimate of £4,000–£6,000. A ruby-and-diamond bracelet, circa 1930, sold for £40,000; while a sapphire-and-diamond tiara went for £26,450, double its estimate.

At Bonham's June 20 sale, an attractive diamond-set swan brooch by Van Cleef & Arpels sold for £11,000. A Burmese ruby-and-diamond cluster ring went for £22,000.

At Sotheby's June 11 New York sale, private American buyers purchased eight of the 10 top lots. A fine cultured pearl necklace sold just below estimate at £68,680; the same price paid for a necklace of natural black pearls was substantially above estimate.

The article also reports on other auctions, including further examples of pieces sold.

<div align="right">MD</div>

PRECIOUS METALS

Platinum demand rises in U.S., China. M. Kletter, *National Jeweler*, June 16, 1997, p. 3.

According to Johnson Matthey's *Platinum 1997*, demand for platinum in jewelry applications rose in both China and the United States in 1996. Worldwide, total demand for jewelry reached 1.85 million ounces, up from 1.81 million ounces in 1995. Demand for platinum jewelry in North America rose around 38%, to 90,000 ounces from 65,000 ounces in 1995. Platinum jewelry in the U.S. is still largely concentrated in the bridal market. China became a significant market for platinum jewelry in the last three years, according to the report, because of demands by a new middle class in that country. Demand was flat in 1996 in Japan, the largest market for platinum jewelry.

Platinum supplies fell by 90,000 ounces to 4.9 million ounces in 1996, largely because of declining shipments from Russia and South Africa, the largest platinum suppliers.

<div align="right">MD</div>

SYNTHETICS AND SIMULANTS

The identity of reddish-brown inclusions in a new type of Russian hydrothermal synthetic emerald. K. Schmetzer and H. J. Bernhardt, *Journal of Gemmology*, Vol. 25, No. 6, 1997, pp. 389–390.

Reddish brown transparent platelets in recent Russian hydrothermal synthetic emeralds are conclusively identified as hematite. They differ from previously observed opaque hematite platelets only in that they are thin enough to achieve transparency.

<div align="right">CMS</div>

TREATMENTS

Identification of B jade by diffuse reflectance infrared Fourier transform (DRIFT) spectroscopy. P. L. Quek and T. L. Tan, *Journal of Gemmology*, Vol. 25, No. 6, 1997, pp. 417–427.

The advantages of DRIFT spectroscopy to detect wax and polymer impregnation of jadeite are spelled out in this article. DRIFT can obtain results even from thick and/or mounted specimens; its sensitivity exceeds that of traditional FTIR spectroscopy.

Three samples of "wax-buffed" (otherwise untreated) jadeite, three of bleached and wax-impregnated jadeite, and four of bleached and polymer-impregnated jadeite (all green) were examined. Ultraviolet (long- and short-wave) fluorescence could not distinguish between the first two sample types, and it only sometimes indicated the third. FTIR results proved similarly ambiguous. However, fine peaks in the 700–6000 cm^{-1} region of the DRIFT spectra enabled the authors to conclusively separate the samples into their three groups. Although 10 samples represent a small population from which to draw sweeping conclusions, this method (and its usefulness in detecting certain treatments) clearly deserves serious consideration and further study.

<div align="right">CMS</div>